Development of a 6 Degree-of-Freedom Manipulator Arm for Use on an Urban Search and Rescue Robot

Prepared by:

Peter M A Henson

Prepared for:

Stephen Marais
Robotics and Agents Research Lab
University of Cape Town
March 2012

Acknowledgments

Firstly I would like to thank the Lord God, who has been right with me the whole way, keeping my spirits up, and giving me good ideas. He has been the source of all my provision; He has been my encourager and has given me the grace and strength to complete it. Thank You Lord!

"Be strong... and work; for I am with you," says the Lord of Hosts (Haggai 2:4)

To my parents: thank you for all the support; both the encouragement and the financial support. You deservedly have as much claim to this document as I do. You have never left me wanting for anything. Thank you Dad and Mom. And Dad, once again thank you very much for all your excellent ideas and solutions.

To Stephen Marais: thank you so much for being an outstanding supervisor! You have pushed me and brought out the best in me. You have been the perfect balance of strict and helpful. I could not have asked for a better supervisor. I wish you all the best in the Mexico competition. Thank you!

To the departmental and workshop staff: thank you for your time, help and for growing my patience.

To Mr M. Uematsu in KHK Japan: who despite torrid natural disasters delivered superb quality gearing on time. You guys are an engineering inspiration.

To Mr Albert Verburg: thank you for making my carbon tubes free of charge, you are most generous.

To friends and family: Thank you all for brightening my days and supporting me over these last two years. Cape Town has been a better place because of you guys.

To Emma: both a distraction and a support, thank you so much for both! You have given me inspiration in completing this masters.

Declaration

1. I know that plagiarism is wrong. Plagiarism is to use another's work and pretend that it is one's own.
2. I have used the ISO 690 convention for citation and referencing. Each significant contribution to, and quotation in, this thesis from the work, or works, of other people has been attributed, and has been cited and referenced.
3. This thesis is my own work.
4. I have not allowed, and will not allow, anyone to copy my work with the intention of passing it off as his or her own work.

Signature..... Date.....

Abstract

This document reports on the design, construction and testing of the manipulator arm that is to be fitted to UCT's Urban Search and Rescue Robot (USRR), named the *Ratel*. The 6 degree-of-freedom manipulator arm is mounted on the crawler base and is shown in Figure I below. It is fitted with the sensor payload and gripper assembly.

Figure I: Rendering of Ratel Complete with Manipulator Arm and Sensor Payload

The USRR is designed to traverse difficult terrain in search of survivors. The base is therefore equipped with variable geometry tracks to enable it to traverse stairs and other tricky terrain. The sensor payload is equipped with life detection equipment and the manipulator arm enables the USRR to manipulate with its environment (opening doors etc.)

and to interact with survivors, passing them water or food packs. Figure II shows the completed manipulator arm, together with the sensor payload and gripper.

Figure II: Left side of Manipulator Arm (Sensor Payload Cover Removed)

The manipulator arm was designed to lift 1kg at full reach, which it exceeded in testing; it was tested to 2kg at full reach, complete with the sensor payload. Figure III shows the arm at full reach, with the sensor payload looking backwards. The turntable, second elbow, wrist and pan (for the sensor payload) all exhibit continuous rotation, making use of slip rings, and the entire arm's wiring is run internally.

Figure III: Photograph of Manipulator Arm in Full Horizontal Reach

It was also required that the arm display low backlash to ensure a steady camera feed, and precise arm control. Adjustable backlash *duplex* worm gears were used in the three lowest joints, and they were tested to have near-zero backlash. Figure IV shows the gearbox design.

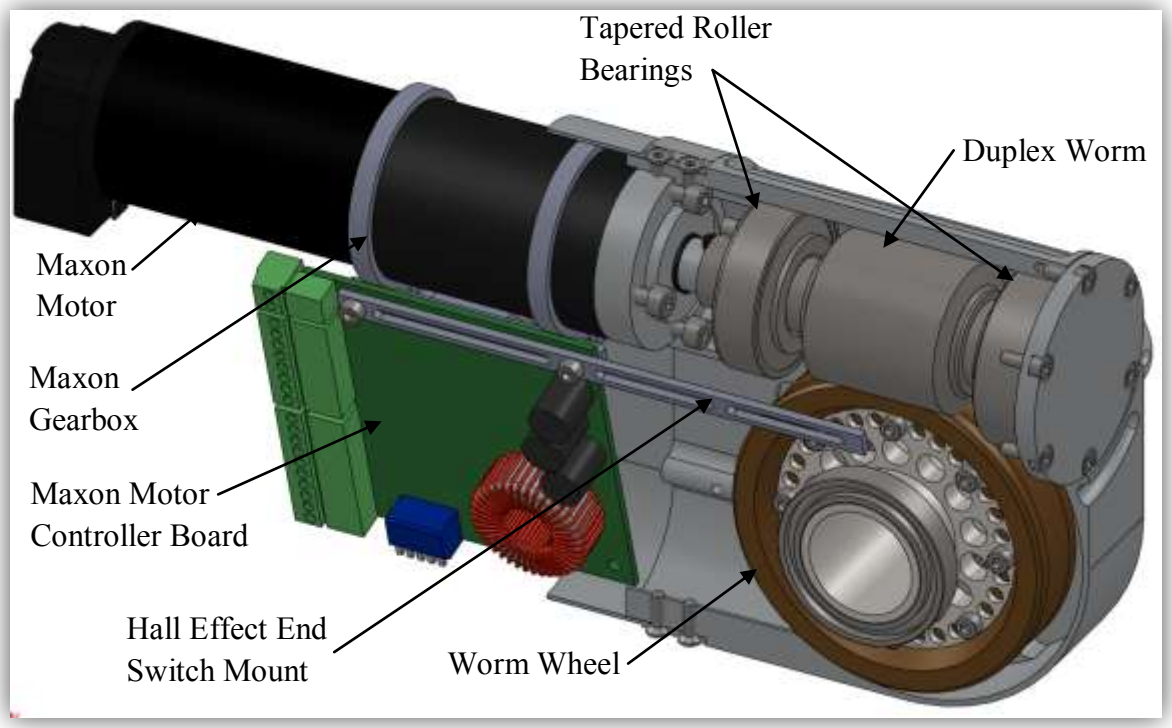

Figure IV: Cutaway of Gearbox Housing showing the Internal Components

To assist in lifting the arm and its payload at large reaches, a gravity compensating torsion spring was designed and fitted into the shoulder joint of the arm. It can be seen in Figure V below and provides the shoulder joint with an additional 40Nm of torque.

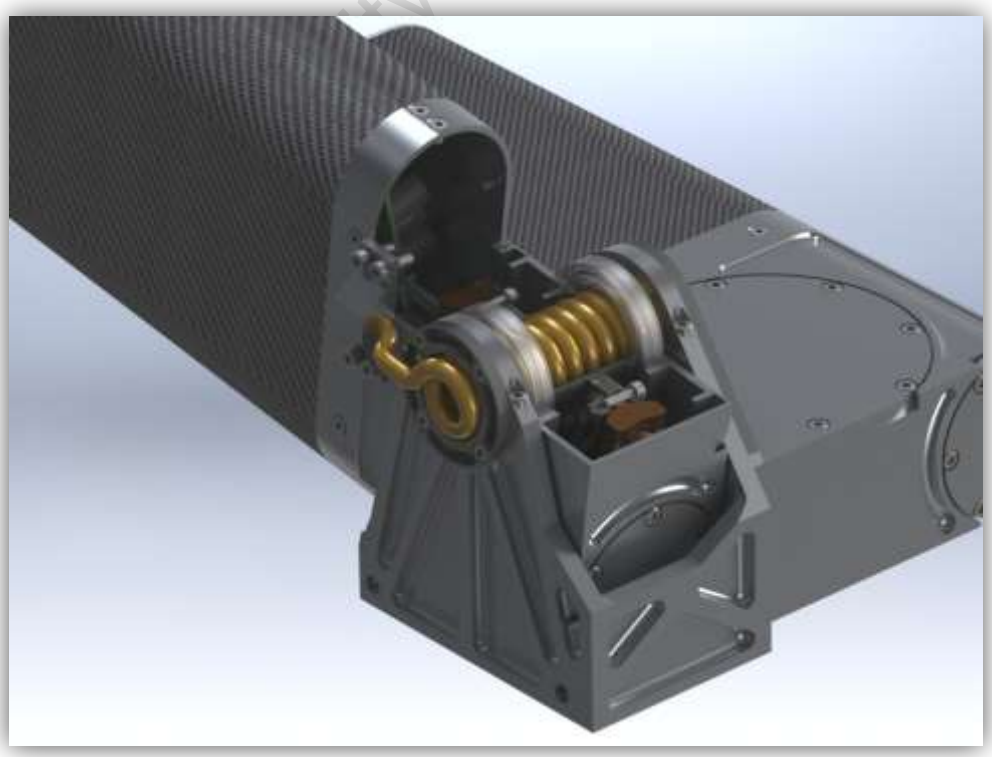

Figure V: Render of Bottom of Arm with Cutaway showing Torsion Spring

It was concluded that the arm performed well overall, exhibiting a good strength to speed compromise. It exceeded all the reach and lifting requirements while only slightly underperforming in joint rotation speed; achieving 17°/s on most joints. It was heavier than specified by 25%, weighing 12.5kg, but this does not adversely affect its performance, as it still manages to lift more than required.

The final elbow of the arm utilises hypoid gears that proved to have excellent strength to weight and strength to size characteristics, as well as being capable of extremely high gear reduction ratios. It is therefore recommended that on future generations hypoid gearboxes be used throughout the arm. It will result in a lighter and more compact arm.

Table of Contents

List of Figures

List of Tables

Glossary of Terms

CAD	Computer Aided Design
Duplex Worm	A worm gear that has an increasing tooth thickness along its axis. That is; its leading and trailing faces are cut with different pitches.
GUI	Graphic User Interface
Home	Default position or orientation of a joint or arm
RARL	Robotics and Agents Research Laboratory
USRR	Urban Search and Rescue Robot
UCT	University of Cape Town

1 Introduction

1.1 Birth of the Urban Search and Rescue Robot

Many true stories exist of people who were pulled out from earthquake wreckage alive, several days after the earthquake. Unfortunately there are also stories of those who were not reached in time. They were either not found or were just inaccessible. Many of the situations are dangerous and the actual rescuer may lose his life trying to find or help trapped survivors. This created a need for a more „disposable' rescue worker, and as technology developed, a new breed of robot emerged to tackle the task; the Urban Search and Rescue Robot (USRR). Figure 1-1 below shows the iRobot Packbot which is an industrial solution that can be purchased.

Figure 1-1: Picture of iRobot PackBot 510 fitted with EOD Manipulator Arm Kit [1]

1.2 Need for a Manipulator on the USRR

USRR's are designed to go where a human or canine rescuer cannot, or should not, due to the danger of risking their lives. These robots started out as passive helpers, serving as

observation vehicles which were designed to find and report survivors, so rescuers would know where to dig.

In order to move from a passive to a more active role, where the USRR can help the survivor by giving him/her water, food, two-way radios, etc, the USRR will need to be fitted with a *manipulator arm*. This basically consists of a movable arm and an *end-effector* that can interact with objects.

If the camera and sensors are mounted on such a manipulator arm, an even better understanding of the environment can be gained as they will be able to look into previously unreachable areas. USRR's may grow to an even more active role, where they could carry the „jaws of life' for example and free survivors that are stuck. The future might even promise USRR's which can perform an entire medical operation on a victim that may be trapped underground. The requirements for such development are precise *control* and a high level of *dexterity*. The manipulator arm and end-effector should be as versatile as possible, much like the human arm and hand.

1.3 RoboCup and RoboCup Rescue

The *RoboCup* is a competition that started in 1997 which initially just involved the development of soccer playing robots, with the vision of fostering artificial intelligence and intelligent autonomous robots. Then in 2005, the *RoboCup Rescue* was introduced to the *RoboCup* with the hope that it will encourage and hasten the development of the USRR. This socially significant competition was brought about following the great „Kobe Earthquake', which claimed the lives of over 6500 people [2].

RoboCup Rescue is a sub-competition in which robots must move through a simulated disaster site, and identify survivors. It also includes mapping challenges and an autonomous section. The arena poses extremely challenging terrain such as step fields, ramps and stairs. It requires identification of certain signs, carbon dioxide emissions, movement, heat and human-like dolls and body parts.

Within the Rescue competition, is the *Blue Arena* which tests the reach and gripping capabilities of the USRR's manipulator. It is a relatively new arena; it was proposed in 2008, and only included in the scoring metric in 2009 [3]. It consists of three tiers: one at ground level, the next 0.5m high and the last 1m. Objects are placed on the shelves at distances of 0.3mm and 0.6m deep, as seen in Figure 1-2. The objects include 500ml full water bottles, handheld radios and 100x100x100mm blocks, which represent sensors or food packs. The objective is to place one of these items in each found victim box.

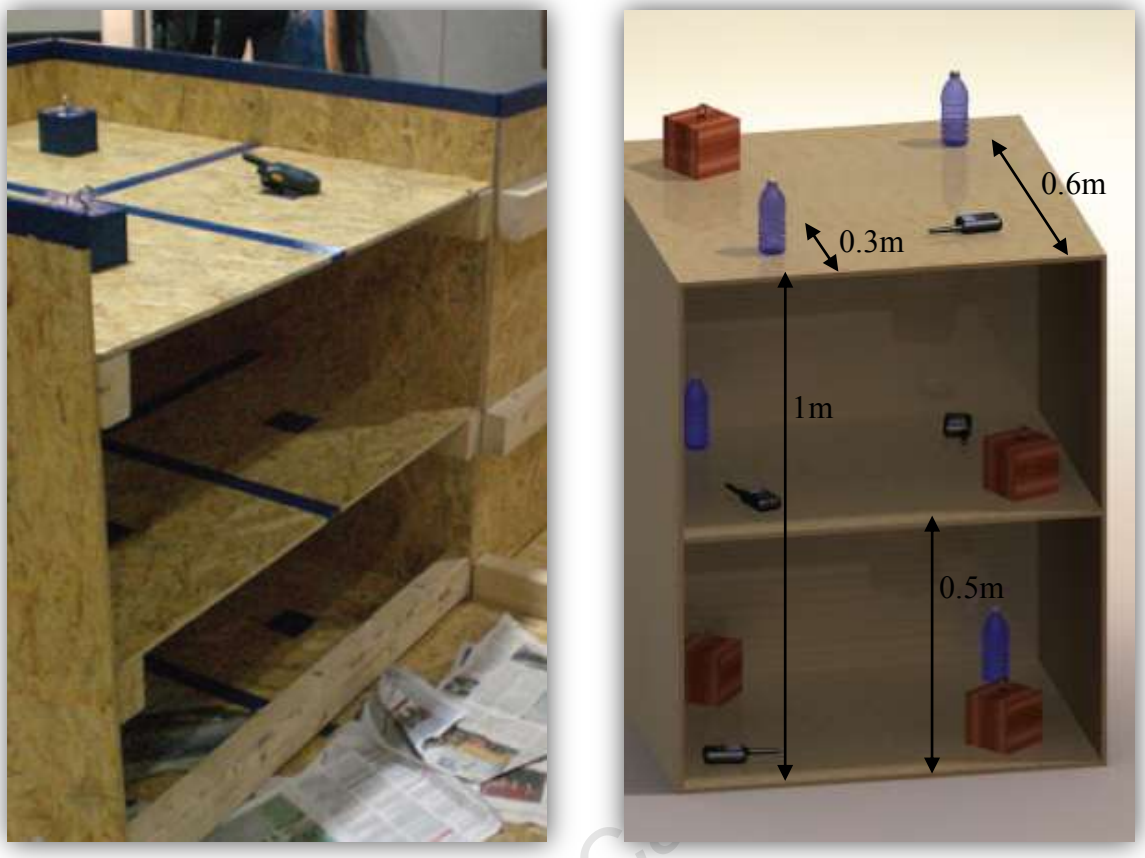

Figure 1-2: Pictures showing layout of Blue Arena [3]

1.4 Control of Manipulator

The manipulator will need to be remotely controlled by the operator, as he/she cannot see the robot in the arena. He/she will have to operate the arm based entirely on the feedback received. This will require the system to have positioning sensors within it. These positions/angles can be processed by the operator station and a three-dimensional representation of the manipulator will be available for the operator. This, in conjunction with the live video streamed from the cameras should be adequate for precision operation of the arm.

1.5 Scope of this Project

This project forms part of the „Ratel' USRR project being developed by the Robotics and Agents Research Laboratory (RARL) at UCT. Ratel is the Afrikaans name given to the honey badger, and has been adopted for the USRR as it is a tenacious creature that survives harsh terrain and never gives up.

This sub-project deals with the design, manufacturing and testing of the mechanical part of the manipulator arm that will be fitted to the Ratel. The arm will be mounted on the USRR base that was designed by Eugene Dreyer and it will carry the sensor pack designed by Cameron Sharp. The current end-effector being used has been designed as a final year

undergraduate project by Terry Scott, and the final end-effector is to be designed by Michael Rieger. This project will be highly integrated with all of these systems as electrical power and signals will be passed through from one to the other. Bradley Springer will be designing the control software and circuitry to control the manipulator arm.

The main objective of the project is to design and build a system that will be able to help in disaster type situations. To evaluate and test this, the sub-objective is win the RoboCup Rescue competition, and in particular, to win the *Best in Class Award* (Manipulator). However, extra functionality that is not specifically required by the competition is also included into the scope of the project. Some of these functions are opening doors with various handles, cutting rope and the ability to use screw-driver tools. All these functions will benefit in real life situations of Urban Search and Rescue.

While industrial solutions of USRRs fitted with manipulator arms exist, this project aims at designing a competitive arm for a significantly lower cost. It also aims to be more precise and to exhibit lower levels of undesired *backlash* and *shake*. This will result in a steadier video stream for the operator, and more precise movement of the end-effector.

1.6 Overview of Report

This report starts with a summary of the specifications of the *Manipulator Arm*. It lists both the desired and achieved specifications. It then briefly covers the conceptual stage of the design of the arm, after which it describes some of the calculations used in the design, including the MATLAB® model that was used to simulate the arm.

It then enters the detailed design phase of the project, and in this section, the final solution is expounded on in detail. This section is divided into subsections which cover each sub-assembly of the final design. The wiring, control and electronics design is then explained.

The testing and the discussion of results is then presented, which is finally followed by the conclusion and future recommendations.

2 List of Main Specifications

The manipulator arm system's desired and achieved specifications are presented in Table 2-1 below.

Table 2-1: List of Main Specifications

No.	D/W	Requirements	Desired	Achieved
1.	**Arm Performance Specifications**			
1.1.	D	Minimum Shelf Reach	1m High 0.65m Deep	1.25m High 0.68m Deep
1.2.	D	Minimum Lift at Full Reach	1kg	>2kg
1.3.	D	Ability to Support Sensor Pack	2kg	2kg
1.4.	D	Minimum Joint Rotation Speed	20°/s	~17°/s
1.5.	D	Maximum Joint Backlash	0.2°	0.5°
1.6.	D	Internal Wiring	Yes	Yes
2.	**End Effector Performance Specifications**			
2.1.	D	Minimum Gripper Bite Size	142mm	113.3mm
2.2.	D	Continuous Wrist Rotation	Yes	Yes
2.3.	D	Cutting Ability	Yes	Yes
2.4.	D	Ability to Use Tools	Yes	No
3.	**Physical Specifications**			
3.1.	D	Fit through *Fireman's Triangle* of 24"	Yes	Yes
3.2.	D	Ability to Fit into Standard Pelican Type Box	Yes	Yes
3.3.	D	Maximum Weight Excluding Sensor Pack	10kg	12.5kg
4.	**Control System Specifications**			
4.1.	D	Master-Slave Controller	Yes	Yes
4.2.	D	Inverse Kinematic Control	Yes	Not Tested
5.	**Power Specifications**			
5.1.	D	Operate Off 36V Supply Batteries	Yes	Yes
5.2.	D	Maximum Current Draw	10A	2.7A per motor
6.	**Budget Specifications**			
6.1.	D	Maximum Cost	R70'000	R75'000

The full justification of these specifications can be found in Appendix B. The testing of these specifications, with the detailed results can be found in the Testing and Results section of this report.

3 Concept Design

3.1 Introduction and Overview of the Design Process

The project started with ascertaining the required specifications of a USRR manipulator arm, as listed in the previous chapter. Using these specifications, initial layout concepts were developed and possible solutions were chosen, and then narrowed down to the best solution. This was then laid out in a 3D CAD model. The initial driving specifications were related to the arm's size and reach requirements.

Once these models were developed, the first iteration of calculations could be carried out, and the process of selecting suitable motors and gearboxes was started. The driving specifications in this stage of the design process were those relating to lifting capabilities and weight restrictions. Computer models of the arm were developed in MATLAB® to aid in these iterations. After the final iteration was completed and motors and gear combinations were selected, the project moved out of the concept design phase and into the detailed design phase. This chapter looks at the concept design phase and expands on some of the concepts developed as well as the mathematics behind the calculations. The concepts are looked at in greater detail in Appendix C (Concept Design).

3.2 Concepts of Joint Layouts

Two general layout concepts of the arm were selected as possible solutions. Both could achieve the reach required and both concepts required 6 functions (motors). Figure 3-1 shows these two schematics.

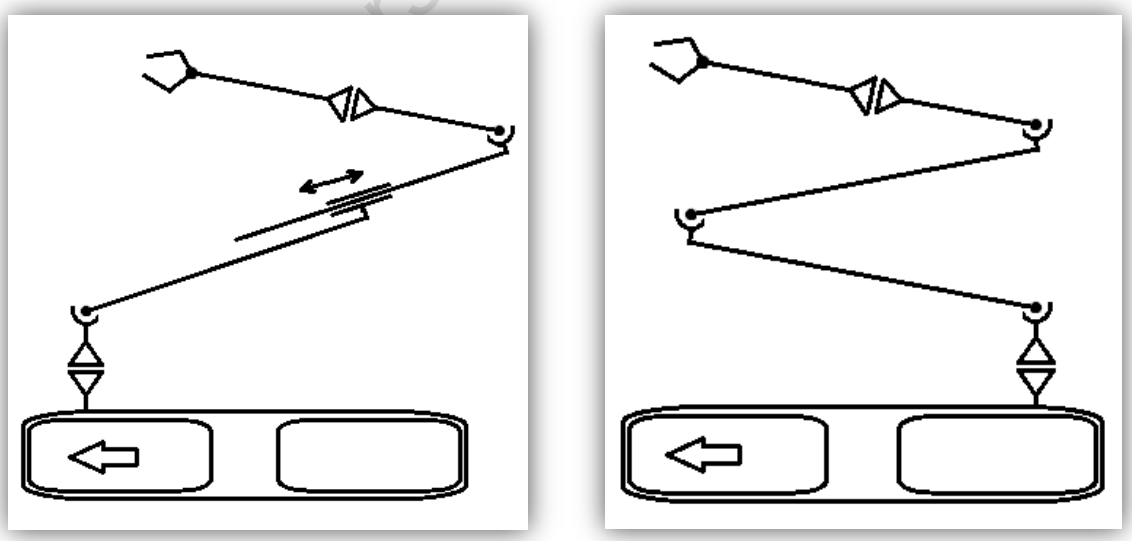

Figure 3-1: Concepts A (left) and B (right) of Manipulator Arm Layouts

There is only a slight difference in functionality between the two concepts. Concept A is slightly easier to operate as the last arm segment does not change angle whilst it is being

extended. For Concept B to have this functionality, advanced control is required. Concept B was chosen as it is less complicated to design, manufacture and maintain.

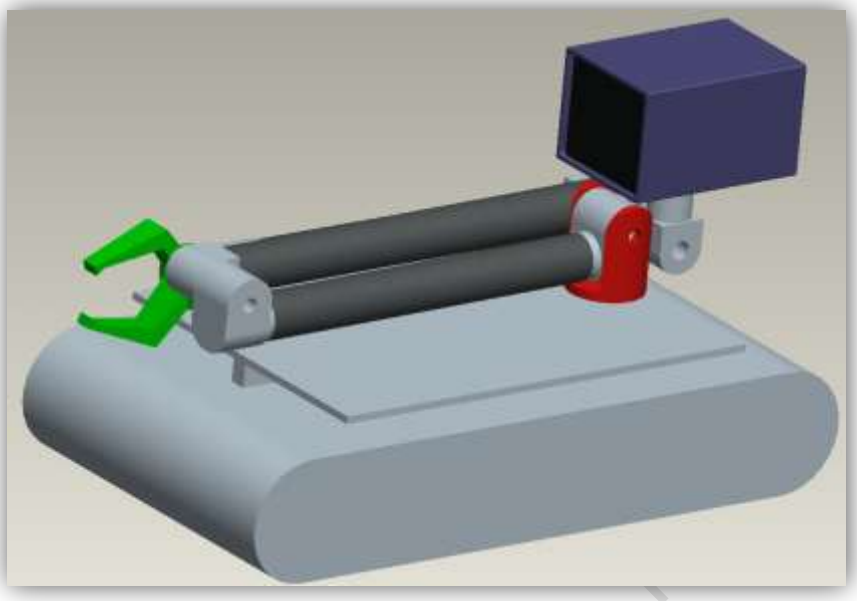

Figure 3-2: 3D View showing Conceptual Layout of Arm and Sensor Pack

These lay-outs were developed into a three dimensional concept as shown in Figure 3-2. The *reach* specification as well as the requirement for the robot to fit through the *fireman's triangle,* were the main driving specifications in the initial stages. Initial motor and gearbox options were chosen to start the iteration process, and a more detailed concept placing the motors in the arm was developed. This more advanced concept can be seen below.

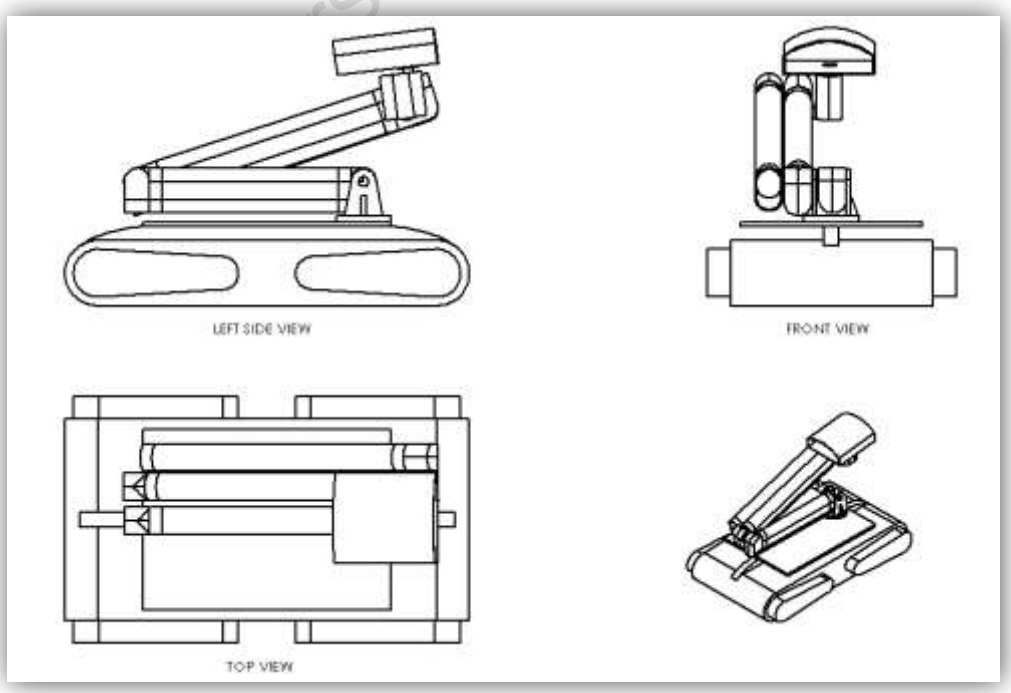

Figure 3-3: Front, Left, Top and Isometric Views of Arm Concept

This was then used to run initial design calculations and to choose a more accurate motor-gearbox combination, after which the next iteration would be carried out. The *lifting capability* specification together with the weight restrictions were the driving specifications in this phase.

3.3 Mathematical Model of System

A mathematical model was developed to assimilate the arm and aid in the iterative process. The model required a substantial amount of three dimensional geometry and mathematics. MATLAB®, a powerful math computing program, was used to create the model. The soft files of the program and its sub-programs can be found on the accompanying DVD.

3.3.1 Position Calculation

The program that was developed takes in the angles of the various joints and plots the arm using these angles and known constants, such as arm lengths, etc. It utilises *Forward Kinematics*, working from the base of the arm up to the tips of the gripper.

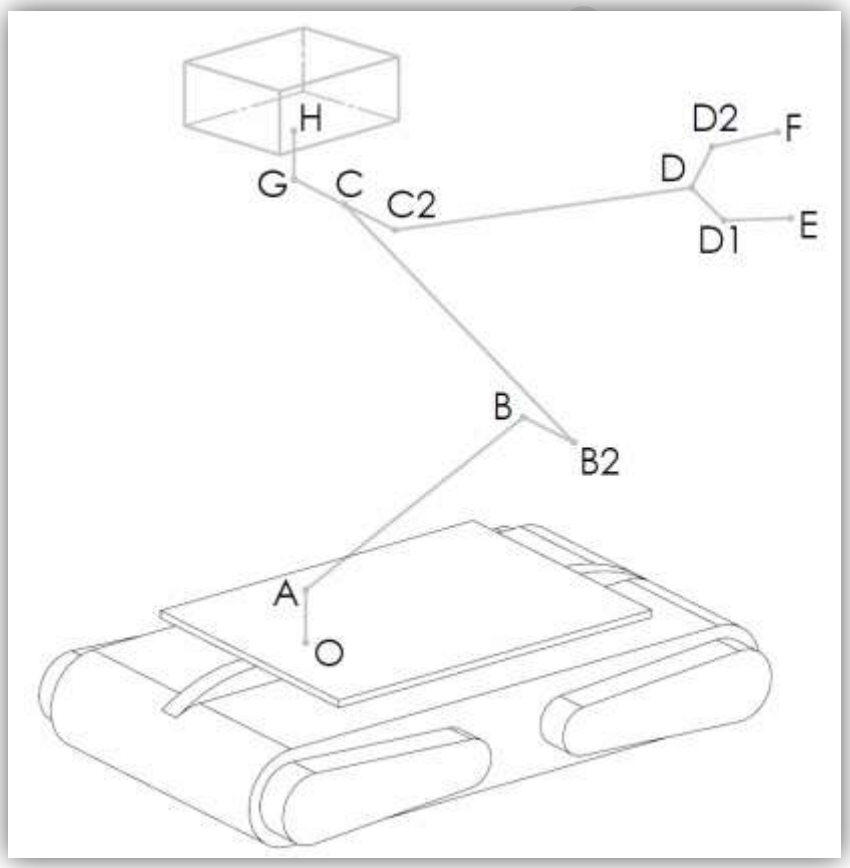

Figure 3-4: Sketch showing Allocation of Points in MATLAB® Model

The allocation of points in this model can be seen in Figure 3-4 above. The first position A is known, relative to the origin, which in this case is the arm's attachment point to the crawler base. From this point, the next point B, along the *series type* arm can be calculated as the arm

length and the angle at A is known. Once this point is known, the next point can be calculated from this point, and so on.

The end point of an arm section is calculated by first determining the *unit direction vector* of the section, and then multiplying it by its length and adding the resultant vector to the start point. An example of this calculation is shown below. Figure 3-5 shows the allocated names of the various angles of the arm.

Calculation of *unit direction vector* of Section AB:

$$nAB = [\cos(Rot_A) * \cos(Ang_A), \sin(Rot_A) * \cos(Ang_A), \sin(Ang_A)]$$

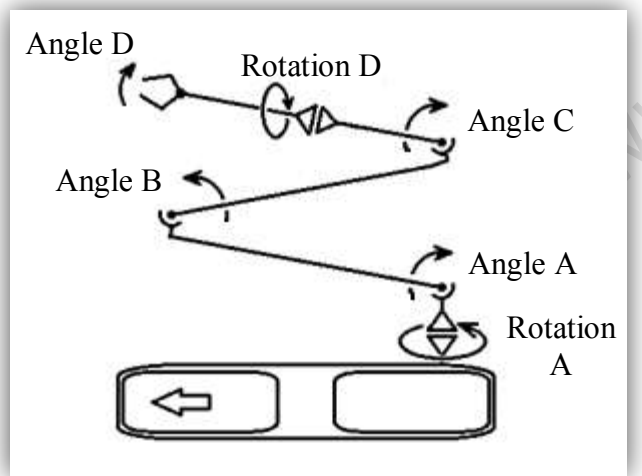

Figure 3-5: Schematic showing Allocation of Joints in MATLAB® Model

Calculation of position B (vector OB):

$$B = A + length_{AB} * nAB$$

This same process of calculation is then carried out to determine position C and so forth. The *unit direction vectors* of each arm section are used again when positioning the centres of mass along each section.

Calculation of centre of mass of section AB:

$$CoM_{AB} = A + length_{ACoM_{AB}} * nAB$$

The USRR will not always be traversing perfectly level terrain. Often it will drive on steep slopes and the loading on the arm's joints will change relative to the angle of the slope. It was necessary then to include into the model, the roll, pitch and yaw of the base of the robot; *roll* being a rotation about the *x-axis*, *pitch* being a rotation about the *y-axis* and *yaw* being a rotation about the *z-axis*. Rotation matrices for each of these three were developed and are listed below.

$$Rotation\ Matrix_{Roll} = \begin{pmatrix} 1 & 0 & 0 \\ 0 & \cos(Roll) & -\sin(Roll) \\ 0 & \sin(Roll) & \cos(Roll) \end{pmatrix}$$

$$Rotation\ Matrix_{Pitch} = \begin{pmatrix} \cos(Pitch) & 0 & \sin(Pitch) \\ 0 & 1 & 0 \\ -\sin(Pitch) & 0 & \cos(Pitch) \end{pmatrix}$$

$$Rotation\ Matrix_{Yaw} = \begin{pmatrix} \cos(Yaw) & -\sin(Yaw) & 0 \\ \sin(Yaw) & \cos(Yaw) & 0 \\ 0 & 0 & 1 \end{pmatrix}$$

Each point of the arm is then updated by multiplying it through by each of the rotation matrices. An example of this operation on point A is shown below. After all of the points are updated, the final orientation of the arm can be plotted.

$$A = \left(\left(\left(A * Rotation\ Matrix_{Roll}\right) * Rotation\ Matrix_{Pitch}\right) * Rotation\ Matrix_{Yaw}\right)$$

3.3.2 Graphic User Interface

This plot is integrated into a *graphic user interface* (GUI) together with slider bars that manipulate the joint angles. Figure 3-6 shows a screenshot of the final GUI. Sliders are also integrated to manipulate the roll, pitch and yaw as well as the Pan and Tilt of the sensor payload. The tags on each of the sliders in the GUI are listed in Figure 3-5.

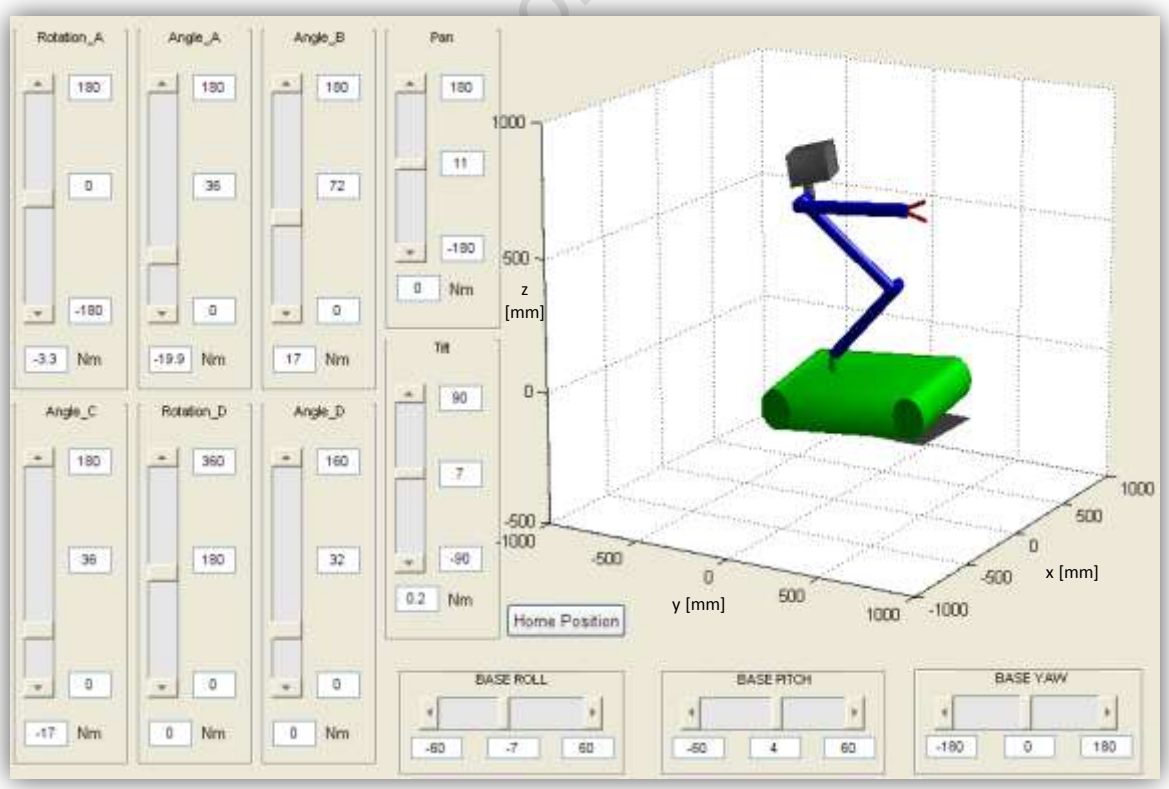

Figure 3-6: Screenshot of Final GUI for Manipulator Arm

3.3.3 Torque Calculations

The torque calculations are done in a separate sub-program that is called on by the main program when needed.

Figure 3-7 shows a simplified schematic of an arm section. Elements $n1$, $n2$ and $n3$ are *unit normal vectors*. That is; they are perpendicular to each other. The vector $n2$ is known as it was calculated as demonstrated in the previous section. Vector $n1$ can be calculated by determining the plane that it is normal to. In this arm, sections AB, BC, and CD rotate in parallel planes. This means they share a common *unit normal vector*; $n1$ in this example. This plane is determined by the angle of *Rotation A*. The vector $n1$ can therefore be calculated as follows:

$$n1 = (sin(Rotation_A), -cos(Rotation_A), 0)$$

Note that this equation assumes that the base is level, and so the unit normal vectors $n1$ and $n2$ must be multiplied through by the roll, pitch and yaw rotation matrices. Vector $n3$ can then be calculated using the *cross product* as follows:

$$n3 = n1 \boldsymbol{x} n2$$

The torque, *T,* required to lift the weight at the end of the section can then be calculated by multiplying the weight, *W,* by the length of the arm, *d* in this example. However this is only true when the arm is lying horizontally. The required torque decreases as the arm is raised, or tilted to the side (which only occurs when the base rolls or pitches), as the horizontal distance decreases. The vertical component of $n3$ is therefore used in the equation as follows to decrease the torque as the arm is lifted or tilted.

$$T = n3(z).m.g.d$$

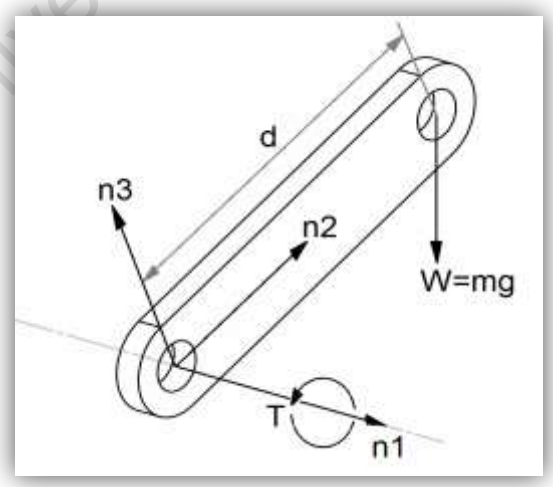

Figure 3-7: Diagram showing Arm Member, Forces, Torques and Unit Normal Vectors

These torques are shown in the GUI, and are updated in real time, as the sliders are moved. Using these known torque requirements, the next iteration of motor and gearbox combinations was selected and the model was updated. Once the chosen motors and

gearboxes satisfied the weight limitations and were strong enough to meet the lifting and joint speed requirements, more detailed gearbox housing concepts and mounting concepts could be developed.

3.4 Mechanical Design Concepts

Several gearbox concepts were looked at, and designed. Figure 3-8 is one such preliminary concept of the worm gearbox layout. It incorporates a slip ring though the centre of the worm wheel to allow for continuous rotation of the joint, and to allow the wiring to remain internal. It was determined from this concept that the inside of the worm wheel chosen was to be of diameter greater than 20mm (16mm for the slip ring and 2mm each side for the steel shaft).

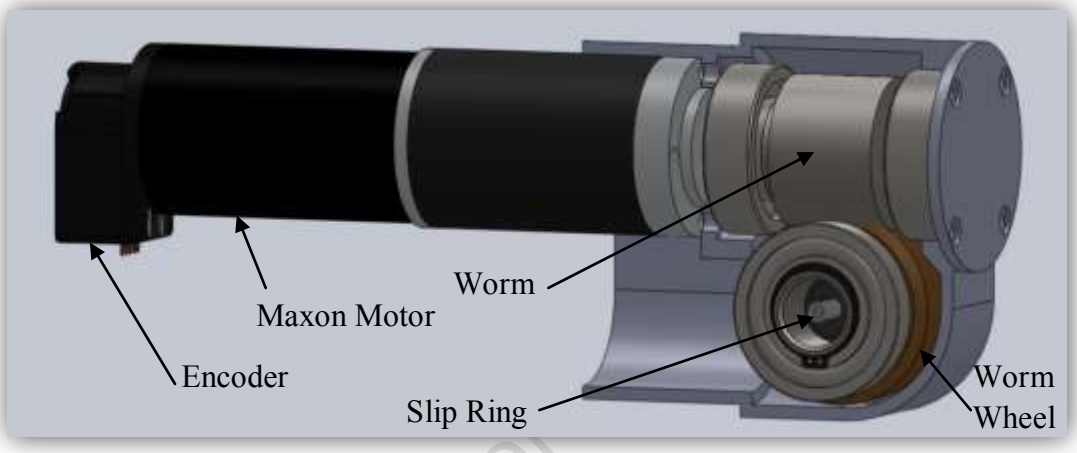

Figure 3-8: Worm Gear Housing Detailed Concept

To satisfy the *low-backlash* specification, several low backlash designs were developed as commercially available options were expensive. One of the concepts developed was this *split-worm wheel* design shown in Figure 3-9.

This concept uses a *torque bar* to force open the teeth of each split *worm wheel* half, in order to completely *fill* the gap in the *worm* and thereby remove all backlash. The shortfall of this concept is that only half of the worm (the driving half) is carrying the load. This means that gears twice as strong need to be selected. Another problem is that because of the clamping force provided by the *torque bar, the* friction is greatly increased, and so the power and torque requirements are much greater. The wear rate will also greatly increase as the driving surface area is halved.

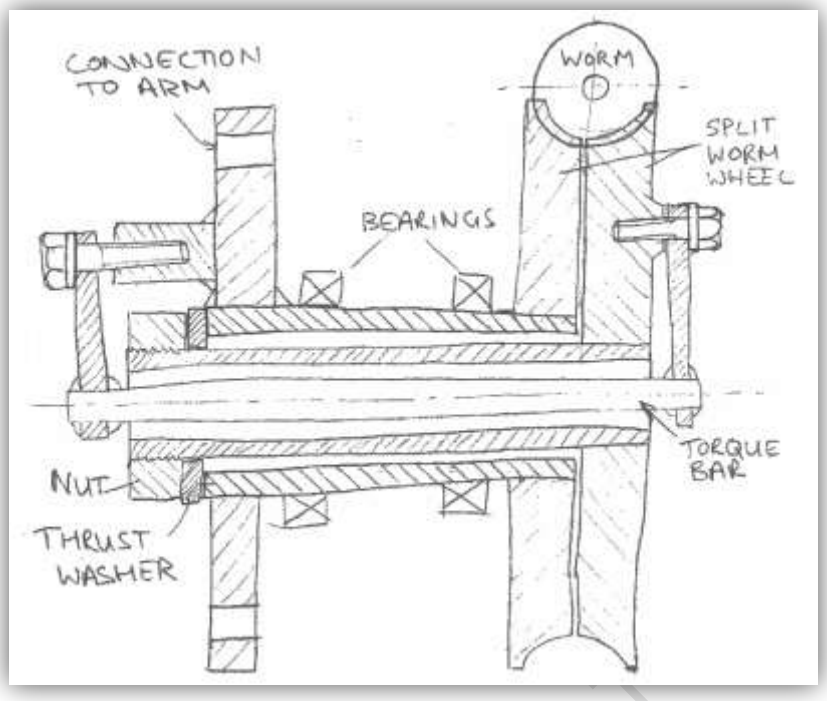

Figure 3-9: Cross Sectional Sketch of Split Worm Wheel Zero Backlash Design

Other similar backlash reducing concepts were developed, but these designs were not chosen however due to their drawbacks and complexities. They are listed in Appendix C (Concept Design).

3.5 Summary

This chapter looked at the concept design phase of the project. It covered the initial layout concepts, and then went on to discuss the mathematical model that was developed to aid in the iterative design process. The GUI that was developed was discussed. These all assisted in selecting suitable motor and gear combinations.

Once suitable combinations were chosen, and their availability ensured, mechanical concepts were developed to ensure their manufacturability and assembly. The project then moved out of the conceptual stage into the detailed design phase. The following chapter will expound on the final product and its mechanical design elements.

4 Mechanical Detailed Design

4.1 Introduction

This section of the report looks at the final design and expands on each of the subsections of the manipulator arm. It commences with the overall system, and the transportation case used for the Ratel. It also discusses the Ratel's ability to fit through the *Fireman's Triangle*, complete with manipulator arm and sensor payload.

The detailed construction and design of the subsections is then looked at, starting with the composite tubes used in the structure of the arm. The tubes use a collapsible mandrel for ease of manufacture, and then have aluminum inserts fitted to each end to ensure a precise mate with the gearbox housings.

The turntable section is the first of the actuators to be looked at, and its gearbox, which is common to the first three arm actuators, is examined in detail under this section. This gearbox incorporates adjustable backlash *duplex* worm gears used to reduce the backlash within the arm.

The remaining subsections of the arm are looked at and various novel features such as the gravity compensating torsion spring are expounded on in detail. The end effectors that have been designed to fit into the manipulator arm are also reviewed. The section ends off by describing the internal wiring of the manipulator arm, including its slip rings which allow for continuous rotation on several joints. The drawings of the assemblies can be found in Appendix E, *Drawings*.

4.2 The Complete System

The render in Figure 4-1 shows the Ratel complete with the manipulator arm, gripper and sensor payload. This is the final design and was produced in SolidWorks®. Figure 4-2 shows the exterior dimensions of the Ratel. The photographs shown on pages 17 through 19 show the completed manipulator arm in various positions. In Figure 4-5 and Figure 4-6, the sensor payload's cover is removed. In all of the photographs, the arm is mounted on a test plate that is clamped to a table. As of writing this document, the manipulator arm has not been assembled together with the crawler base.

All of the entities, (crawler base, manipulator arm, gripper and sensor payload) are standalone modular systems, which draw only power and communication from each other. This means they can quite easily be used on other platforms, or changed out with future revisions of their design.

The manipulator arm system can be divided into subsections. These subsections will be looked at individually in detail in the following sub-chapters. The sections are Turntable, Bottom, Mid, Top and Pan Sections and are shown in Figure 4-1.

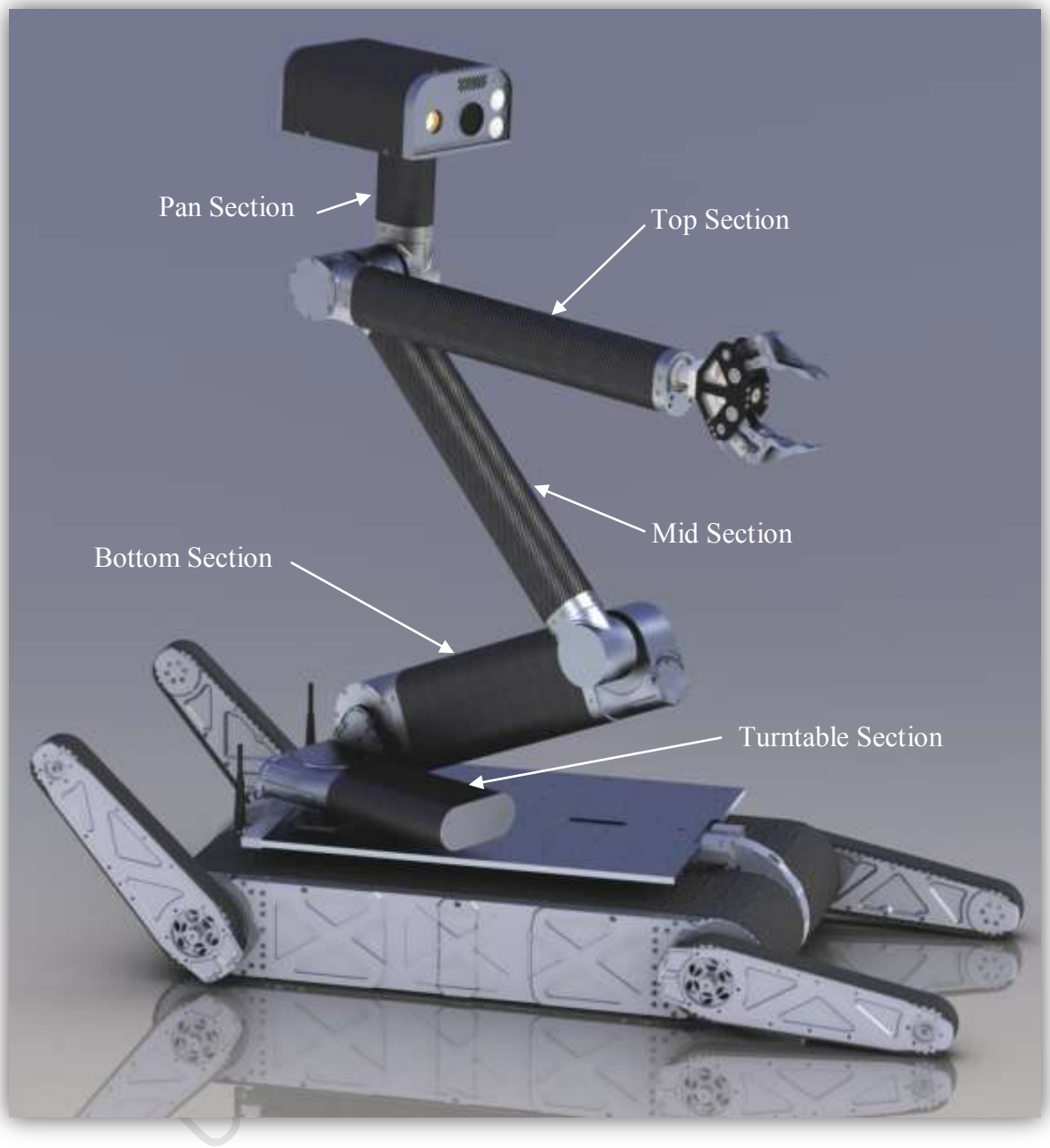

Figure 4-1: Rendering of Ratel Complete with Manipulator Arm and Sensor Payload

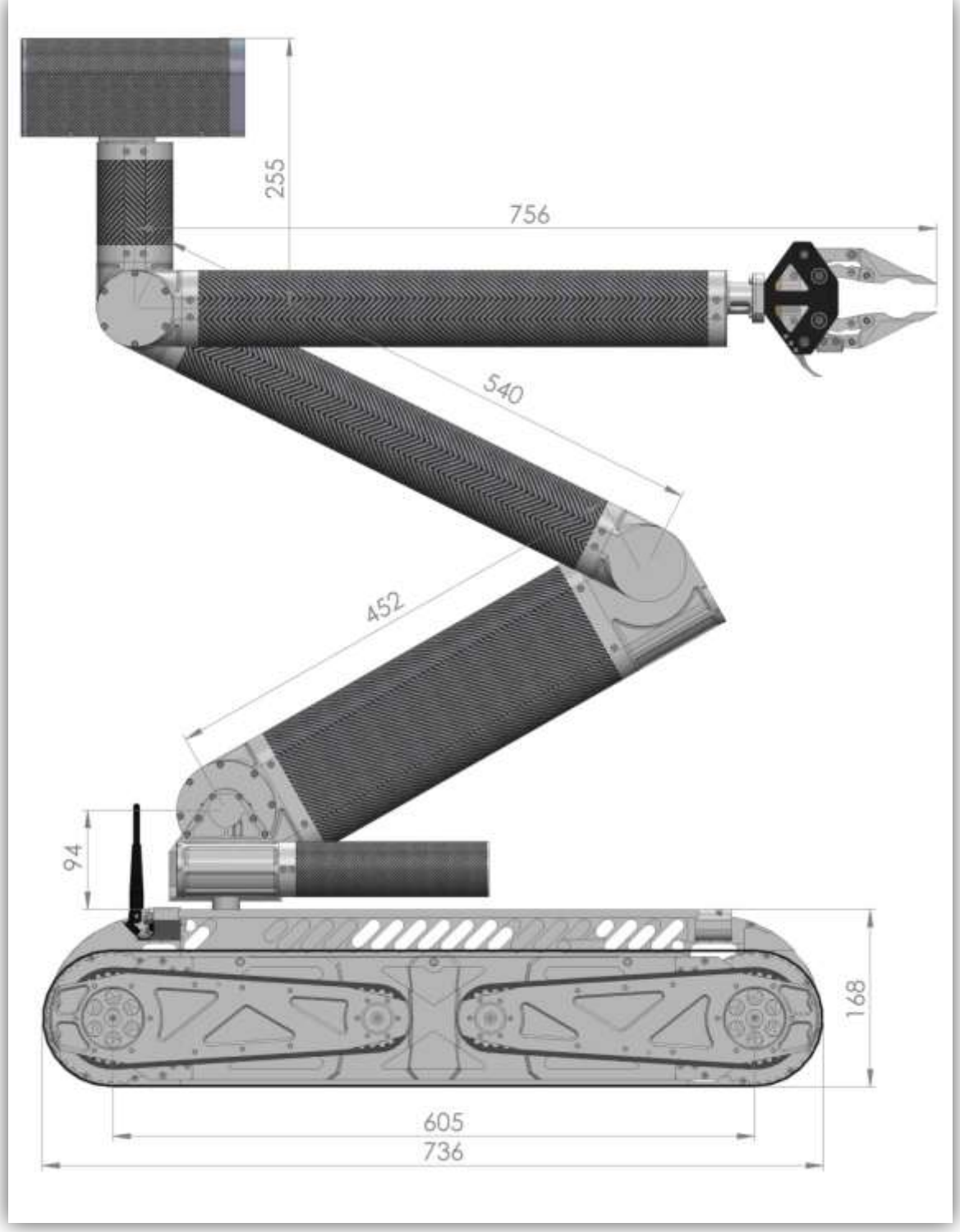

Figure 4-2: Side View of Ratel with Dimensions

Figure 4-3: Photograph of Manipulator Arm complete with Sensor Payload and Gripper

Figure 4-4: Photograph of Manipulator Arm in Full Horizontal Reach

Figure 4-5: Left side of Manipulator Arm (Sensor Payload Cover Removed)

Figure 4-6: Manipulator Arm in Home Position (Sensor Payload Cover Removed)

Figure 4-7: Photograph of Manipulator Arm Reaching Up at 45°

4.2.1 Transportation Design

The Ratel will need to be easily and safely transported. It was therefore necessary for it to fit in a standard sized Pelican Case. The Pelican 1780 was chosen; it is hardy and easy to move, as it is a wheeled case. The case had not been delivered by the time of writing this document.

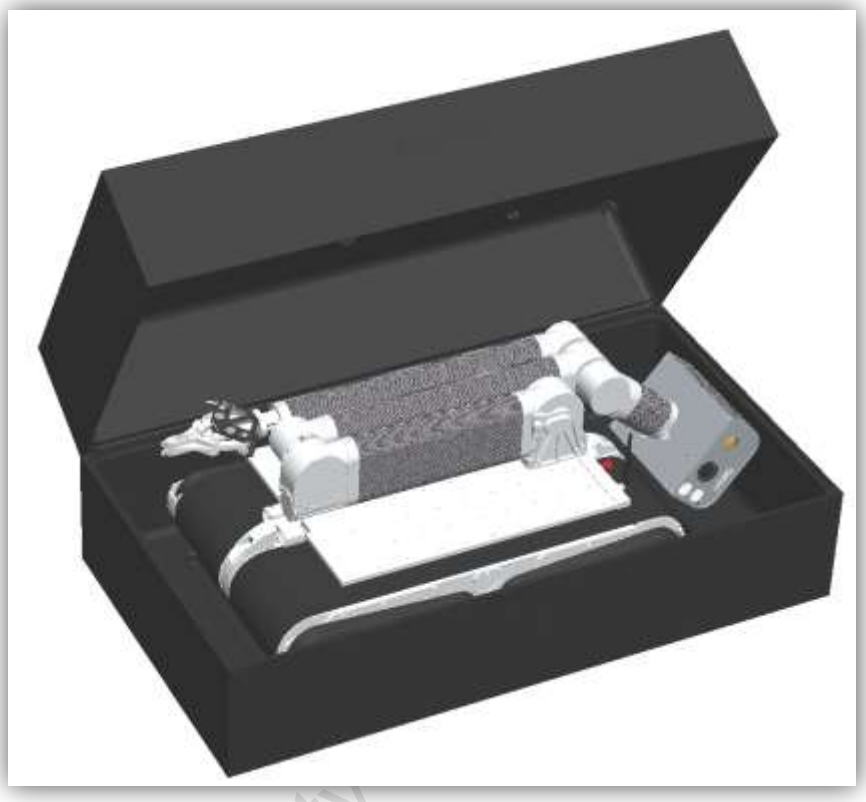

Figure 4-8: Solidworks Screenshot of Ratel in 1780 Pelican Transport Case

Figure 4-8 shows the Ratel in the Pelican 1780 Transport Case. For the most compact position, the sensor payload needs to be folded back and rotated 90 degrees to the side. This results in a comfortable fit in the Pelican case, as can also be seen in the cutaway in Figure 4-9. Hard foam will be cut to fit the robot snugly, and prevent any movement within the case.

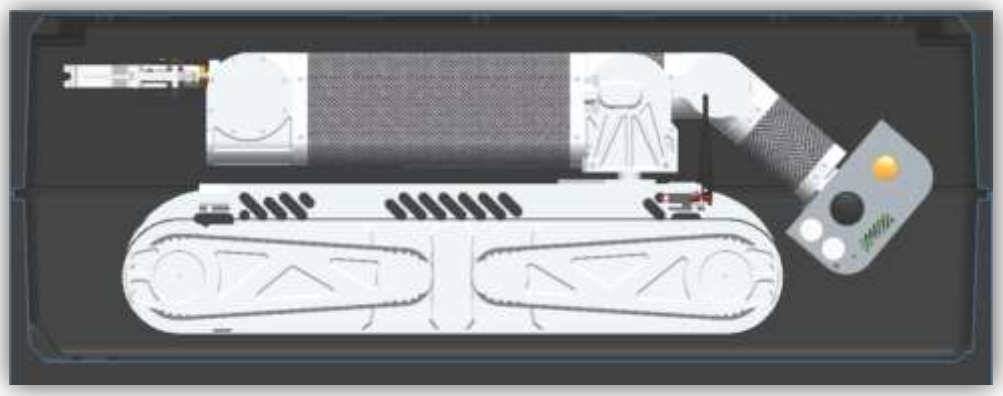

Figure 4-9: Side View Cutaway showing Ratel in 1780 Pelican Transport Case

4.2.2 Entry Triangle

As the robot will be used for search and rescue in complicated terrains such as a collapsed building, it needs to navigate though small openings. A 24" equilateral triangle is often cut into building to allow rescue workers to enter. This is also known as a *Fireman's Triangle.* The entire robot will have to enter through this triangle. The Ratel has been designed to fit through the 24" equilateral entry triangle.

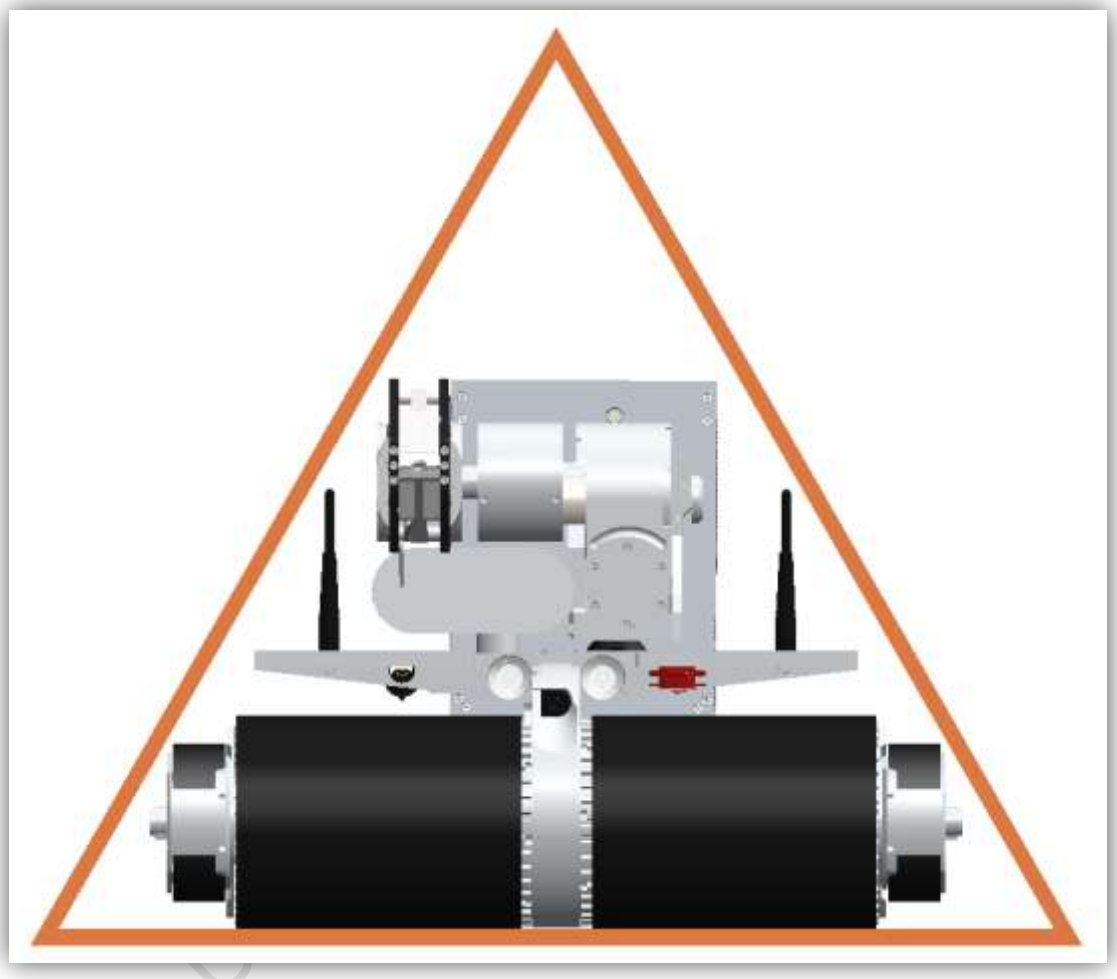

Figure 4-10: Front View of Ratel in Entry Triangle

However, to do this, it needs to fold the sensor payload back, as seen in Figure 4-10 and Figure 4-11. While driving forward or backward through the triangle, the front and rear drive cameras are used. The main camera only needs to be folded back at the last moment, and so it can help with negotiating the front flippers through.

Figure 4-11: Ratel in Entry Triangle with Sensor Payload Folded Back

If the gap is particularly tricky, the arm can fold out backwards, and lower the sensor head so that it obtains a third person perspective on the main body, to help navigate very tight gaps. This can be seen in Figure 4-12 below.

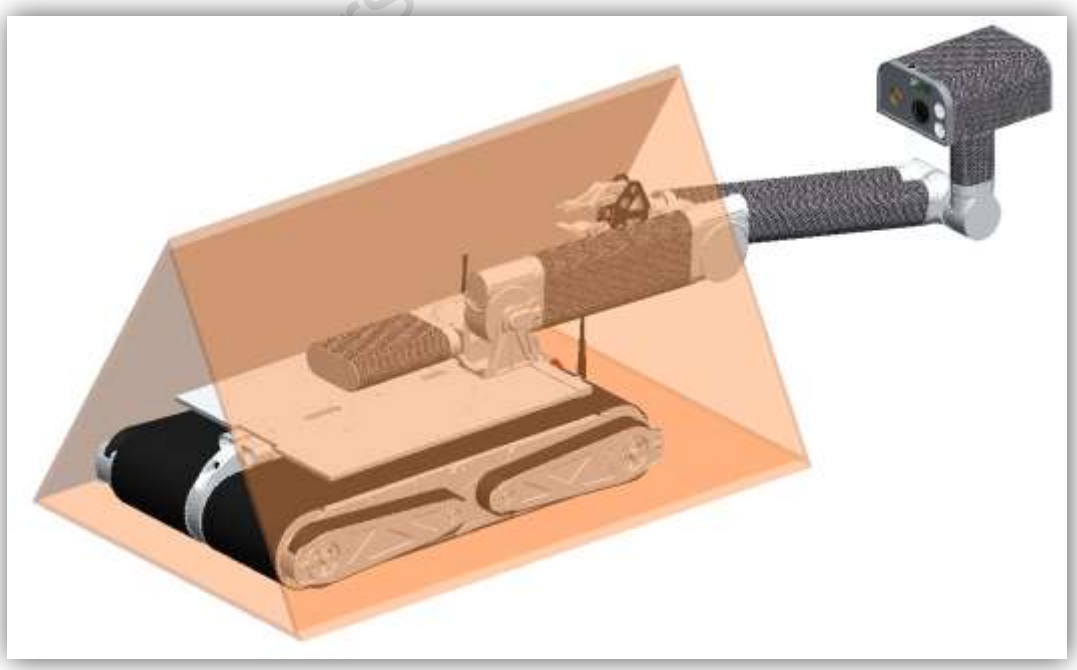

Figure 4-12: Ratel Navigating Entry Triangle with Arm Extended in Third Person View

4.3 Carbon Fibre Composite Tubes

The design of the arm necessitated custom carbon fibre composite tubes. The tubes were used as structural links; linking one joint to the next. The manufacturing of the tubes was outsourced, and the company, GRP Tubing, kindly offered to produce them for free as it was a small order, and providing we machined the internal mandrels in-house.

In order to avoid the requirement for tapered tubes, a collapsible mandrel was designed. This can be seen in the diagram below. To remove the mandrel after the tube had cured, the *Blue* centre part is first knocked out. The *Green* parts are then clamped together, into the middle, into the space created by the *Blue* part, and can then be knocked out. Finally the *Red* semi-cylinders are brought into the middle and removed.

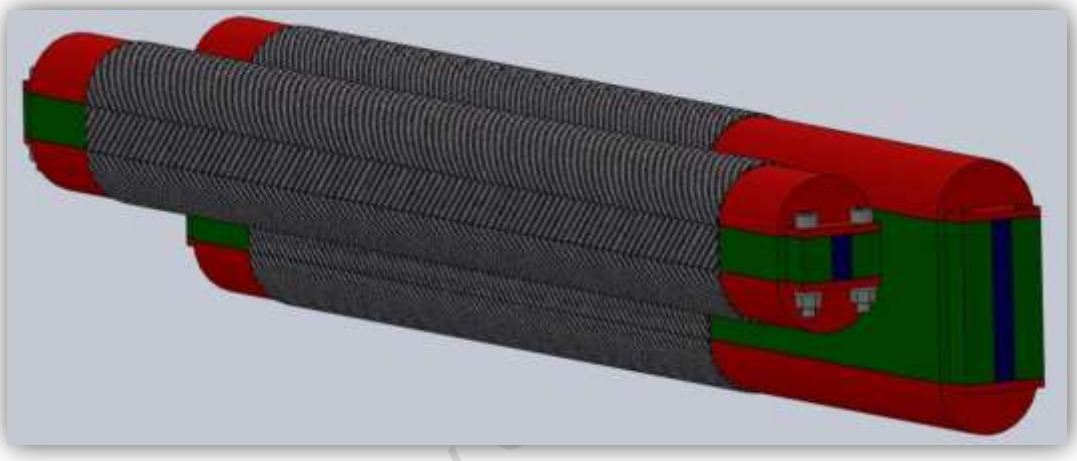

Figure 4-13: Figure Showing Mandrel Design for Small and Big Section Tubes

The advantage of this design is that the two semi-circular parts shown in red can be used for both the small section and large section tubes, reducing the mandrel costs and reducing machining time. To ensure a good fit with the gearbox housings, it was decided to have aluminium interfaces inserted into the tube ends. These could be machined to an adequate fit. A cut-away of the interface in the tube is shown in Figure 4-14. The interfaces were anodised to increase their hardness, and then bonded into the tubes using resin and cured in an oven.

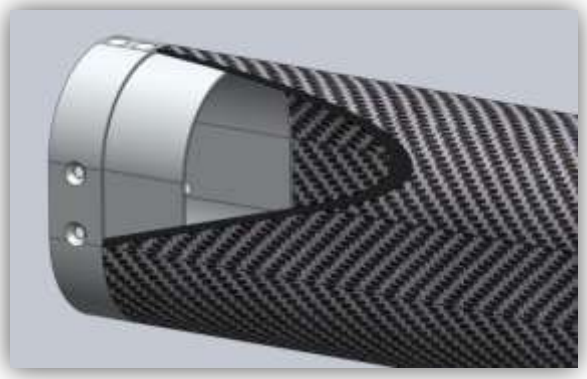

Figure 4-14: Figure Showing Cut-away of Carbon Tube with Aluminium Insert

The arm consists of two large section tubes and three small section tubes. Two of the finished tubes can be seen below, along with the mandrels. Their finish is poor, and they were manufactured with a greater wall thickness than specified, increasing their stiffness (strength) but also increasing their weight.

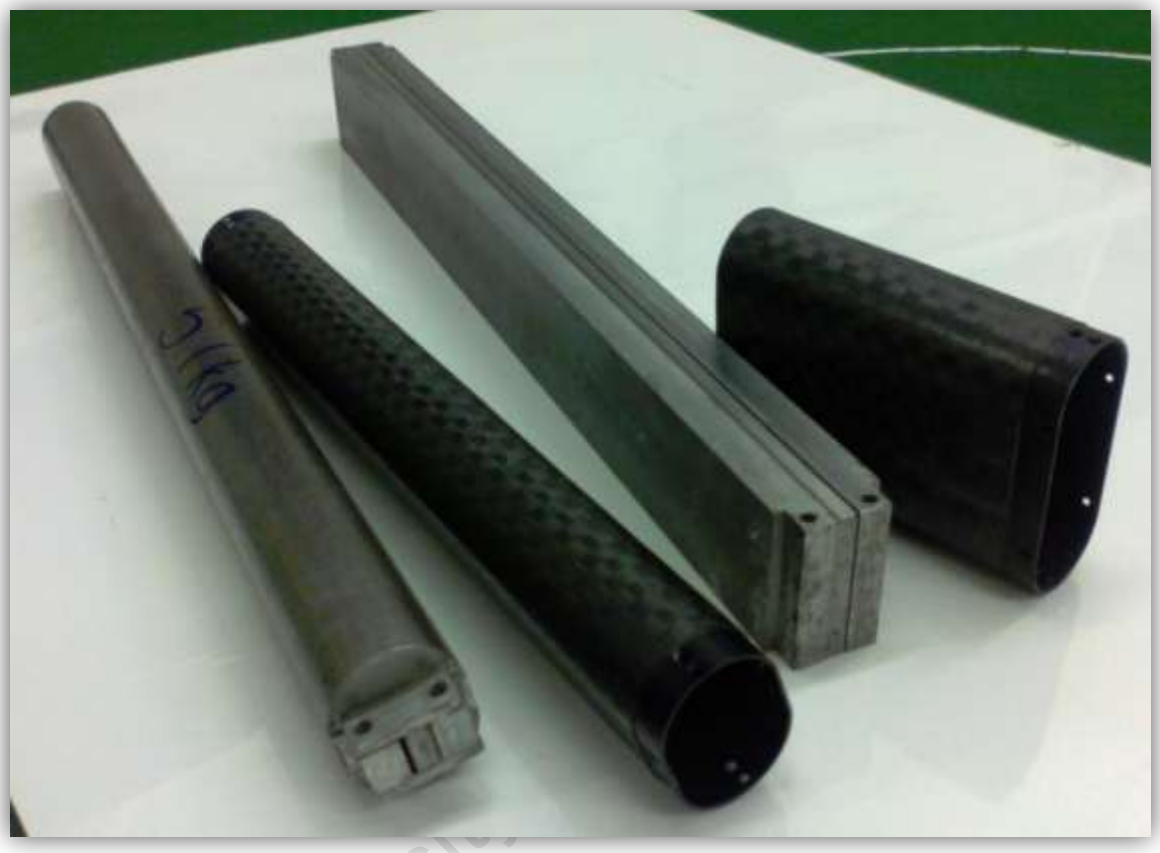

Figure 4-15: Small and Large Section Carbon Fibre Composite Tubes with Mandrels

The poor surface quality is believed to be partly due to the carbon sheets used, as the carbon weave was quite broad. It is believed to be also partly due to the method of wrapping used. Once the carbon sheet and resin was wrapped around the mandrel, a plastic sheet was then put over, and finally tightly wrapped with broad tape to squeeze it onto the mandrel.

New tubes are to be manufactured in the near future, using pre-woven carbon *socks*, which will improve the surface finish and aesthetic appeal of the tubes. A vacuum will be used to squeeze the carbon onto the mandrels.

4.4 Turntable Section

Figure 4-16: Turntable Section of Manipulator Arm

The turntable section houses the turntable motor and worm gear set, and provides rotation to the entire arm. It can be seen as the most significant degree of freedom, along with the shoulder joint, as one degree of movement of these joints will result in the greatest movement of the arm tip.

The manipulator arm's turntable has continuous rotation. This is achieved using a slip-ring. Figure 4-17 and Figure 4-18 show the turntable section exploded and fully assembled respectively. This joint as well as both the joints in the *bottom section*, (the *shoulder* and the *elbow 1)* all have the same motors and gearboxes. This was chosen to reduce complexity, for ease of manufacturing and to standardise parts. The assembly procedure of these gearboxes is described in detail in following section.

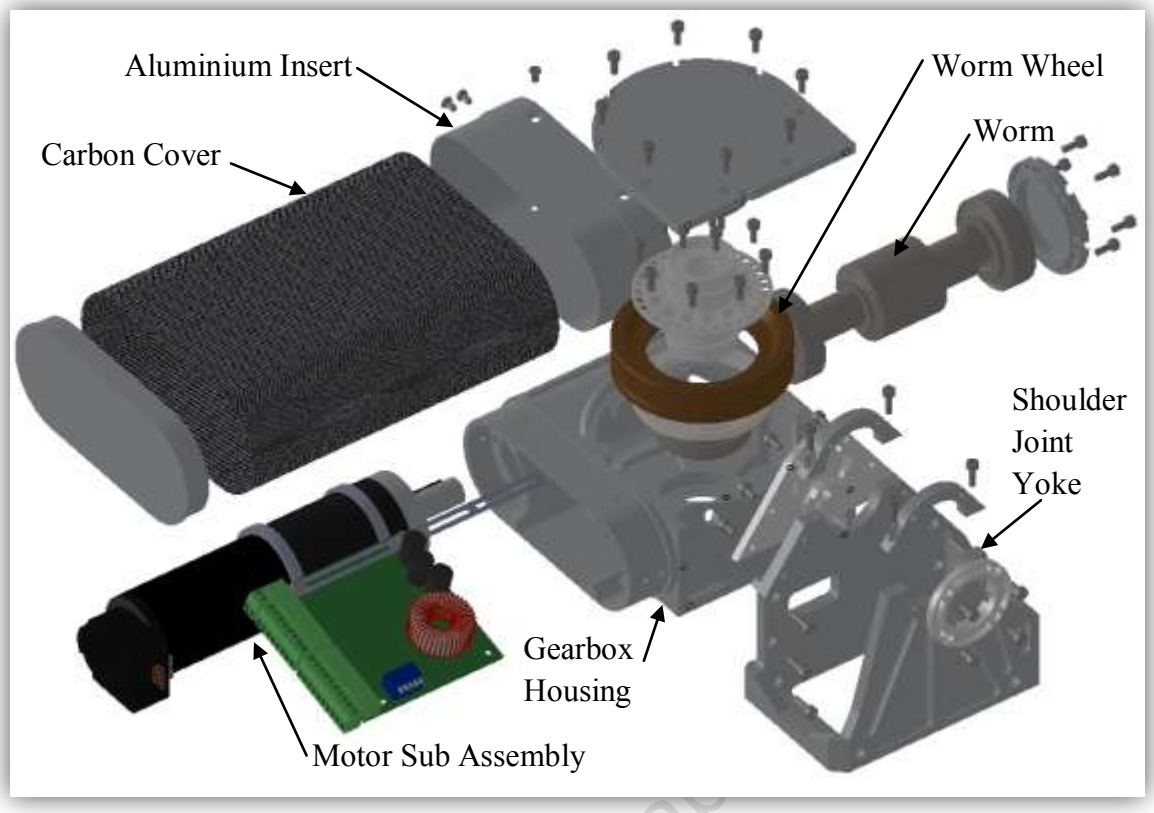

Figure 4-17: Exploded View of Turntable Section of Manipulator Arm

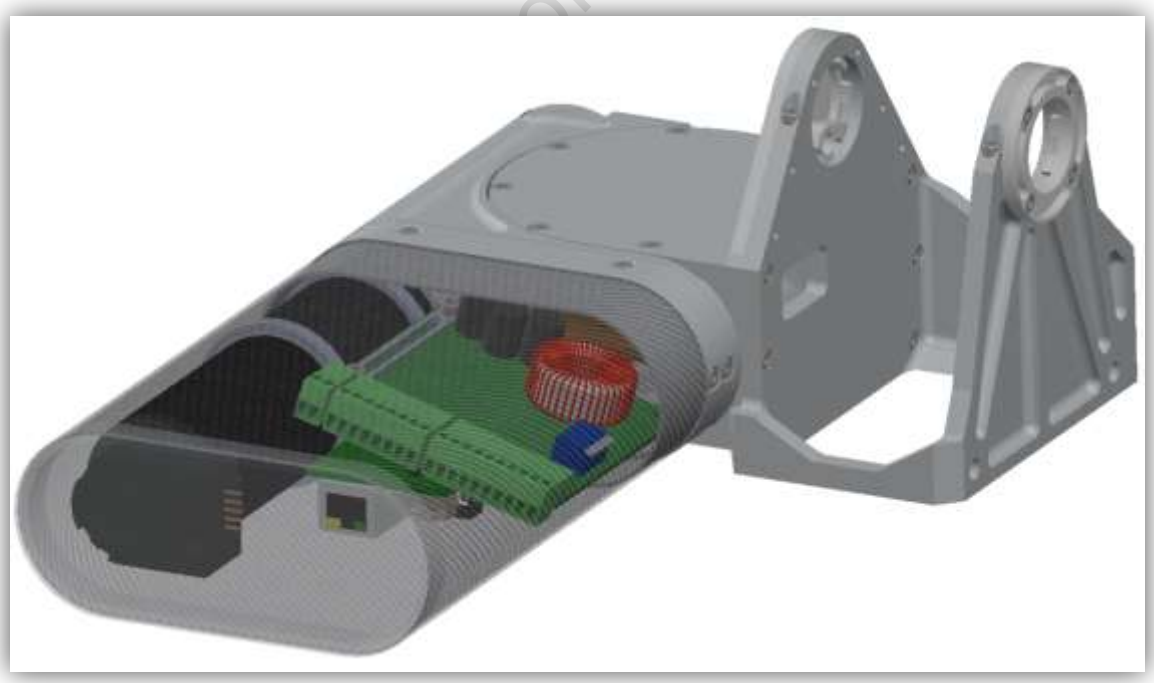

Figure 4-18: Turntable Section Assembled

The motor used in the turntable is an EC40 120W Maxon motor, coupled with a GP42C 74:1 Maxon planetary gearbox. The motor is fitted with a HEDS 5540 Maxon position encoder. These are pointed out in Figure 4-20 under the next section.

4.4.1 Adjustable Backlash Duplex Worm Gearbox

Duplex worms are worm gears that are designed to accommodate wear throughout the life span, whilst maintaining minimal backlash [4]. They achieve this characteristic by increasing the tooth thickness on the screw from one end of the worm to the other whilst maintaining the pitch. The designer then allows the worm to be moved axially along its shaft every so often to re-tighten the worm and reduce the backlash to a minimum. It is also compensates for manufacturing errors in the centre distance between the gears. A diagram showing the duplex gear and how it operates can be seen below in Figure 4-19.

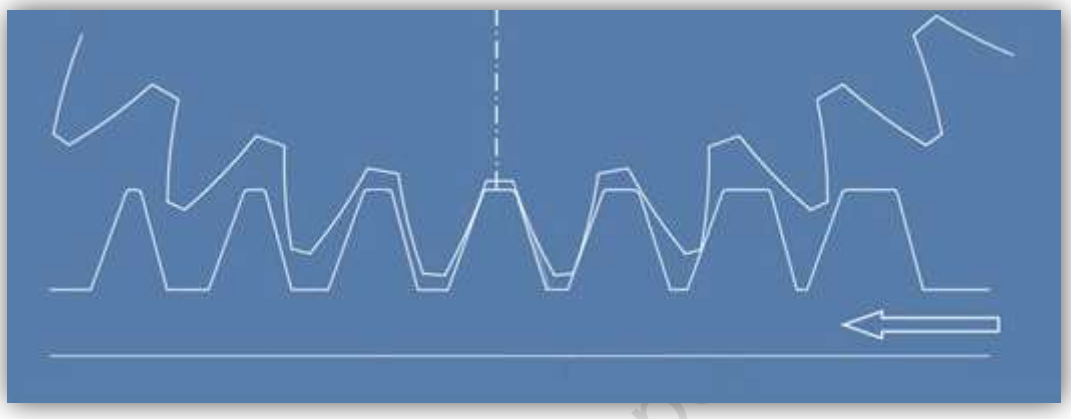

Figure 4-19: Diagram Showing Duplex Worm Gear Eliminating Backlash [5]

As low-backlash was one of the main specifications, it was decided to go with *duplex* gears. The housing design can be seen in the cutaway below.

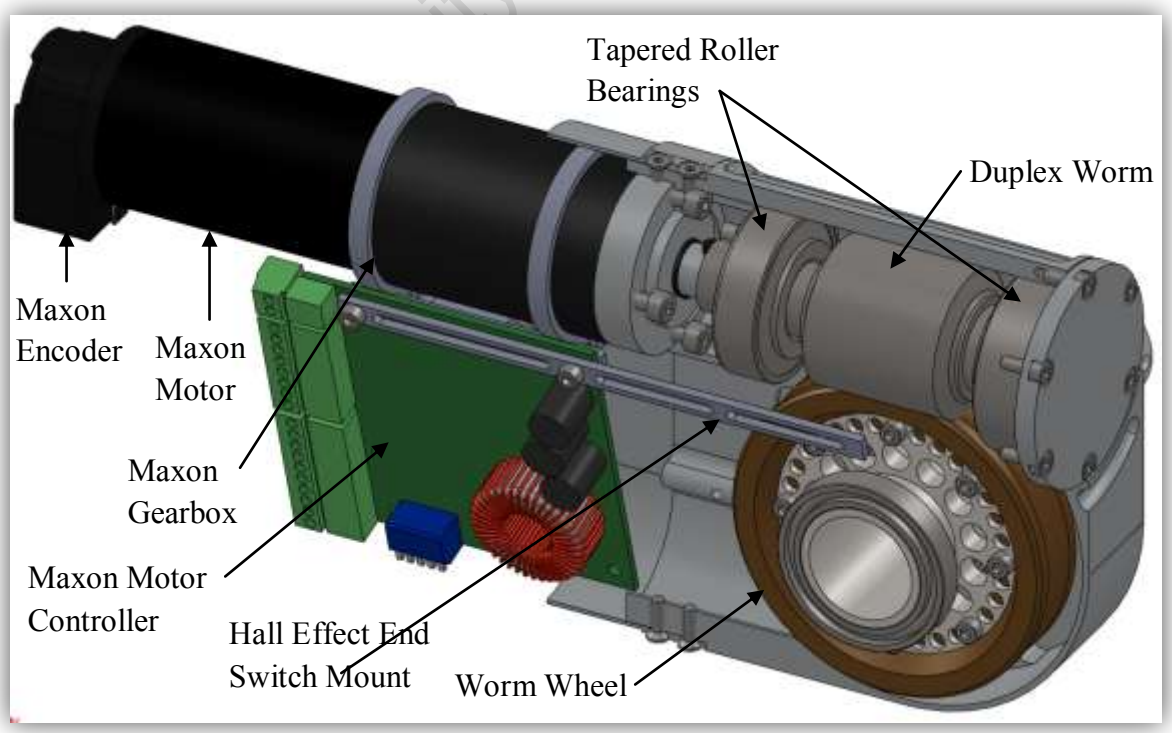

Figure 4-20: Cutaway of Gearbox Housing showing the Internal Components

Figure 4-21: Photo of Worm Gearbox Exploded

This gearbox as shown in Figure 4-21 is assembled by first inserting the motor and fastening it with 4 M4 cap screws. The outer race of the smaller tapered roller bearing is then inserted. The worm wheel along with its shaft and bearings are then inserted. Note that the worm wheel has a direction, and so cannot be inserted either way. The arrow on the worm wheel must point in the direction of narrowing thread when touching the worm. The inner races of both the tapered roller bearings as well as the spacers are then mounted on the shaft. This is then inserted. Note, that as this is inserted, the worm wheel rotates (it is therefore required that the wheel and housing are free to rotate and is therefore preferable if the gearbox is assembled separate to the rest of the arm). Note also that the worm shaft must be oriented so that the keyway and the motor key line up. It was found that it assembled easier if the inner race of the smaller tapered roller bearing is on the end of the worm shaft, and later pushed tight against the spacers. Finally the outer race of the large tapered roller bearing is inserted.

The end cover on the worm shaft has been designed with a 0.5mm gap when fully tightened. This is to ensure a certain amount of pre-loading on the tapered roller bearings, while accounting for machining tolerances smaller than this distance. Over pre-loading the end cover „locks' these bearings and the motor will stall. Under loading will result in free play and will add to any backlash experienced in the worm gears. The correct tightness is determined by running the motor with no load on the worm wheel while slowly and evenly tightening the cap screws until the motor current starts to increase; at this point, the bearings are correctly loaded.

However, as the correct tightness is shared by all 6 cap screws in the end cover, the individual tightness is insufficient to ensure that the screws do not vibrate loose. Therefore, after correct tightness is achieved, the gap should be measured. Several shims of different thickness were manufactured. The correct thickness shim should then be inserted and the cover can then be fully tightened onto this shim, ensuring that both a) the bearings are not excessively preloaded, and b) the screws are tight enough to not shake loose. Figure 4-22 shows the shim in the gearbox assembly.

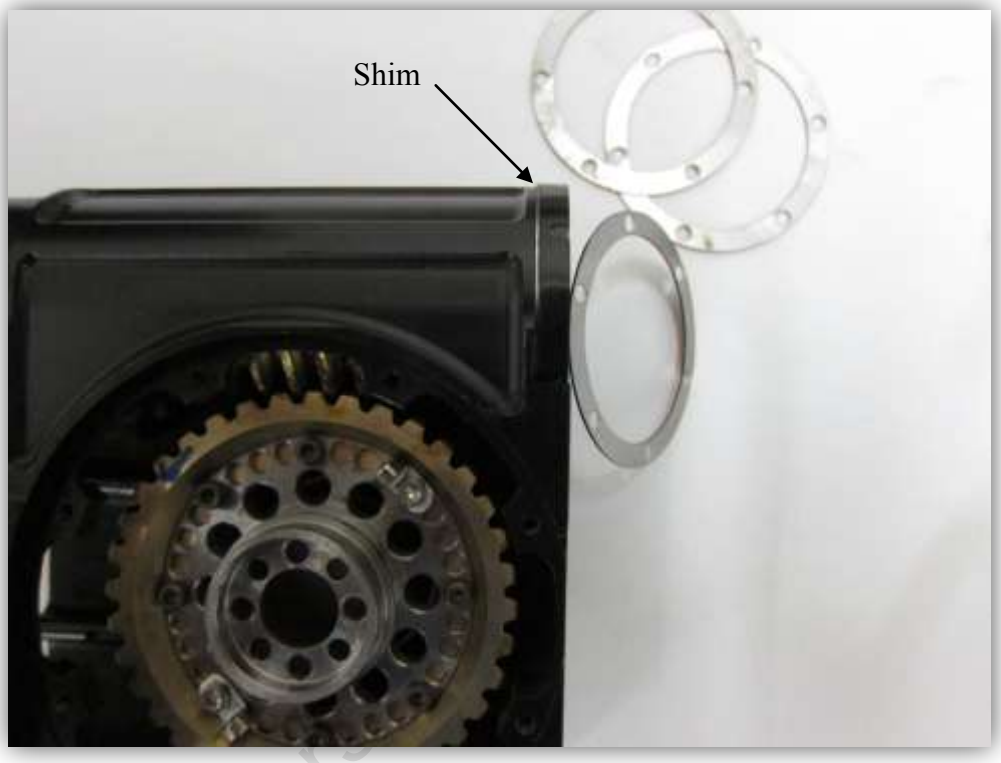

Figure 4-22: Picture of Gearbox Housing with Shim and End Cover

4.4.1.1 Adjusting the Backlash of the Duplex Gears

In this design the worm needed to be able to be shifted axially and locked. It is preferable for the bearings to be further apart from each other, to better support the worm's moment loads. It was also discovered that if the bearings were to move with the worm, they would interfere with the brass worm wheel. It was decided that the worm would be preset using cylindrical spacers of different thicknesses to offset it from the bearings, which would remain stationary in the housing. These spacers would go in the gap on either side of the worm, hence locking it in a certain axial position relative to the two bearings. Figure 4-23 shows the worm in its „loosest' and „tightest' positions. Figure 4-24 shows the worm with the aluminium spacers.

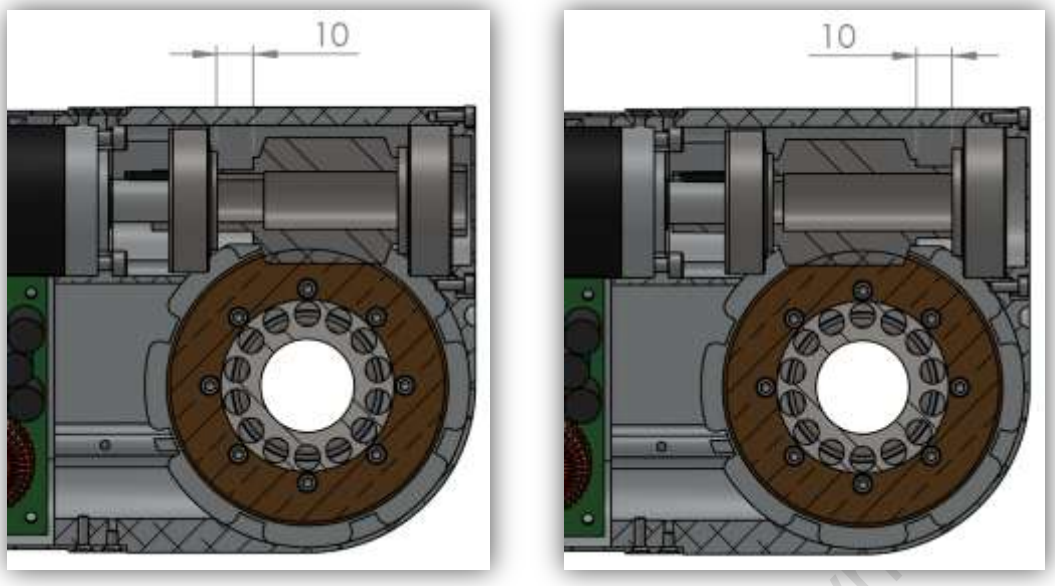

Figure 4-23: Cross-Section of Gear Housing in a) 'Loosest Position' b) 'Tightest Position'

Figure 4-24: Duplex Worm with Varying Size Spacers

The distance between the loosest and the tightest positions is 10mm, providing the worm with 5mm of leeway in either direction from the design size (which is the hypothetical situation of every part being manufactured to a zero tolerance). The thinnest spacer is 1.00mm thick, giving the worm a *shift resolution* of 1.00mm. This means that the worm can be shifted in 1.00mm increments between the loosest and tightest position.

KHK, the supplier of the duplex worm gears, manufacture worm gears of all modules with an increase of tooth thickness of 0.02mm per 1mm. This means that a shift of 1mm will reduce or increase the backlash by 0.02mm. The gears chosen have a reduction ratio of 36:1 and a module of 2mm. KHK use a *normal pressure angle* of 17.5° on their duplex gears as opposed to the 20° used on normal worms.

4.5 Bottom Section

Figure 4-25: Bottom Section of Manipulator Arm

The bottom section of the arm as shown in Figure 4-25 houses the motors and gear sets for both the shoulder joint and the elbow joint. The centre to centre distance between the shoulder axis and the first elbow axis is 422mm. To reduce the overall torque requirement on the shoulder actuator this section of the arm is the shortest of the three main sections. This is because this section is the heaviest as it houses two of the duplex worm gearboxes complete with motors etc, and so by reducing its length, the torque moment is reduced. This obviously affected the reach of the arm, and so the lighter mid section and top section were lengthened to make up for it. It was designed to be just long enough to fit the two gearbox sub assemblies with a small amount of extra space for wiring.

Exploded and assembled views of the bottom section of the arm can be seen below in Figure 4-26 and Figure 4-27 respectively. It is assembled in a modular fashion, with each gearbox being assembled separately. The completed gearboxes can then be wired together, and mounted into the carbon tube. In all of the sections, the carbon tubes act as interfaces, and are the last parts to be assembled.

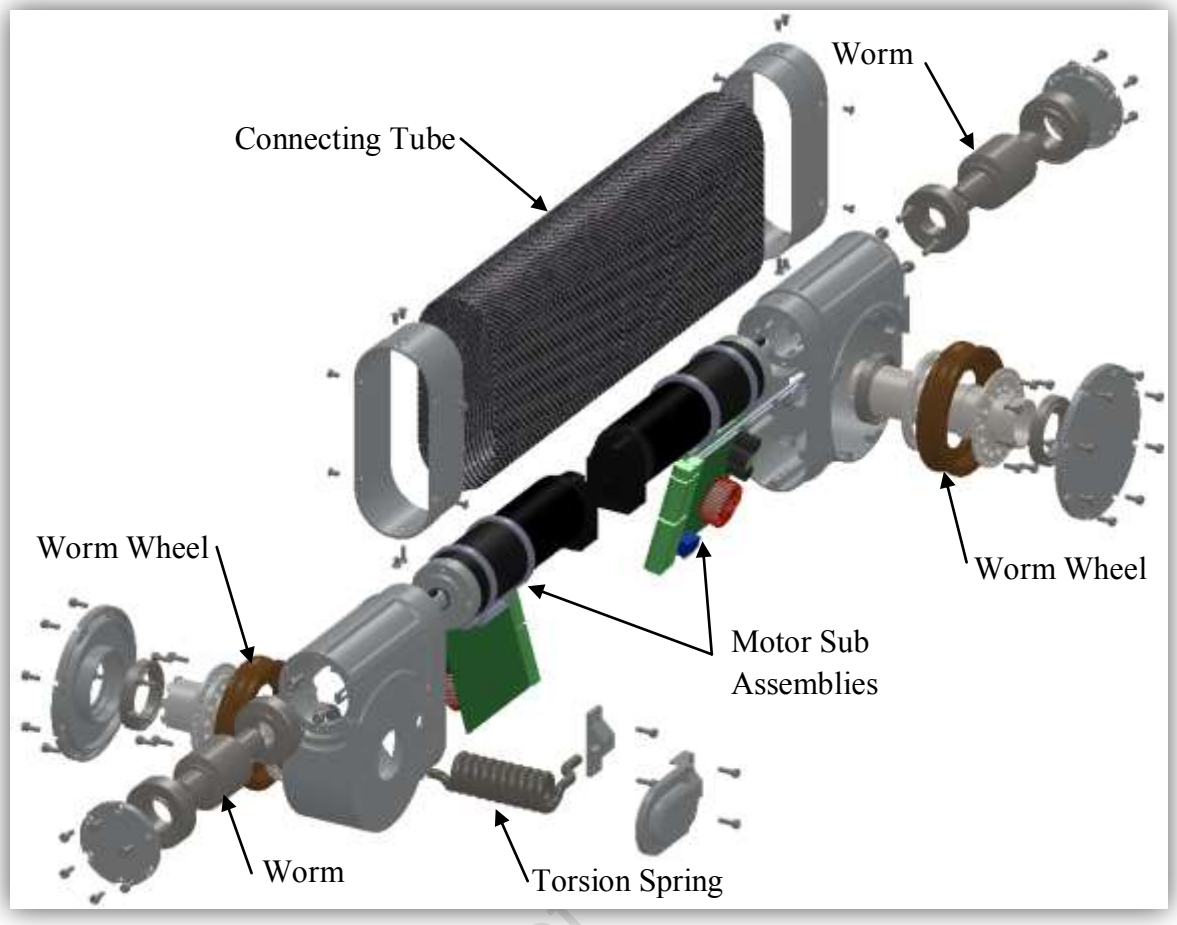

Figure 4-26: Exploded View of Bottom Section of Manipulator Arm

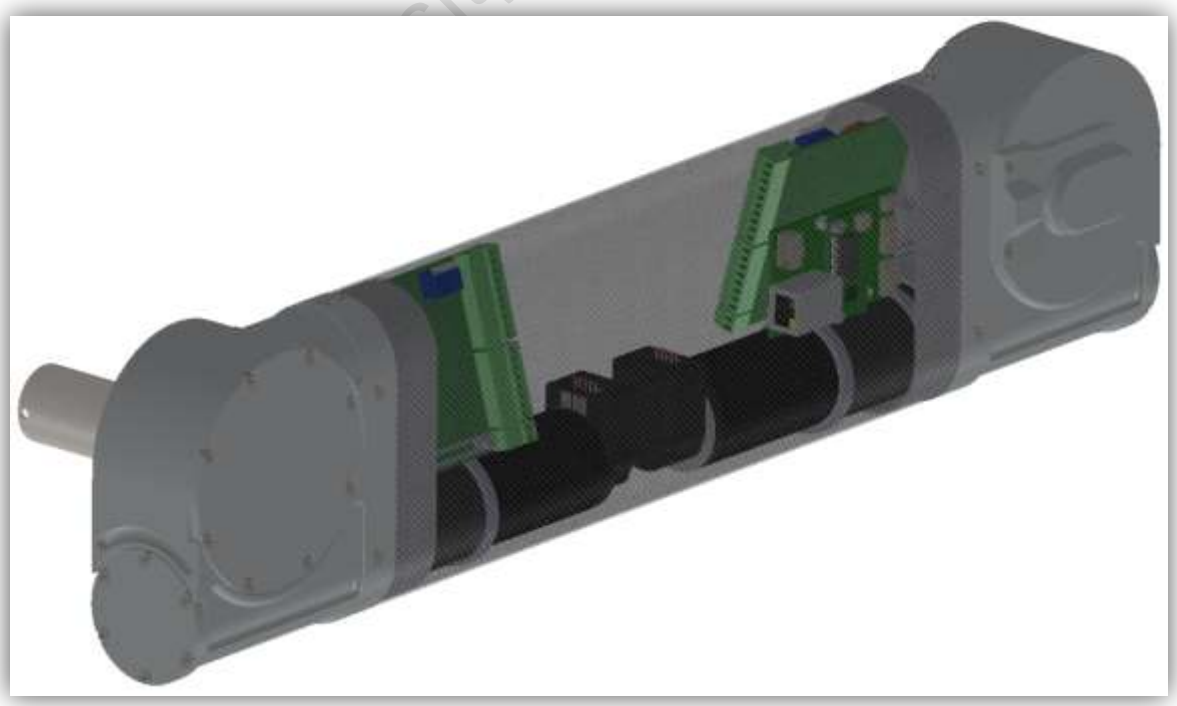

Figure 4-27: Bottom Section Assembled

4.5.1 Gravity Compensating Torsion Spring

Included in the shoulder joint is a gravity compensating torsion spring. After running calculations, it was seen that the base actuator would be required to provide 120 Nm of torque. This is extremely high and posed a problem in worm gear selection. The brass worm gears were not strong enough to handle this torque, and so gears with a large diameter had to be chosen. This increased the size of the housing and further increased the weight, increasing the torque requirements even more.

A solution to reduce the required base torque was developed. It consisted of a torsion spring that would offset the torque due to gravity. The spring is unloaded in the vertical position; deflection occurs when the arm moves down in either direction from the vertical. The spring will resist this deflection, and thereby assists in lifting the arm.

The spring strength was decided to be equal to the torque experienced when the arm is in its collapsed position. This would mean, the motors would see a near-zero (weightless) loading, when the arm is collapsed.

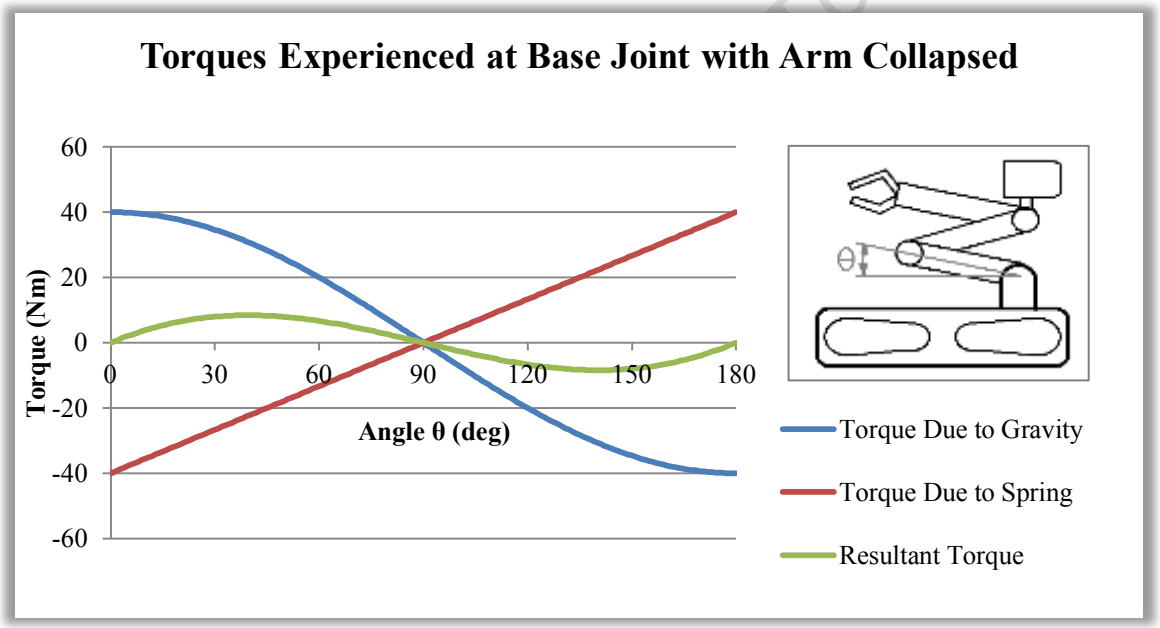

Figure 4-28: Graph Showing Torque Offset due to Spring with Arm Collapsed

The green line in Figure 4-28 shows the resultant torque that is required of the actuator. It can be noted that the maximum torque experienced moves from angular positions 0° and 180° to 40° and 140°.

When the manipulator is extended, the moment arm to the centre of mass increases, and the torque due to gravity therefore increases. The spring however is only affected by the angle from the vertical and is not affected by the extension. Figure 4-29 shows the relationship when the arm is fully extended. In this instance, the spring reduces the maximum required torque from 120Nm to just above 80Nm. Once again it can be noted that the angular positions of maximum torque shift from positions 0° and 180° to 12° and 168°.

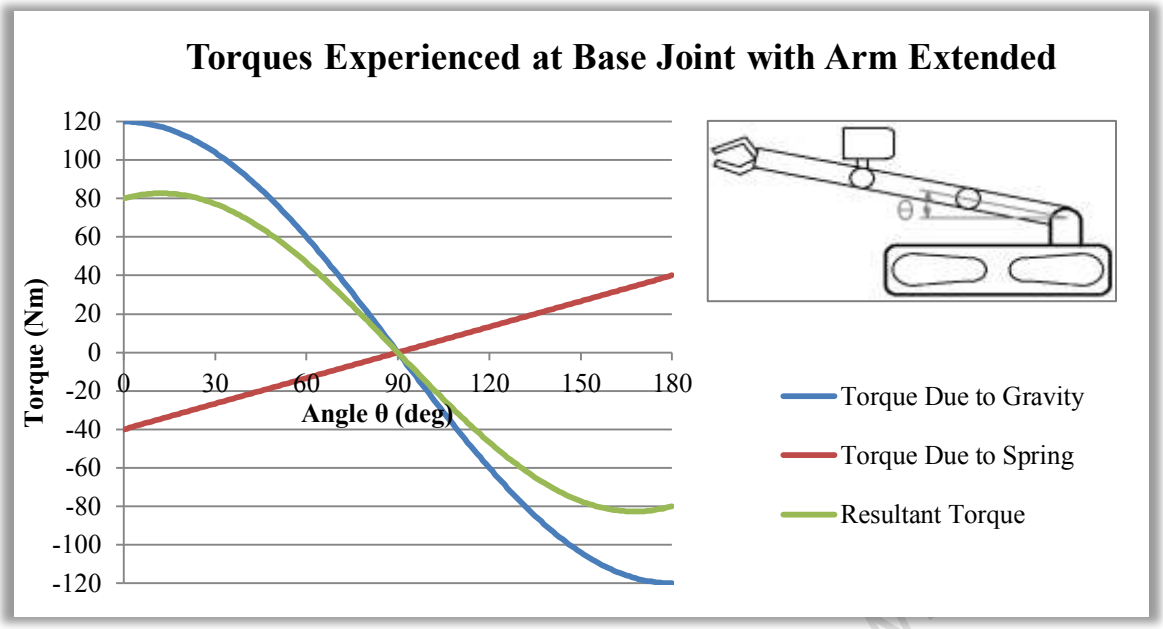

Figure 4-29 Graph Showing Torque Offset due to Spring with Arm Extended

The springs design and mounting can be seen in Figure 4-30 and Figure 4-31. The short end is secured in a steel part, as it experiences a crush force up to 13kN when fully deformed (this is due to the small moment arm on this end). The longer leg is clamped to the bottom section using an aluminium part mounted on the arm. The spring is constrained within the steel worm wheel shaft, and is designed with just enough free space for the small expansion in diameter that occurs when „unwinding' the spring (turning clockwise). The spring was also designed with a pitch of 6.2mm which is just greater than the wire thickness of 6mm, to allow space for when the spring winds anti-clockwise and lengthens by a quarter turn.

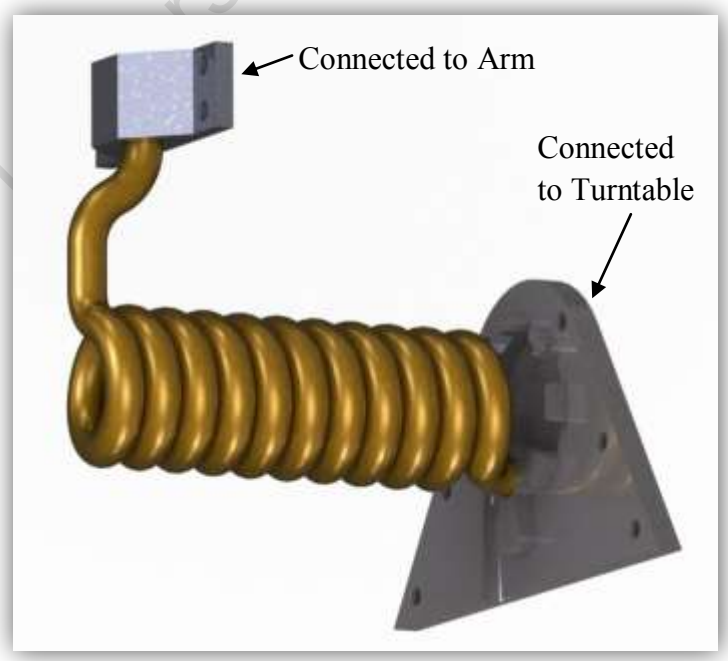

Figure 4-30: Rendering of Torsion Spring with End Constraints

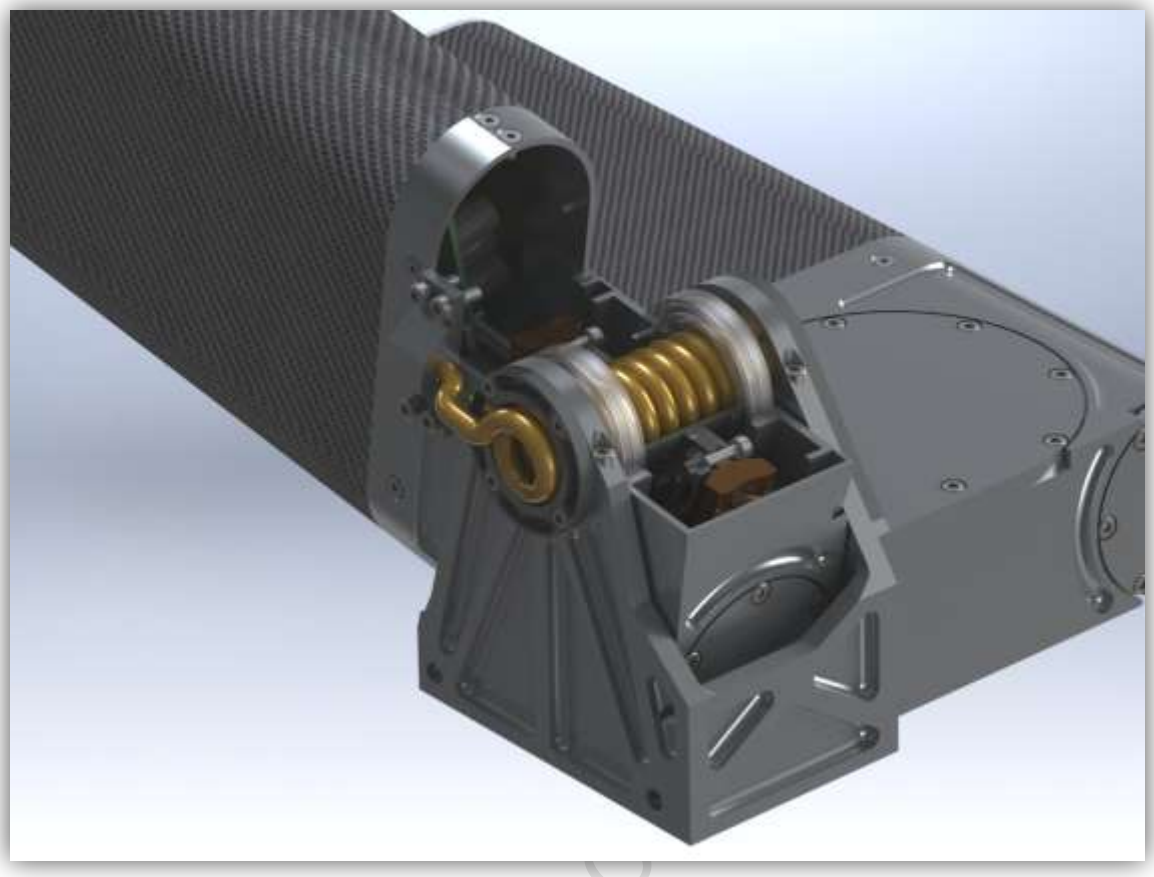

Figure 4-31: Render of Bottom of Arm with Cutaway showing Torsion Spring (Bearings Transparent and Spring Cover Hidden)

The electrical wiring from the turntable to the bottom section passes down the centre of the spring. It does not use a slip ring as it is only rotated 90° either side of its neutral position. The spring chosen is a 6mm DIN17223 Grade C (the tensile strength is between > 1590-1770 MPa) spring with a mean diameter of 19mm, a pitch of 6.2mm and has 10.5 turns. As mentioned it was designed to provide 40Nm of torque when rotated through 90°. This provides an effective additional lifting capability of 2.4kg at full reach.

A second spring was also ordered with the same dimensions except in 5mm wire. This was to have a lower strength option available should it be deemed necessary. It was designed to provide 20Nm of torque. This translates to an additional lifting capability of 1.2kg at full reach.

4.6 Mid Section

Figure 4-32: Mid Section of Manipulator Arm

The mid section of the arm is very light, containing only the tilt actuator for the sensor payload. It uses spiral bevel gears with a module of 1.5mm and a ratio of 20:40 teeth. Spiral bevel gears were chosen as they are quieter and run smoother than straight bevel gears. The 1.5 module was chosen for its size benefits, rather than its strength; it was needed to fit the wiring through the shaft. These gears are therefore oversized and so lightly stressed.

This section was designed to be long enough to allow the sensor head to fold behind the end of the bottom section. At the bottom end of this section is the housing that clamps to the shaft of the 1st elbow. It uses two steel pins to transmit the torque from the 1st elbow's worm wheel shaft to the mid section. These pins are custom made with threads on the end to ensure they can be removed after being assembled, as they fit into blind holes.

An exploded view and a fully assembled model of the mid section can be seen in Figure 4-33 and Figure 4-34 respectively.

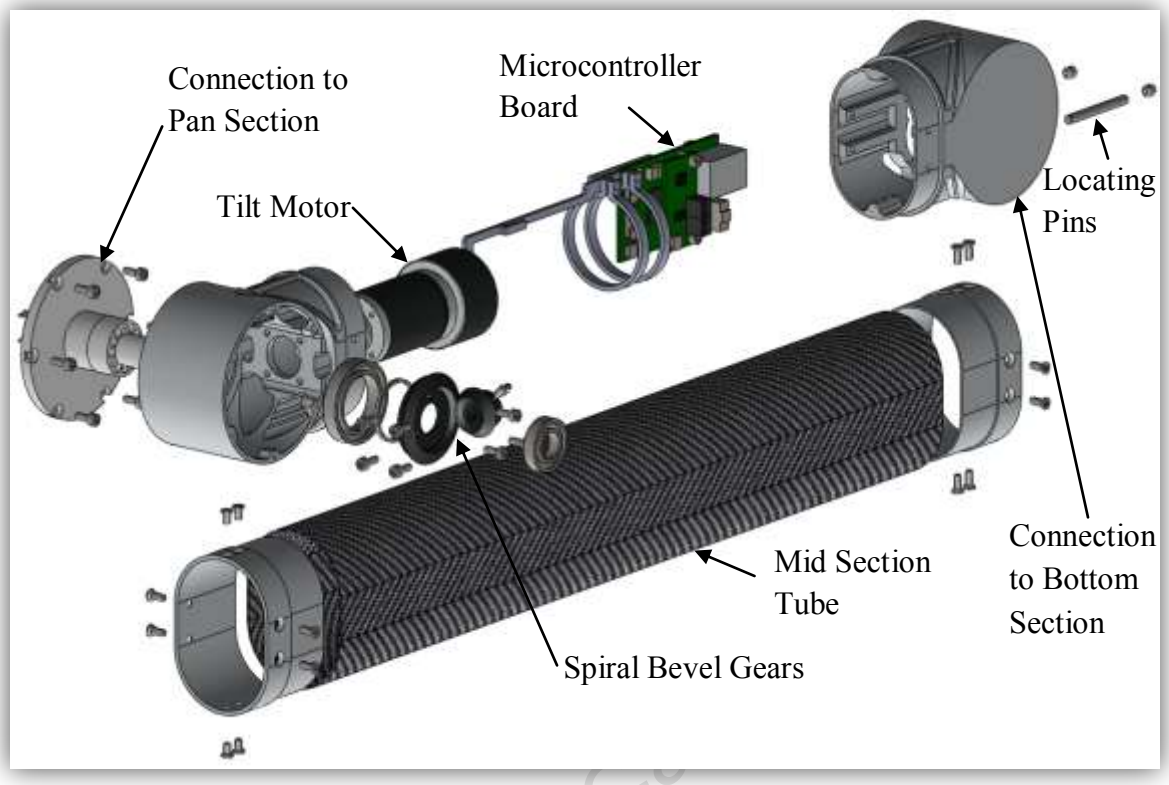

Figure 4-33: Exploded View of Mid Section of Manipulator Arm

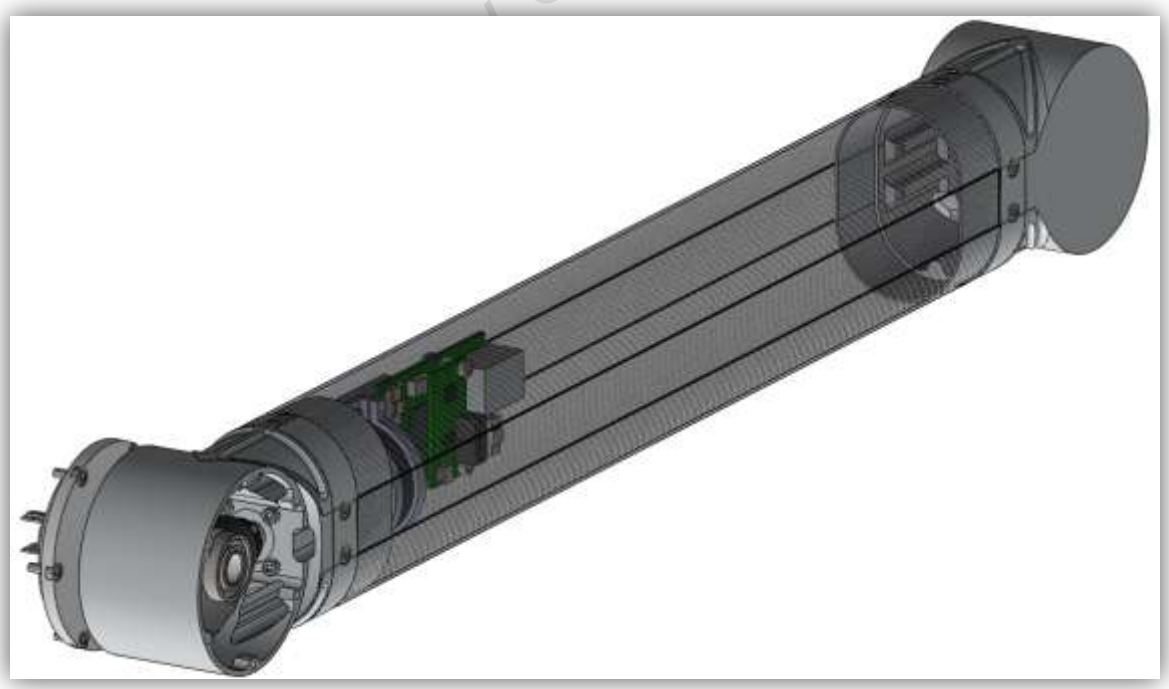

Figure 4-34: Mid Section Assembled

The initial motor chosen for the tilt actuator was a EC Flat 32mm 15 watt Maxon motor, with an integrated speed controller. The motor was coupled to a 190:1 Maxon planetary gearbox.

After testing however, it was discovered that the integrated speed controllers could not hold a zero speed, and so after moving the sensor payload, it had the tendency to „flop' down and hang from the arm. The motor was strong enough to lift the head again, but the controller could not maintain a position. The same problem was experienced in the *pan* actuator which had the same motor and gearbox combination. This is discussed in greater depth in the Testing section of this report.

New motors with encoders and more advanced controllers were ordered. These were Maxon EC-max 30mm, 25 watt motors, coupled with 531:1 GP32C Maxon gearboxes and MR Maxon encoders. These gearboxes had identical interfaces and therefore can be easily swapped out.

4.7 Top Section

Figure 4-35: Top Section of Manipulator Arm

The top section of the arm houses three actuators: the *2nd elbow,* the *wrist* and the *gripper.* This section will focus on the *2nd elbow* joint. The following two figures show the top section exploded and assembled, without the wrist or gripper.

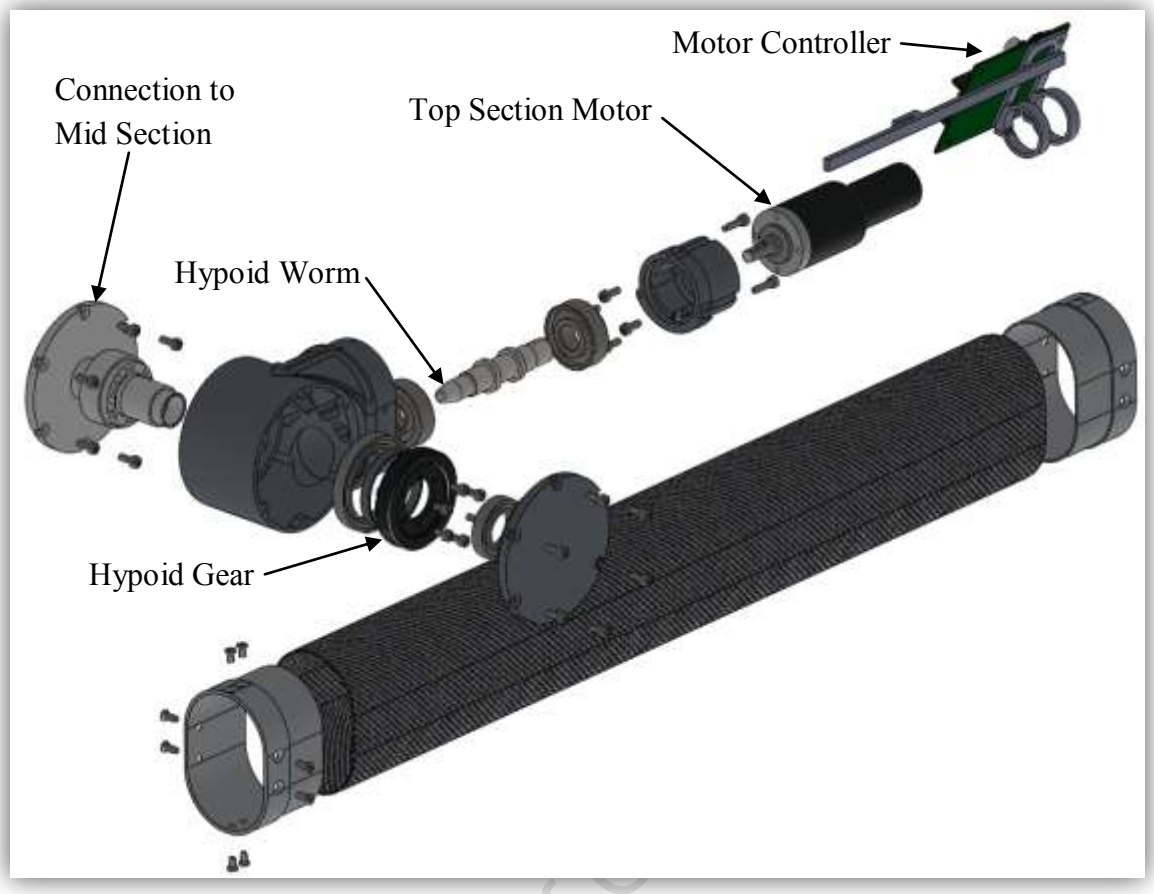

Figure 4-36: Exploded View of Top Section of Manipulator Arm

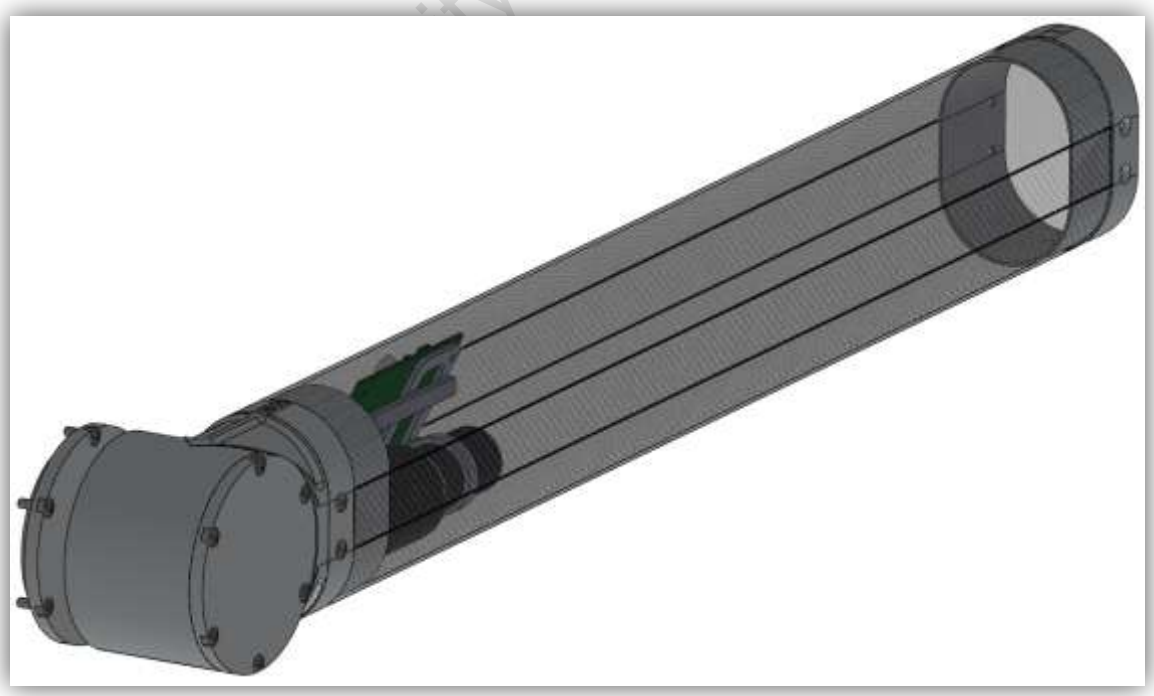

Figure 4-37: Top Section Assembled

The 2nd elbow joint utilises KHK high-ratio hypoid gears. These gears can be seen in Figure 4-38. These boast many good qualities including:

- High reduction ratio.
- High efficiency when compared to worm gears.
- High strength. Carburised steel alloy allows for a comparably smaller module to be chosen, than the softer brass worm gears.
- Compact gear assembly, as the screw does not sit on top of the gears, but rather next to the gear.

They do not however exhibit the low backlash characteristics of the duplex worm gear. In this joint, 45:1 hypoid gears with a module of 1.5mm were chosen. As with a worm gear, a hypoid is a self locking gear, provided it has a sufficiently high reduction ratio and a low number of starts on the worm. It also, like worm gears, carries a large axial loading. Sufficiently strong bearings therefore need to be chosen to handle the loading.

Figure 4-38: Picture Showing Hypoid Gearbox with Slip Ring

The motor used in this section is an EC22 40 watt Maxon motor coupled with a 190:1 EC32C planetary Maxon gearbox and a MR Maxon encoder. This joint also has the ability to rotate continuously and so it has been designed to house a slip ring.

4.8 End Effectors

As mentioned, Mr. Michael Rieger is designing the latest version of the wrist and gripper, shown in Figure 4-40 and Figure 4-41. The gripper seen in the pictures of this report is the previous generation version designed by Mr. Terry Scott and is shown in Figure 4-39. Each design was required to fit with the previously mentioned Aluminium Interface bonded into the end of the tubes.

Figure 4-39: First Generation Wrist and Gripper (Terry Scott)

Figure 4-40: Rendering of Second Generation Wrist and Gripper (Michael Rieger)

This latest generation version will boast the following sensors (Michael Rieger):

- Weiss Robotics 84 cell tactile sensing arrays
- Object presence sensors
- Micro VGA colour camera
- LED lighting
- High precision current sensors to aid in force feedback.

The purpose of the pressure sensing pads is to better provide the operator with feedback on the object being picked up. The lights and camera will give the operator better situational awareness and will help him or her to interact with the object.

Both designs are two finger parallel grippers, and use Maxon EC22 40W brushless DC motors coupled to Maxon EC22HP 157:1 planetary gearboxes, and MR Encoders. The first gripper shown in Figure 4-39 was tested to a closing force of over 300N. It also includes an integrated cutter (not shown in the picture).

Figure 4-41: Ratel Fitted with Second Generation Wrist and Gripper

4.9 Pan Section

Figure 4-42: Pan Section of Manipulator Arm

As the name suggests, the pan section of the arm houses the sensor payload's pan actuator. It uses an identical motor-gearbox combination as the tilt motor. This is then coupled to a 1:1 helical gear set of 1mm module and 25 teeth. The reason for the helical gears is to offset the motor from the pan axis. This allows the slip ring and wires to pass through the centre of the gears, and allows for continuous rotation on this joint. Helical gears were chosen above spur gears as they run smoother and are quieter. This is important as vibrations could be transmitted to the sensor payload and cause shake on the camera's picture.

An exploded view of the pan section can be seen below, together with an assembled view. In the exploded view, the slip ring can be seen just next to the motor. Due to the same problem of position control discussed about in the mid section, the motor in this section will also be replaced with one fitted with a position encoder. Due to space constraints in this section, its associated electronics are mounted in the mid section.

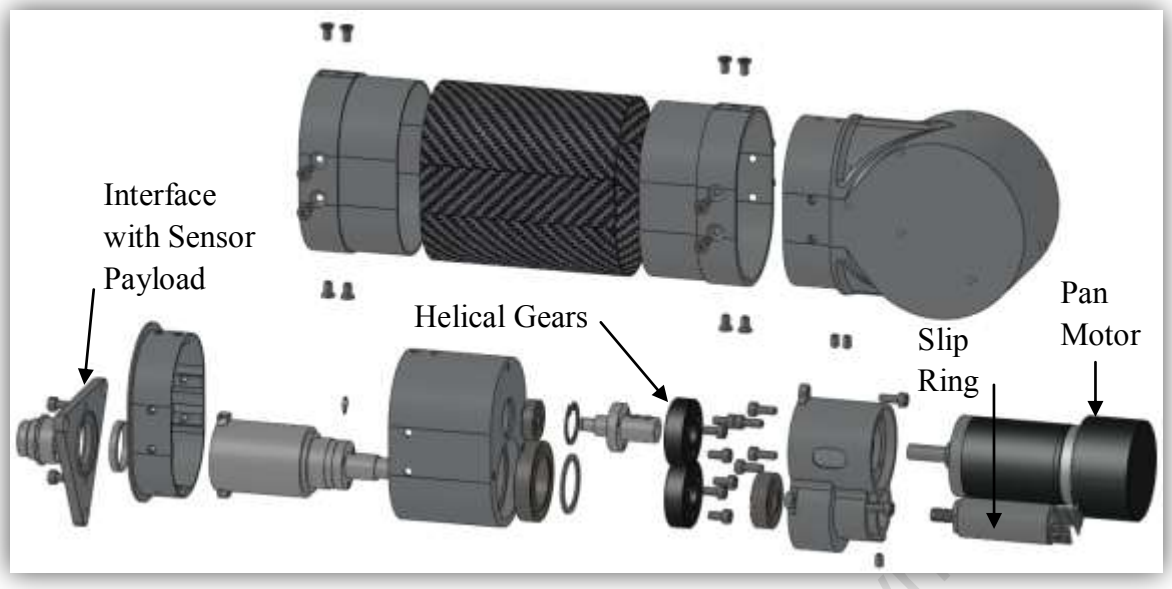

Figure 4-43: Exploded View of Pan Section of Manipulator Arm

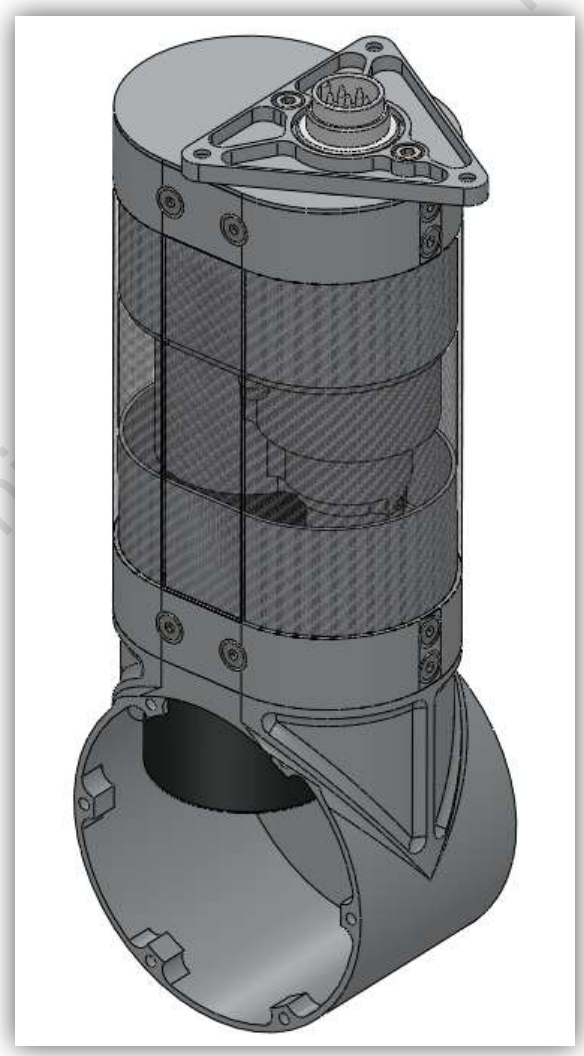

Figure 4-44: Pan Section Assembled

4.10 Wiring

The complete system has internal wiring, with circuit boards placed as shown below. The wiring runs through several slip rings which allow for continuous rotation on various joints.

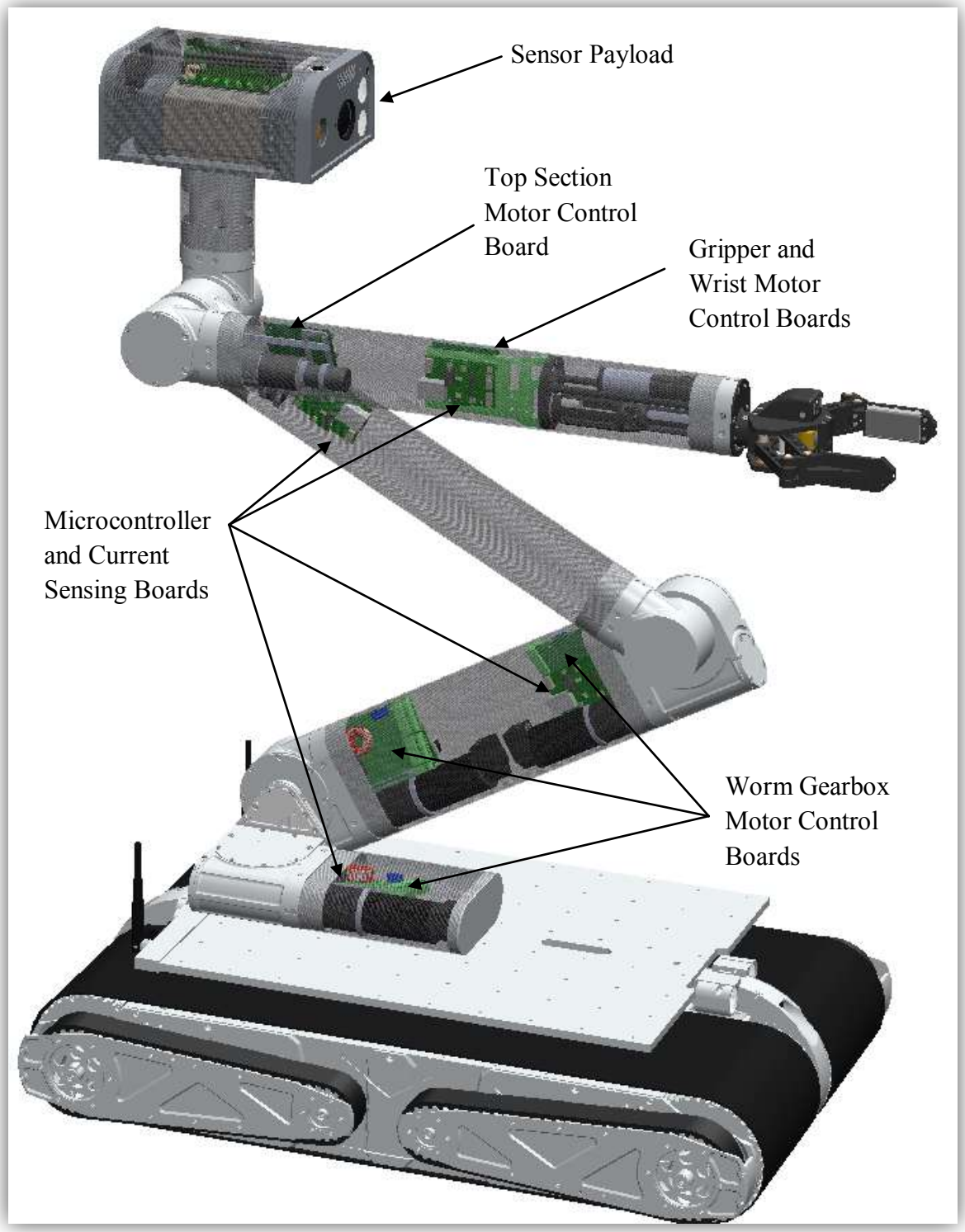

Figure 4-45: Ratel with Carbon Tubes Transparent to Show Circuit Board Layout

The wiring diagram can be seen overleaf showing the slip ring and wiring layout.

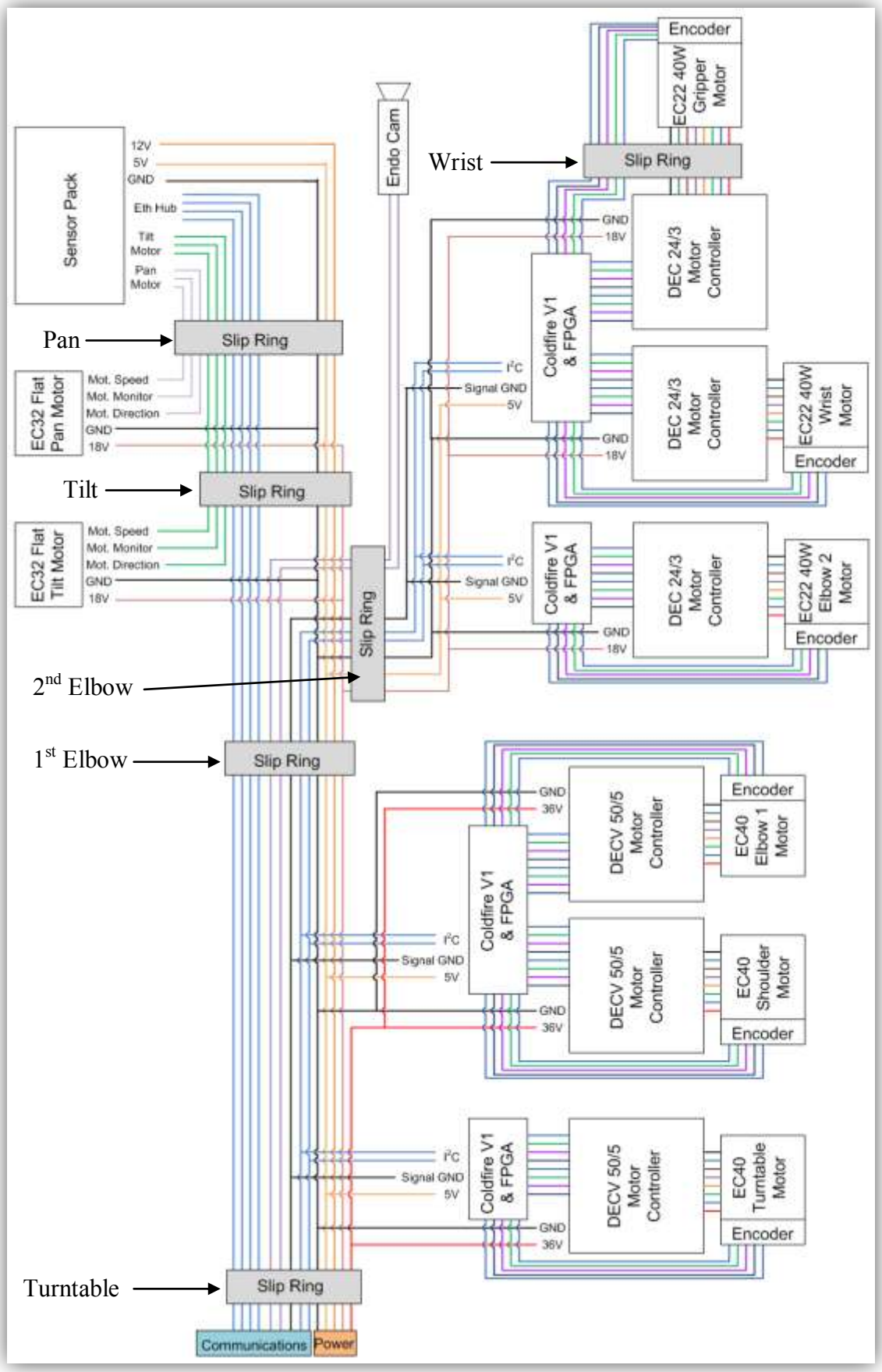

Figure 4-46: Wiring Diagram of Manipulator Arm

The slip rings used in the manipulator arm are ByTune BT016 slip rings, imported from China. They have an outside radius of 16mm and have 30 *ways* passing through them, each with a maximum current rating of 2A. The slip ring can be seen in the rendering below. The rotational friction of the slip ring is sufficiently low for the wires themselves to be strong enough to rotate the inner ring. This greatly reduces design complexity as the inner assembly of the slip ring need not be clamped.

Figure 4-47: Rendering of BT016 30Way Slip Ring

The wires to the right of the picture are connected to gold plated rings which rotate within the housing. Running on these rings are gold brushes which are connected to the wires exiting on the left of the picture. Each wire has a current rating of 2A [6]. For high current requirements, such as those of the power lines, several slip ring wires may be joined together to share the loading.

4.11 Summary

This chapter has looked at the mechanical detailed design of the manipulator arm, and has also given an overview of the two interfacing gripper options. It discussed in detail the adjustable backlash design of the duplex worm gearboxes. It also described the gravity compensating torsion spring developed to lighten the load on the shoulder motor.

Once the mechanical part of the manipulator arm was assembled, with the wiring and circuit boards in place, it needed to be tested. A simple test control board needed to be developed to run the tests, and this is looked at in the next chapter, along with other control interfaces.

5 Control and Electronics

5.1 Introduction

The control of the manipulator arm is outside of the scope of this project, as this project deals mainly with the mechanical design and development of the arm. This chapter therefore gives only an overview of the control systems to be used on the arm. It also includes the design of the test board used in testing the arm. This simply consists of a forward and backward push button for each actuator, and some logic circuitry which is discussed in detail. The Hall Effect electronic end stops used on the arm are also discussed.

5.2 Control Interface

As mentioned in the scope of this project, Mr Bradley Springer is designing the advanced control systems to operate the arm to its full potential. It shall include the second generation master-slave controller designed by Mr Matthew Thorne. This controller is shown in the Figure 5-1 below. It uses advanced servomotors which have the ability to be both *driven*, and to *drive* themselves. This means that the controller can either be used to drive the manipulator arm, or the controller can be used to follow the arm, and thereby show the arms position. Also shown is a 3D mouse, which will be used for *inverse kinematics* type control where the tip of the arm is manipulated with the 3D mouse and the program calculates the required joint angles on each of the motors, to achieve this tip position.

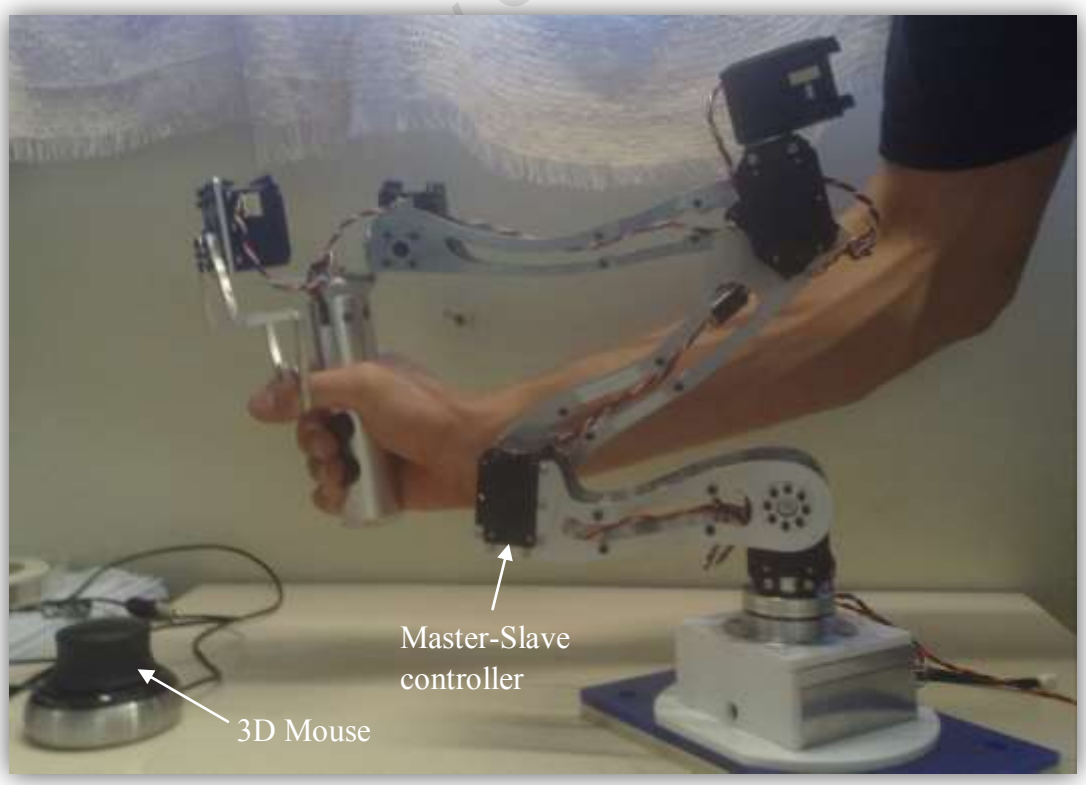

Figure 5-1: Picture showing Master-Slave Controller and 3D Mouse

5.3 Test Board

For testing purposes, a simple speed controller board was built. This can be seen in Figure 5-3. It comprises of a forward and backward button for each of the eight motors, a potentiometer for the speed control of the six arm motors, and a potentiometer for each of the Pan and Tilt joints. The Maxon controllers require their *Enable* pin to be pulled high, and an analogue voltage of 0-5V on the *Speed* input. The direction of the motor is controlled by either a *high* or *low* on the *Direction* pin. The button allocation is given in Figure 5-3.

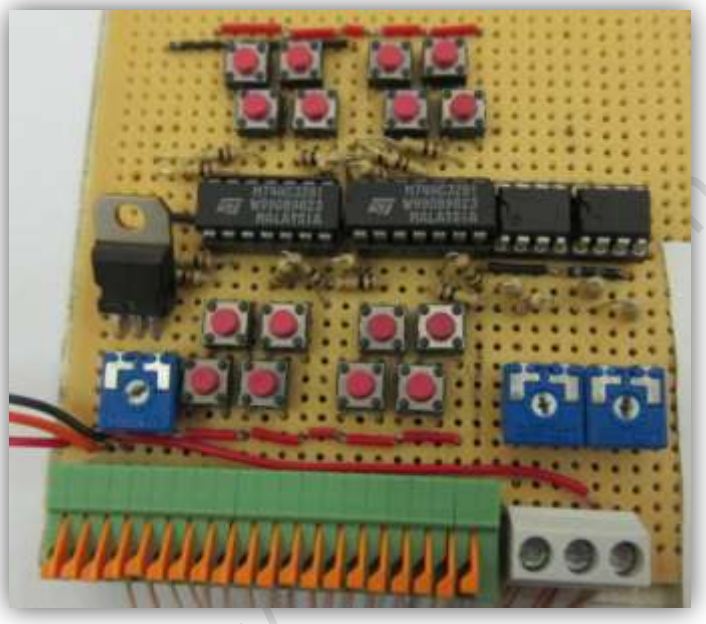

Figure 5-2: Push Button Test Board

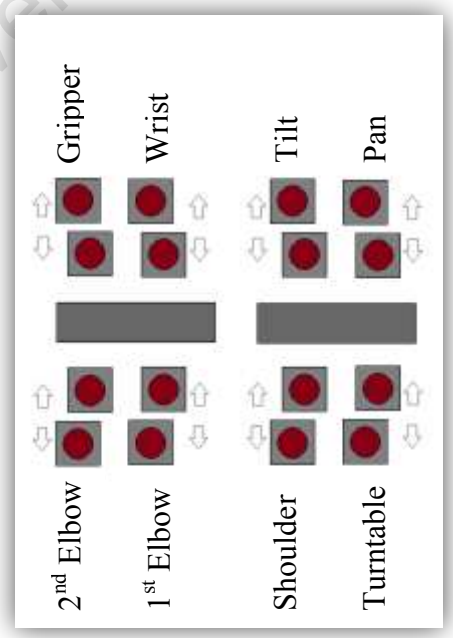

Figure 5-3: Push Button Motor Allocations

The test board uses OR gate logic chips to pull the enable high when either direction button is closed. This logic can be seen in Figure 5-4 below.

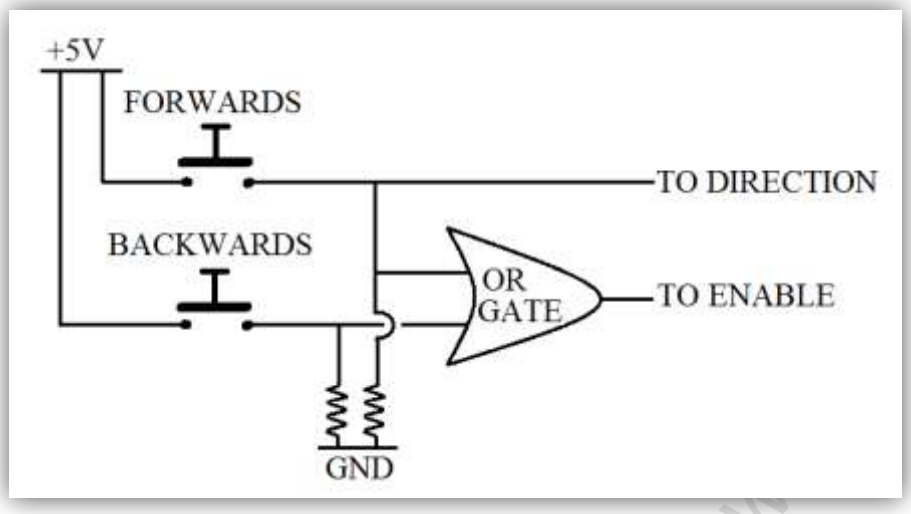

Figure 5-4: Figure showing Test Board's Circuit Logic

On the Pan and Tilt motors, which require only a direction and a speed input, it was found that the OR gate logic chip was not ‚strong' enough to hold the output *low*, and the motors were running slowly without any button input. LM358 operational amplifiers were then added to the test board for these two motors, to force the output to ground.

5.4 Hall Effect End Switches

Each actuator is fitted with a Hall Effect switch which acts as an electronic end stop. They ensure the arm remains within a safe *work envelope*. The Hall Effect sensors chosen are Allegro A1101 unipolar digital Hall Effect switches. They have a preset threshold, and turn on digital signal when a sufficiently strong magnetic north field is experienced.

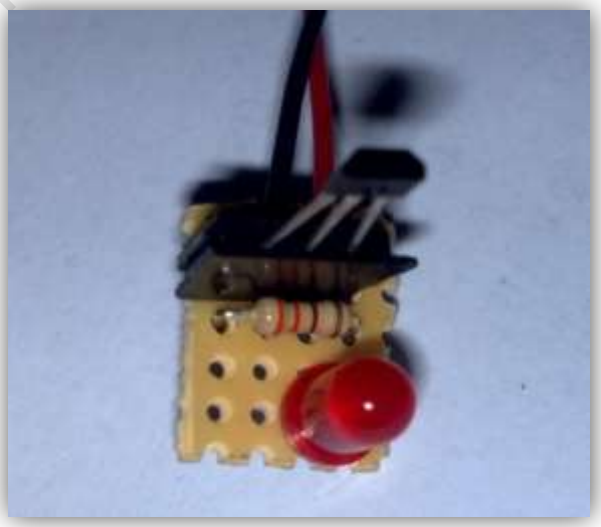

Figure 5-5: Hall Effect Switch Test Board

Figure 5-5 above shows a test board built to investigate the switch's characteristics. The unipolar characteristic is beneficial as one can pass a magnet of varying strength past the Hall Effect switch, and as the centre line of the magnet passes the centre of the switch, it will turn on, giving a very accurate threshold that is not dependant on the magnet's strength, or its distance from the switch. A schematic is shown in Figure 5-6.

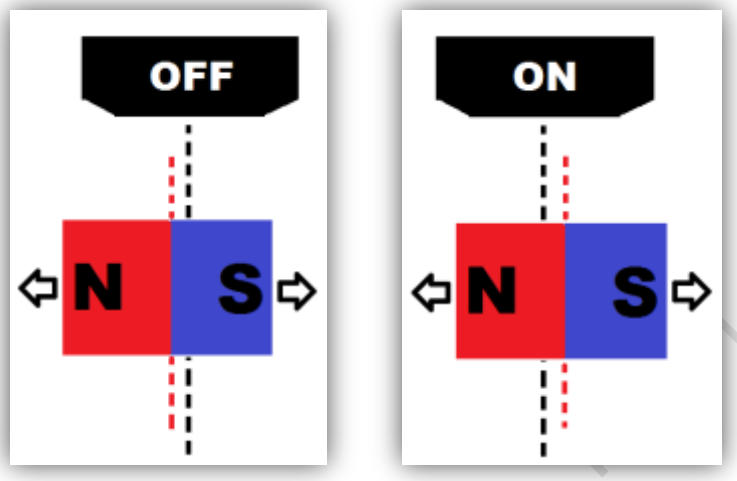

Figure 5-6: Schematic of Unipolar Hall Effect Switch in a) OFF and b) ON Postion

This method results in the ON and OFF thresholds being almost exactly together. The other option would be to bring the magnet close to the switch parallel to its projected centre, as shown below, but this results in a large ‚dead band' where the ON and OFF thresholds are far apart. That is; it turns ON closer to the switch than the position at which it turns OFF.

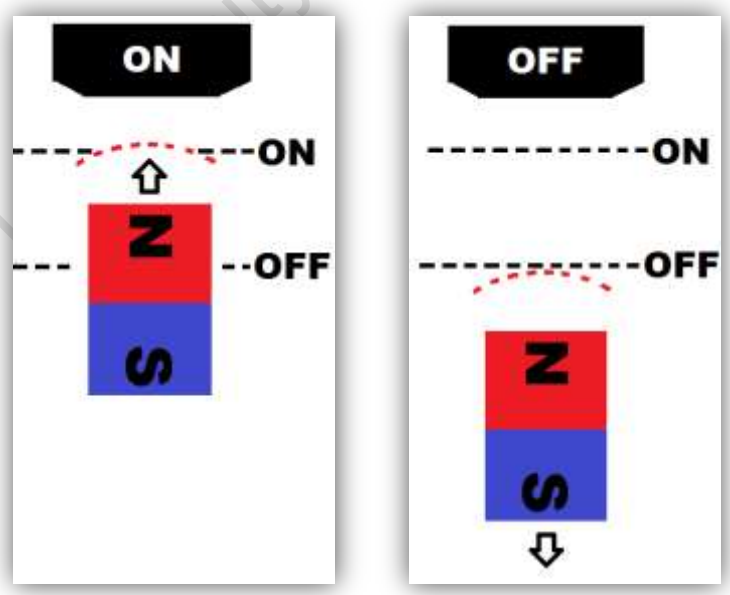

Figure 5-7: Schematic showing Dead Band with Magnet Approaching Switch

A further disadvantage is that varying magnets will give different threshold positions (i.e. the dotted red line will be further or closer in).

The Hall Effect switch with magnet can be seen in Figure 5-8 below in the turntable's gearbox housing.

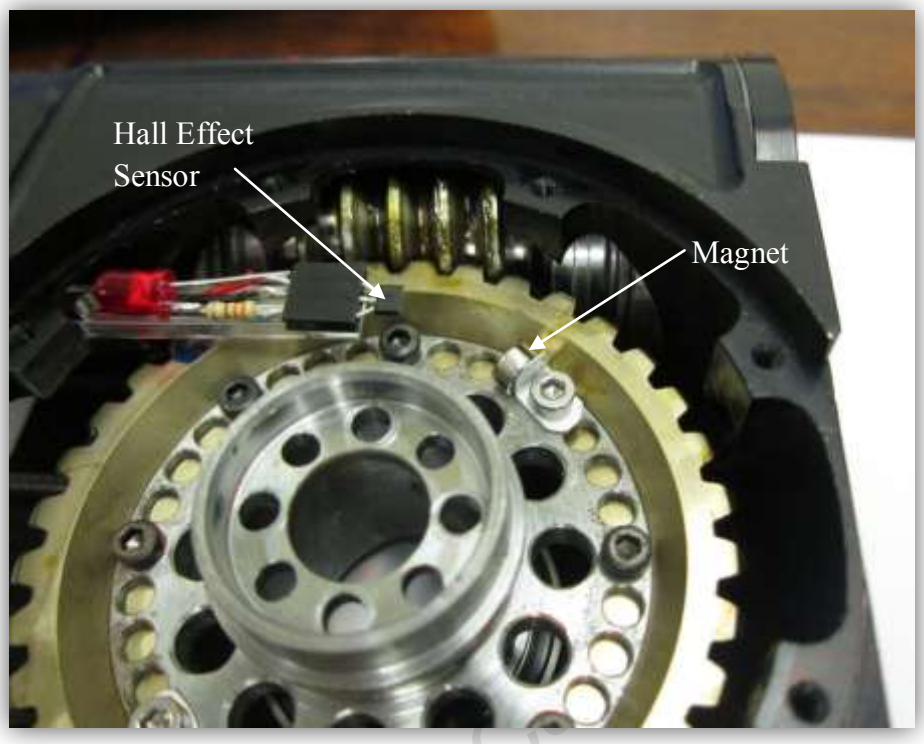

Figure 5-8: Hall Effect Switch in Turntable Housing

5.5 Summary

This section has dealt with the control and electronics used in the testing of the robot, as well as those to be used for final deployment. It also included the design and use of the Hall Effect end stops, and the required orientation of the magnets. Once the test board was built, the testing phase was started. The next chapter covers the tests and their respective results.

6 Testing and Results

6.1 Introduction

The manipulator arm was tested to determine how it performed with respect to its required specifications. This chapter lists the tests performed and their results. It also looks at other specifications such as the overall cost of the manipulator arm.

The detailed testing documentation with respective photographs is listed in Appendix D, *Testing Documentation*. The specific joints talked about in the testing procedures are shown on the below diagram. The Ratel's manipulator arm has 6 degrees of freedom plus a pan and tilt for the sensor payload, equalling a total of 8 actuators, or joints.

Figure 6-1: Picture of Manipulator Arm showing the Different Joints

6.2 Cost

The cost of machining is unknown, as it was done in-house, and not billed. The carbon tubes were manufactured for free. Fasteners and electronics were also supplied in house. The costs of the parts ordered are listed in Table 6-1. The total of these costs is R75 000.

Table 6-1: Table Listing Costs of Supplied Parts

	Supplier/ Manufacturer	Cost
Bearings	Bearing Man Group (BMG) [7]	R2 100
Motors, Planetary Gearboxes and Controllers	Maxon Motors [8]	R45 900
Gears	KHK Stock Gears [9]	R18 100
Slip Rings	ByTune Slip Rings [6]	R8 900
Total		**R75 000**

6.3 Work Envelope

The first tests completed investigated the reach of the arm to determine its work envelope. To determine the work envelope, each joint's angle of rotation and the length of the arm were measured. Figure 6-2 shows the work envelope of the arm with all joints locked in an extended state, and only moving the shoulder and turntable joints. The result is a hemisphere with a diameter measuring 3.46m.

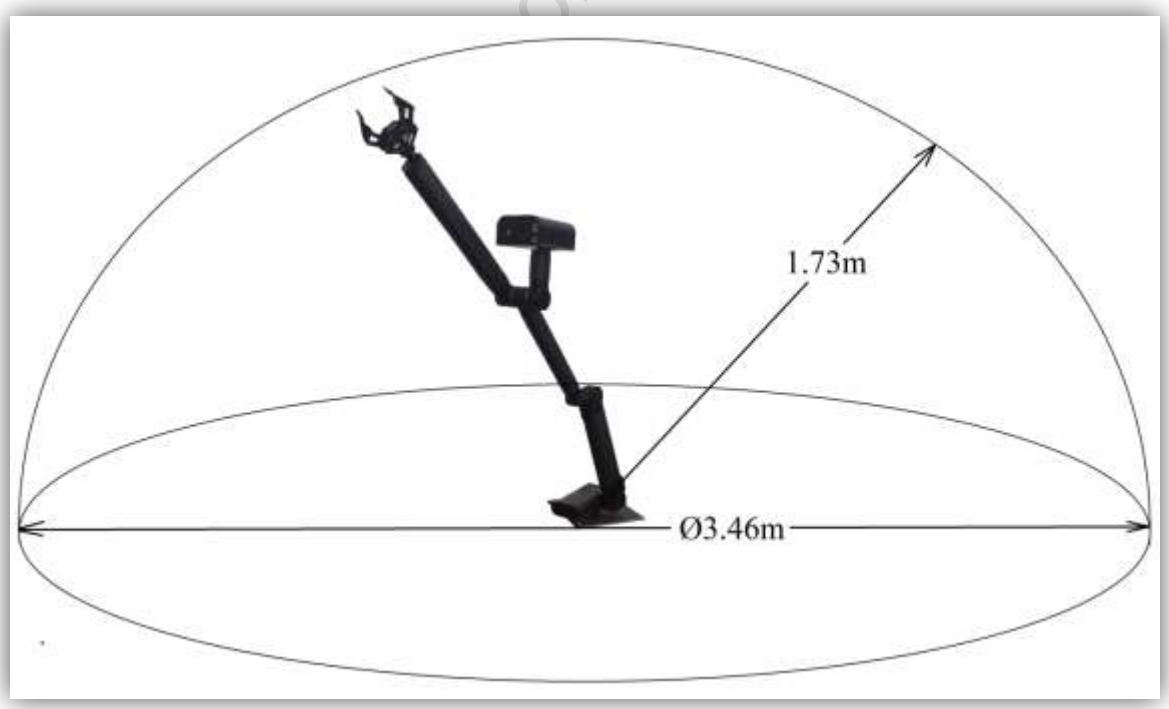

Figure 6-2: Picture showing Work Envelope Hemisphere of Turntable and Shoulder

Figure 6-3 shows the work envelope if the turntable was to be locked perpendicular to the tracks, and the rest of the joints free to move. It can be seen that the arm can reach right under

the body, should the Ratel be driving on a ledge or bridge. It also means that if the base were to stand up on its flippers, it would be possible to inspect the underbelly of the robot with the main camera, and even perhaps loose debris that might be jamming the tracks, with the gripper.

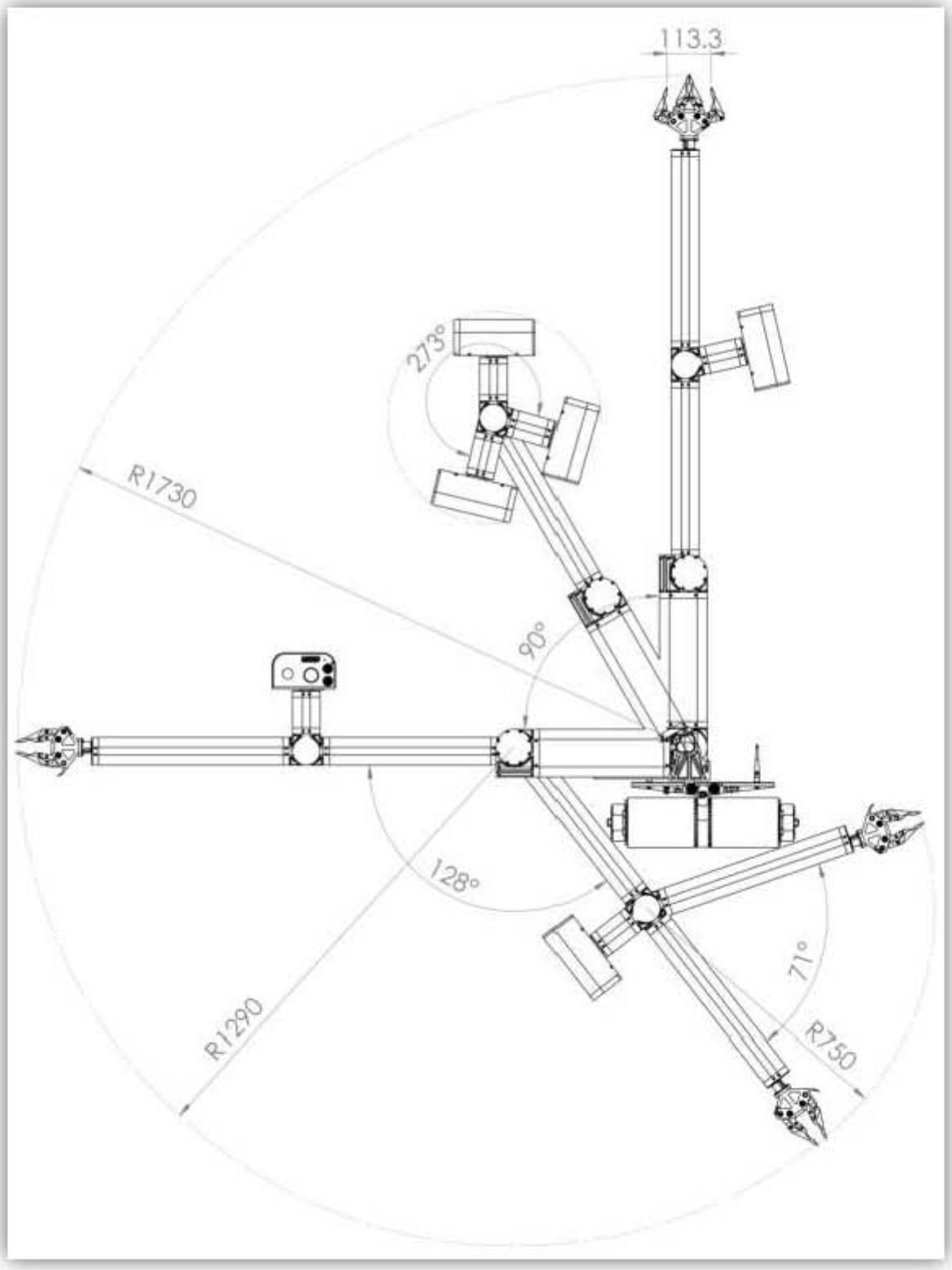

Figure 6-3: Manipulator Arm Work Envelope with Turntable Perpendicular to Tracks

Continuous rotation on the turntable, 2nd elbow, wrist and pan joints was tested. For the entire duration of the testing, and up to the date of publishing, there has not been a breakage or interruption in signal through the slip rings. An estimate of between 50 and 100 cycles were run on each joint, and all wiring is still intact.

In summary, all joints rotated to their designed limits and so the desired work envelope has been achieved. A summary of the joint's ranges can be seen in the Table 6-2.

Table 6-2: Table of Results for Work Envelope Test

Test 1	Joint	Dimension	Speed
a	Turntable	360° Continuous	16.5°/s
b	Shoulder	180°	14°/s
c	Elbow 1	360°	16.5°/s
d	Elbow 2	360° Continuous	18°/s
e	Tilt	273°	45°/s
f	Pan	360° Continuous	90°/s
g	Wrist	360° Continuous	570°/s
h	Gripper	113.3mm	45mm/s

6.3.1 Problem with Tilt and Pan Motors

During testing it was discovered that the pan and tilt motor's could not hold their position. The motors specified were brushless DC motors, with integrated electronics (speed controllers). These motors do not have position encoders, but rather give out a digital pulse that can be monitored to calculate their position [8]. It was incorrectly assumed that the speed controllers were capable of maintaining a speed of zero; it was assumed that the motors would be provided with a reverse current that would hold a zero speed. The controllers however assume a *blocked-shaft* error and cut the power to the motor, allowing it to be driven.

The result is that while the motor has sufficient torque to raise the 2kg sensor payload, it cannot stop and hold it in a horizontal position. Instead, the sensor payload „flops' back down when the motor is stopped. When the sensor payload is within 20° of the vertical, it is able to maintain its position, just due to the friction in the gearboxes. So for the period of the testing it was driven in such a way so as to maintain a near level orientation.

This is in fact the case with all the speed controllers, however because the worm and hypoid boxes restrict the arm from driving the motors, the problem does not affect the arm's joints. It is only the pan and tilt joints which are affected by it, as they have helical and bevel gearboxes, which can be driven backwards.

Mr. Bradley Springer, who is designing the advanced control for the arm, will design a control solution to hold the position of the tilt and pan motors. It will however require encoders to be fitted to the motors, and so new motors with encoders have been ordered to be fitted into these joints.

6.4 Loading Capabilities and Speed Tests

The loading capabilities of the manipulator arm were then tested. Initially, each of the lifting joints was tested to raise and lower the specified payload of 1kg, with the current and time taken to rotate being measured. A table of results of these measurements can be seen below.

Table 6-3: Table of Results for Loading Test

	Joint	Max Current (A)	Time per 90deg (s)
a	Elbow 2	1.2	6
b	Elbow 1	2.7	6
c	Shoulder	2.9	7

The maximum continuous current allowed through the motor controllers is 5A for the shoulder and elbow 1 joints, and 3A for the elbow 2 joint. From the table it can be seen that even at maximum speed, the motors are not reaching even 60% of their maximum continuous current specification. Below is a picture of the arm about to raise the 1kg payload.

Figure 6-4: Manipulator Arm holding 1kg Water Bottle at full Extension

6.4.1 PackBot Manipulator 1.0 Comparison Tests

From all the literature reviewed, it was determined that the PackBot was the industry leader in the search and rescue world. It was therefore decided to run tests comparative to the PackBot's specifications, in order to properly judge the Ratel's manipulator arm. At a manipulator reach of 1.54m, the *PackBot Manipulator 1.0* can lift 4.5kg (10lbs), and at its close-in reach, it is capable of lifting 13.6kg (30lbs).

The Ratel was then extended to a reach of 1.54m and was loaded with a 5.1kg bright steel semi-cylinder (used as a mandrel for the manufacturing of the carbon composite tubes). The arm raised and lowered the payload without any perceived difficulty. The speed however was reduced to roughly 25% so that the jerking momentum forces might be reduced. At this slower speed, the current draw for the 5.1kg payload was low; only 1.8A. This test was also used to determine safe operating limits for the arm. The test setup can be seen below.

Figure 6-5: Picture showing Manipulator Arm lifting 5.1kg at 1.54m Reach

A close-in lifting test was then performed. Its setup can be seen below.

Figure 6-6: Pictures showing Manipulator Arm lifing 15.7kg at Close in Position

The arm was driven to a position simulating picking something off the ground next to a flipper. The arm was initially tested to 14.7kg, and then loaded to 15.7kg. The manipulator arm managed to raise and lower the payload, again with no apparent difficulty. The current draw remained under 2A for the test.

Table 6-4: Table of Results for PackBot Comparison Test.

	Reach	Payload Mass (kg)
a	1.54m	5.1
b	Close-in Position	15.7

The table above shows a summary of the two tests and these values can be taken as the safe operation limits for the arm.

6.4.2 Speed Tests

As can be calculated from Table 6-3, the rotation speed is slightly below the desired 20°/s, at 13°/s for the shoulder and 15°/s for the two elbow joints. However, at the time of running these tests, a 32V power supply was being used for testing. Later, when using a 36V power source, speeds of 17°/s and 15°/s were achieved on the elbow joints and shoulder joints respectively. The turntable was tested and also achieved 17°/s, with a very low current draw of around 1A. While these speeds are less than specified, the arm performed fast enough in the Blue Arena test as described below.

6.4.3 Blue Arena (RoboCup Rescue) Test

In order to test the arm's performance within the RoboCup Rescue's Blue Arena, a time-to-extend test was performed. In the competition the robots are allowed a limited time of 20 minutes to complete as many tasks as possible. It is therefore beneficial for the USRR to move quickly and thereby achieve more tasks.

With the arm mounted at base height (180mm), and stowed in its „home position', it was extended as fast as possible to pick up a wooden block 600mm deep on a 1m high shelf. As the more advanced control of the arm is not yet developed, the time was recorded for the end-effector to reach the block's theoretical position, but not to pick it up. The desired specification was a time of less than 10s. The manipulator arm achieved it in 10.5s, which is only 5% out, and it is assumed that with more accurate control, this will be quicker.

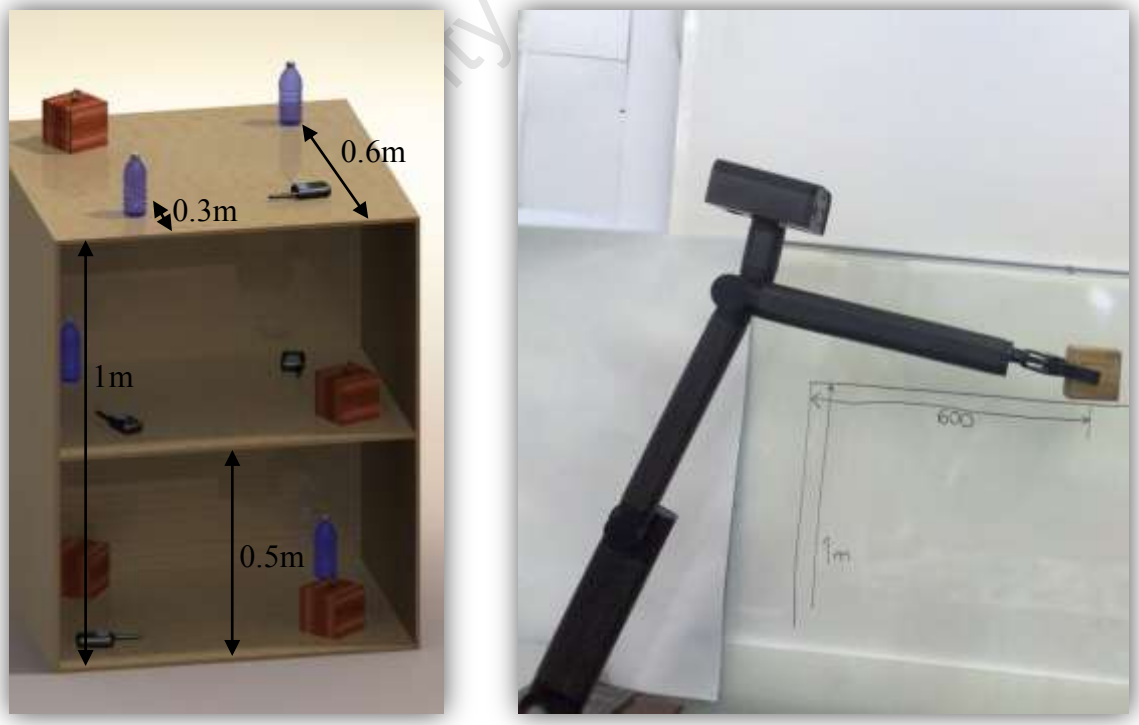

Figure 6-7: Blue Arena Test Setup

6.5 Determination of Overall Mass

The mass of the arm was measured using an electronic scale. The arm was attached to its mounting plate used during testing, which weighed 4.2kg. The overall calculated mass of the arm is 14.5kg (18.7kg - 4.2kg) including the sensor payload. As the sensor payload weighed 2kg, the arm comes to 12.5kg. These results can be seen in the table below.

Table 6-5: Table of Results for Mass Measurement

	Configuration	Mass (kg)
a	With Sensor Payload	14.5
b	Without Sensor Payload	12.5

The desired maximum mass was 10kg excluding the sensor payload. This means that the arm is 25% heavier than specified. This is undesirable, and will negatively affect the perfomance of the base. The extra wieght can be accounted forin several of the gearboxes. In order to save time and reduce machining complexity several of the *undercutting* weight saving machining operations were left out. The majority of the mass however is in the worm gearboxes. Their motors alone weigh 1kg each and the brass worm wheel and steel worm are also very heavy.

6.6 Backlash Testing on Joints

One of the main focuses of this arm, as previously discussed is the requirement for it to have low backlash. Much of the complexity in the design is due to this requirement. The resultant achieved backlash was therefore tested to determine the success of the design. The backlash was tested using a needle and protractor as seen in Figure 6-8 below. This picture is of the backlash test on the turntable joint. Close up photographs were then used to accurately determine the backlash angle. Similar setups were used for all the other joints.

Figure 6-8: Pictures showing Backlash Test on Turntable Joint

The needle's thickness is the width of one division on the protractor. The protractor was adjusted to calibrate the needle to the zero point (90° in the case below) with the joint lightly loaded in the anti-clockwise direction. The joint was then lightly loaded in the clockwise direction and the backlash was recorded as the new position of the needle minus the old position of the needle. A *light* loading is used, as only backlash is being tested; not deflection. While deflection will cause an error in the end position and is therefore undesirable, it does not contribute so much to the *shake* on the camera picture, as backlash does.

All three duplex gearboxes exhibited very low backlashes of near zero. The hypoid gearbox has a backlash of 0.5° which is significantly over the specified backlash of 0.2°. A backlash of 0.5° on this joint results in a tip error of 6.5mm which is considerably large.

Table 6-6: Table of Results for Backlash Tests

	Joint	Type of Gears Used	Angle of Backlash (deg)	Respective End Tip Displacement (mm)
a	Turntable	Duplex Gears	0~0.1	1.5
b	Shoulder	Duplex Gears	0~0.1	1.5
c	Elbow 1	Duplex Gears	0~0.1	1.1
d	Elbow 2	Hypoid Gears	0.5	6.5
e	Pan	Helical Gears	0.8	1.6
f	Tilt	Spiral Bevel Gears	0.3	1.0

This table shows a summary of the backlash results, as well as the respective displacement of the end tip of the arm due to the angular error.

6.7 Summary

This chapter has reported on the tests performed on the manipulator arm, and has listed the results of these tests. The cost breakdown was given, of which the ordered parts came to R75 000. The work envelope was tested and the arm achieved a horizontal reach of 1.73m. Loading and speed tests were performed. The arm lifted 5.1kg at a reach of 1.54m and 15.7kg at a close in position. The shoulder joint achieved a rotational speed of 15°/s while the others achieved speeds of higher than 17°/s.

The arm was weighed and came to a mass of 12.5kg. The backlash of each joint was tested; the duplex worm joints exhibited near-zero backlash, while the 2nd elbow, Pan and Tilt came to 0.5°, 0.8° and 0.3° respectively.

Conclusions on the performance of the arm in these tests are drawn in the following chapter and recommendations for future work are listed in the chapter after that.

7 Conclusion

7.1 Duplex Worm Gearboxes

The turntable, shoulder and first elbows, which used the duplex worm gear boxes, were a very successful design, exhibiting very low levels of backlash, and being strong enough to easily lift the specified weight. Their motor pairing proved to be ideal, lifting a tested amount of twice the specified amount, and only rotating slightly slower (15% less) than specified. The motor choice was also ideal in the fact that it has never exceeded 3A, keeping the controllers well within their normal operating range (0-5A). These gearboxes are slightly heavy however, and do not lend themselves to a small and compact housing.

7.2 Hypoid Gearbox

The second elbow joint, which operates with a hypoid gearbox, was also a successful design in all areas barring its backlash qualities. See Recommendations for a suggested fix to this problem. It exhibited excellent strength and speed qualities; above those specified, while maintaining a low weight. It is the author's favoured design of gearbox, as it showed extremely beneficial strength-to-weight and strength-to-size ratios making it very strong whilst being very compact and light. See Recommendations for further use of this design in future generation arms.

7.3 Pan and Tilt Joints

The pan and tilt motor and gearbox combinations were not entirely successful. They exhibited sufficient speed and strength to achieve the required specifications, and were relatively low weight designs. The pan joint successfully incorporated continuous rotation and both designs were compact. They were very smooth, quiet and low in vibration. However they were unsuccessful in that they could not hold their position, and were able to be driven in reverse order causing the sensor payload to ‚flop' around. A solution to this is being designed by the control engineer, and better motor and controller options have been ordered.

The interface between the arm and sensor payload was also very successful; being both sturdy and quick and easy to detach.

7.4 Torsion Spring

The gravity compensating torsion spring also proved very successful, assisting in the arms high strength lifting capabilities. Its design is small and compact, (fitting inside the worm wheel's shaft) while it provides considerable help to the shoulder joint.

7.5 Internal Wiring

The incorporation of internal wiring worked as expected, with continuous rotation on several joints. The slip rings worked continuously, and robustly. The manipulator arm therefore has a very clean exterior and is unlikely to catch on debris. The wires are also protected from damage, being safely housed in the arm's tubes.

7.6 Overall Performance

When compared to the iRobot PackBot Manipulator 1.0, which is considered by some to be the industry leader, it can be concluded that the UCT Ratel manipulator arm is a successful design. A summary of their comparisons is shown in Table 7-1.

Table 7-1: Comparison of PackBot Manipulator 1.0 [10] and UCT Ratel Manipulator

	iRobot PackBot 510 Manipulator 1.0 [10]	**UCT Ratel Manipulator Arm**
Degrees of Freedom	6 + Pan and Tilt	6 + Pan and Tilt
Full Extension of Camera	1.87m	1.18m
Full Extension of Gripper	1.54m	1.73m
Lift at 1.54m Reach	4.5kg	5.1kg
Lift at Close-in Position	13.6kg	15.7kg
Overall Mass	9.3kg	12.5kg
Internal Wiring	Yes	Yes
Continuous Rotation at Turntable, Wrist and Pan Joints	Yes	Yes
Other Features	Waterproof	Low Backlash
Cost	R650'000	R75'000 + Machining

It proves to be stronger and reach further than the PackBot. It is 34.4% heavier, but this does not affect its own performance, as it still manages to lift more. It is estimated that with machining, the cost will be less than 20% of the cost of the Packbot's Manipulator 1.0 which is a considerable saving, and makes the arm more of a viable option for third world countries' rescue teams.

Furthermore if the arm was to move from the prototype stage into production and aluminium gearbox castings could be made (like those of the PackBot's arm), it would further save on cost, production time and a lighter arm could be produced, making it even more competitive.

The final conclusion is therefore that the manipulator arm designed, built and tested in this project is successful, and meets the required specifications. It is a global competitor at a significantly lower cost. Coupled with a user-friendly and accurate control system, it will perform well in the search and rescue role. It is versatile and dexterous enough to be implemented in both the military and mining environments as well.

8 Recommendations

8.1 Hypoid Backlash Reduction

To reduce the backlash of the hypoid gearbox, it is recommended that the aluminium spacer be lengthened by 0.1-0.2mm to ‚push' the wheel further into the worm. Various size spacers can be manufactured and tested. This will effectively reduce the centre distance slightly, and could thereby reduce the backlash. A similar quick fix could be applied to the worm, instead of the wheel, ‚pushing' the worm into the wheel, again effectively reducing the centre distance. A theoretical estimate of the resultant backlash due to this modification is 0.10mm which is taken from the KHK Gear Catalogue [9] which assumes correct mounting.

8.2 Next Generation Arm Suggestions

If the backlash of the hypoid gearbox could be reduced, it is recommended that the next generation arm to be built uses only this type of gearbox, on all of the joints. Its low weight and compact design and high strength make it the obvious gearbox choice for a more compact arm. The PackBot Manipulator 1.0 is believed to use these gearboxes, and while they do not exhibit as low backlash as that of the *duplex* worm gearboxes, they are superior in almost all the other areas.

I would also suggest that, on the next generation arm, high viscosity fluid dampers be investigated, for use on the joints, to dampen quick shake and provide smoother motion. High quality video camera tripods utilise such dampers to allow only smooth motions to be made. That is: the operator can move the camera smoothly, but any sharp movements are prohibited by the high viscosity fluid. These fluid dampers are also used on paper reels to prevent an over-wind when the paper is pulled and the reel is accelerated. If the implementation of these dampers is successful, then the requirement of low backlash will be less important and smoother arm and camera movements will be achieved.

9 Main Body References

[1] iRobot, "PackBot 510," [Online]. Available: http://www.boston.com/business/ticker/packbot102902.jpg. [Accessed 10 8 2010].

[2] NIST, "RoboCup Rescue," [Online]. Available: http://www.robocuprescue.org/. [Accessed 6 August 2010].

[3] RoboCup, "RoboCupRescue Robot League Rules 2009.1," [Online]. Available: http://robotarenas.nist.gov/2010/RoboCupRescueRobotLeagueRules(v2009.1D)pdf.pdf. [Accessed 10 04 2010].

[4] W. P. Crosher, Design and Application of the Worm Gear, New York: ASME Press, 2002.

[5] Allytech, "OTT Dual Lead Concept - Duplex Design," [Online]. Available: http://www.allytech.eu/index_fichiers/DualLeadwormgearswithoutbacklah.htm. [Accessed 26 October 2010].

[6] ByTune Electronics, *BT016 Series Slip Ring,* 2012.

[7] SKF, *General Catalogue,* 1994.

[8] Maxon Motor, *Program 2011/12,* 2011.

[9] KHK Co., Ltd., *Product Guide and Technical Data,* 2009.

[10] iRobot, "PackBot, 510," [Online]. Available: http://www.irobot.com/gi/ground/510_PackBot. [Accessed 28 Jan 2012].

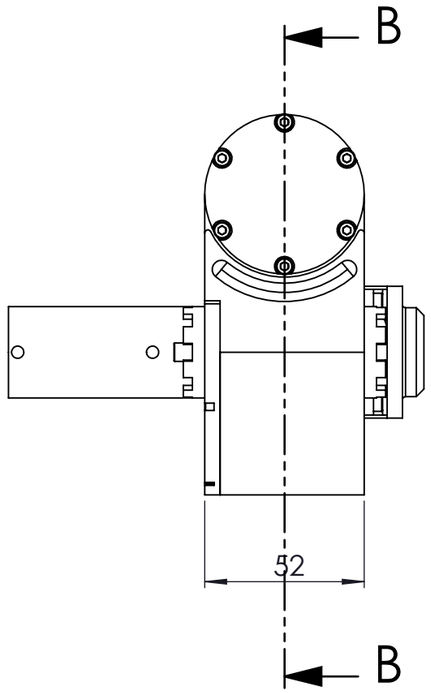

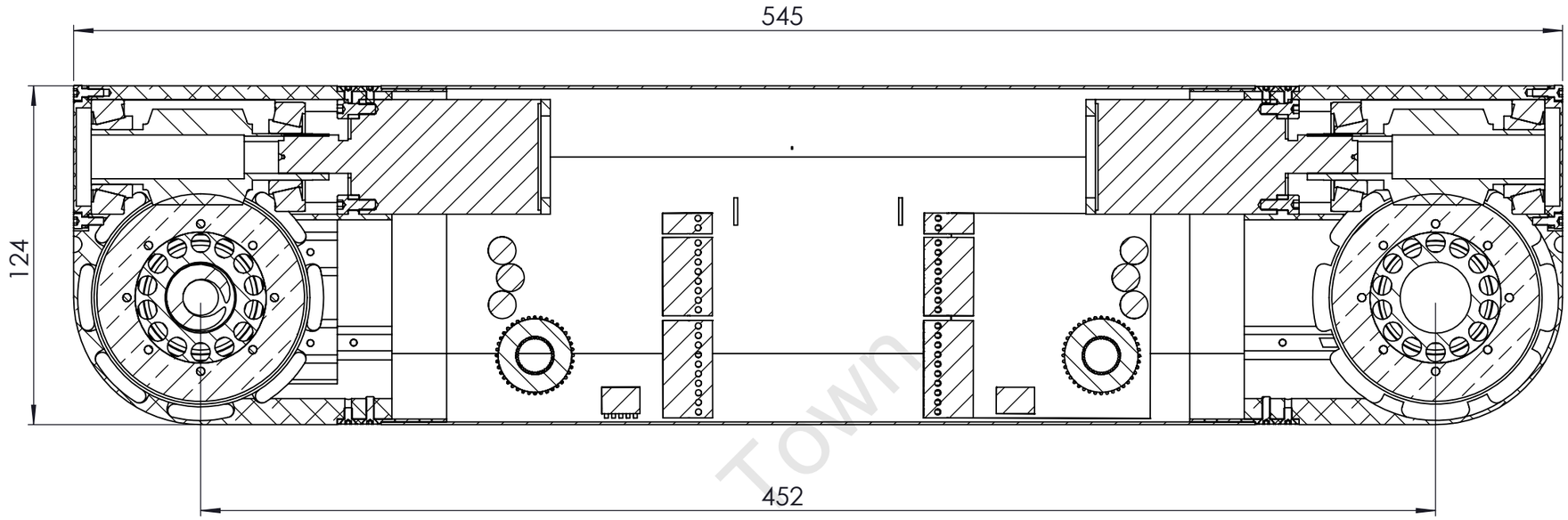

SECTION B-B
SCALE 1 : 2

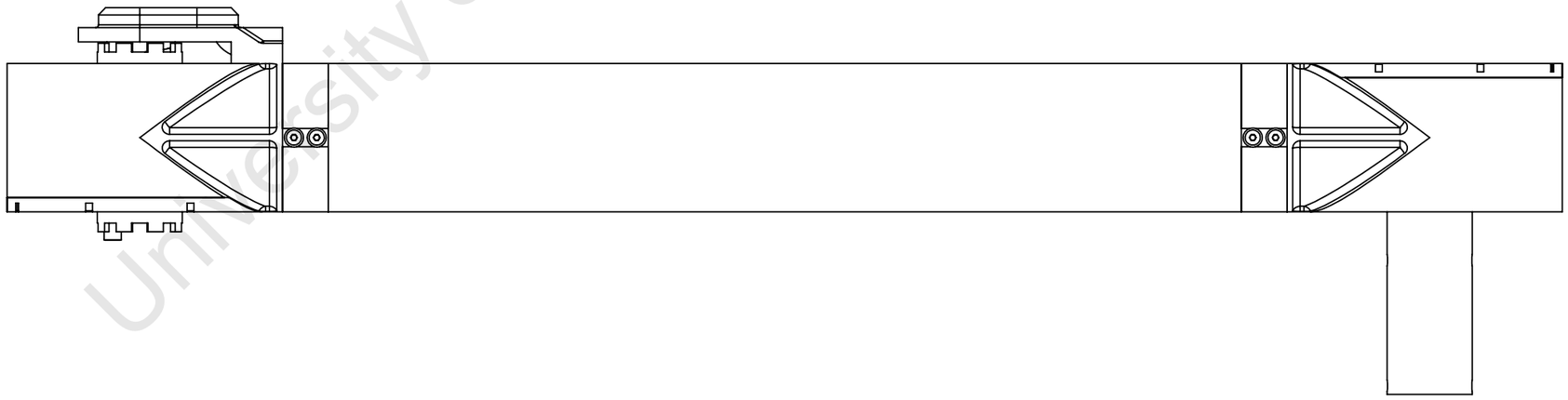

A3 Landscape	University of Cape Town Department of Mechanical Engineering			
	Title: Bottom Section Sub Assembly			
Assembly Drawing	Scale: 1:2.5	Date: 08/09/2011	Sheet 1	of 1
	Drawn By: Peter Henson RARL Mech. Eng.		Drawing Number E5	

ITEM NO.	PART NUMBER	QTY.
1	Spring End Clamp	1
2	Spring and Cable Cover	1
3	Torsion Spring 3	1
4	Gear Housing Sub-Assembly A	1
4.1	AGDL2-36R1_edited	1
4.2	KWGDLS2-R1_edited	1
4.3	ec40ass	1
4.3.1	GP-42 3 stage	1
4.3.2	gearbox_adaptor	1
4.3.3	ec40-120w	1
4.3.4	heds-5540	1
4.4	DECV 505	1
4.5	Large Composite Tube	1
4.6	SKF - 32004 X	1
4.7	SKF - 30203	1
4.8	Gear Housing Sub-Assembly A	2
4.9	Worm Bearing End Cover	1
4.10	SKF - 61806	2
4.11	Wormgear Bearing Side Cover	1
4.12	Worm Gear Shaft Nut	1
4.13	M3 x 0.5 x 10 Hex SHCS	8
4.14	Large Tube End Interface	1
4.15	M3 x 0.5 x 8 Hex SHCS	14
4.16	M3 x 0.5 x 6 Socket FCHS	7
4.17	M3 x 0.5 x 10 Socket FCHS	1
4.18	M 4 x 0.7 x 10 Hex SHCS	4
5	Gear Housing Sub-Assembly B	1
5.1	AGDL2-36R1_edited	1
5.2	KWGDLS2-R1_edited	1
5.3	ec40ass	1
5.3.1	GP-42 3 stage	1
5.3.2	gearbox_adaptor	1
5.3.3	ec40-120w	1
5.3.4	heds-5540	1
5.4	DECV 505	1
5.5	SKF - 32004 X	1
5.6	SKF - 30203	1
5.7	Gear Housing Sub-Assembly B	2
5.8	Worm Bearing End Cover	1
5.9	SKF - 61806	2
5.10	Wormgear Bearing Side Cover	1
5.11	Worm Gear Shaft Nut	1
5.12	M3 x 0.5 x 8 Hex SHCS	22
5.13	Large Tube End Interface	1
5.14	M3 x 0.5 x 6 Socket FCHS	7
5.15	M3 x 0.5 x 10 Socket FCHS	1
5.16	M4 x 0.7 x 10 Hex SHCS	4
5.6	M3 x 0.5 x 10 Hex SHCS	4

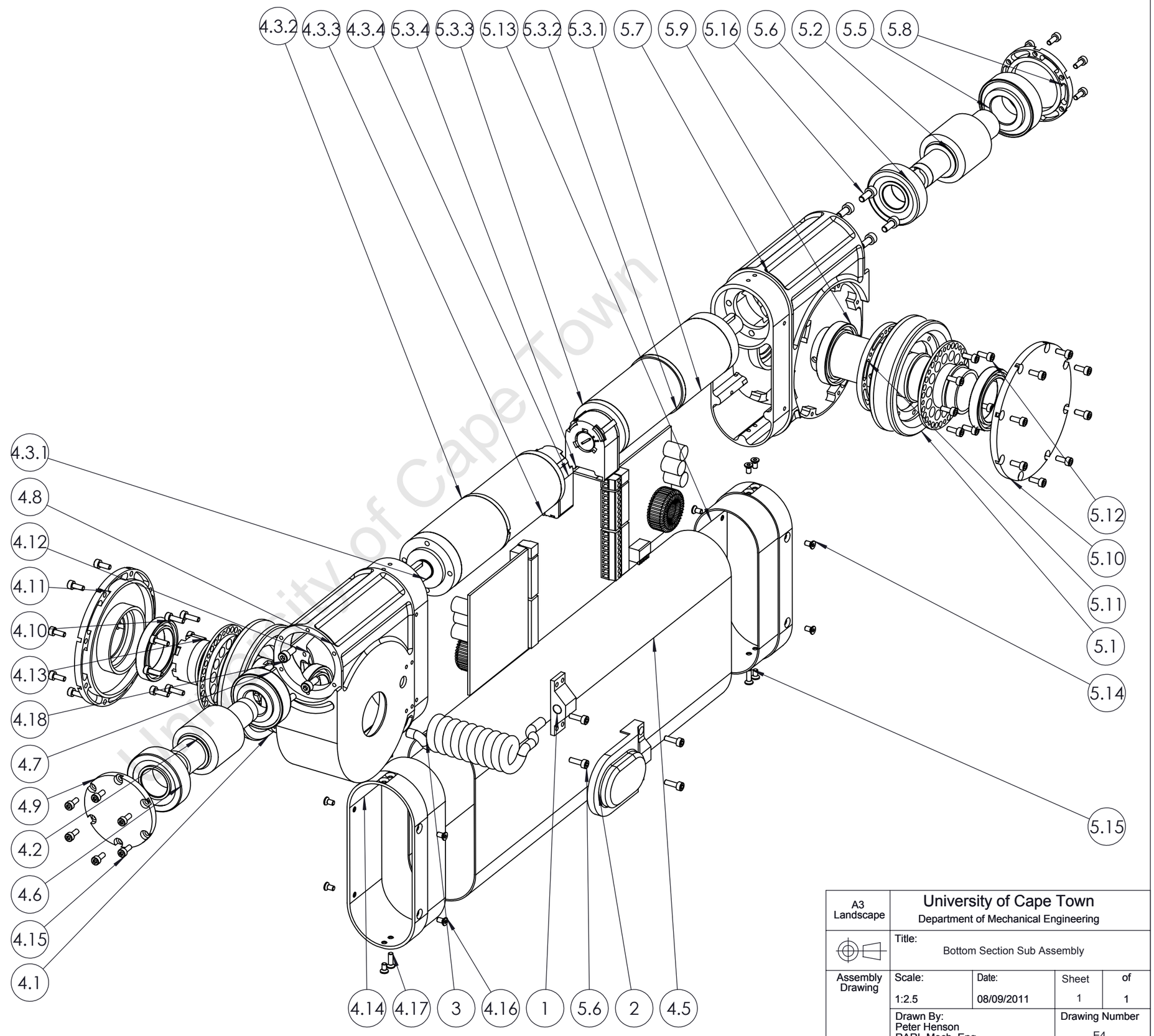

A3 Landscape	University of Cape Town Department of Mechanical Engineering			
	Title: Bottom Section Sub Assembly			
Assembly Drawing	Scale: 1:2.5	Date: 08/09/2011	Sheet 1	of 1
	Drawn By: Peter Henson RARL Mech. Eng.		Drawing Number E4	

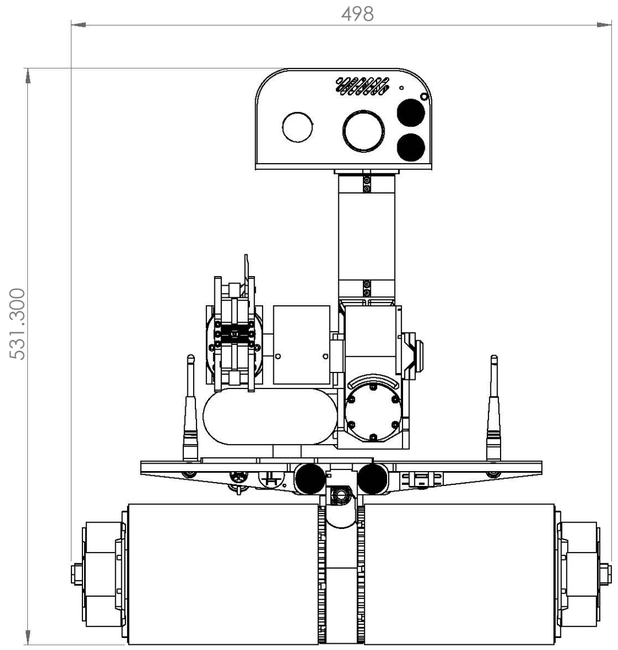

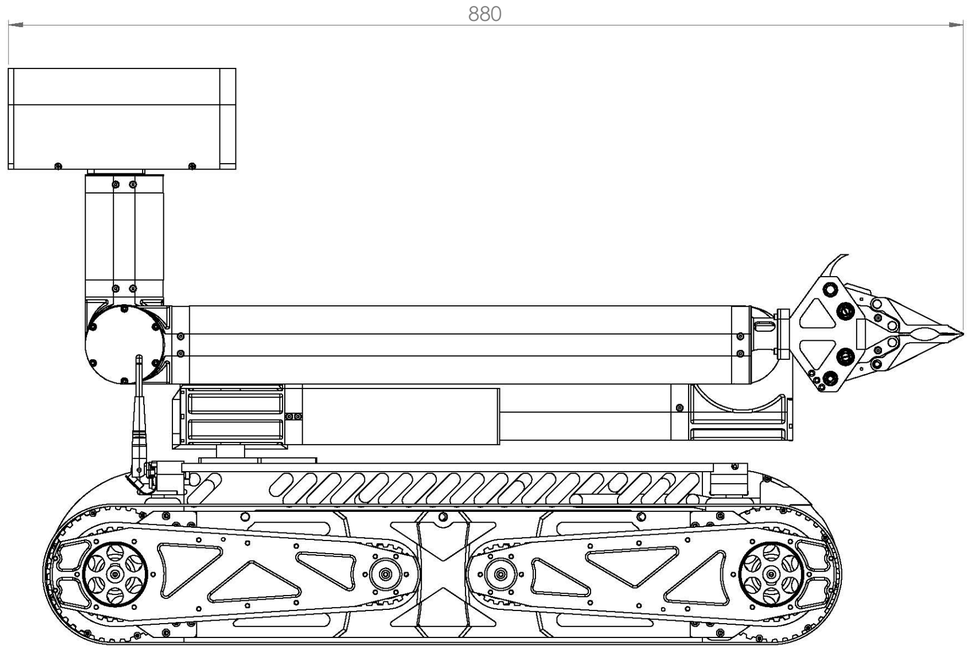

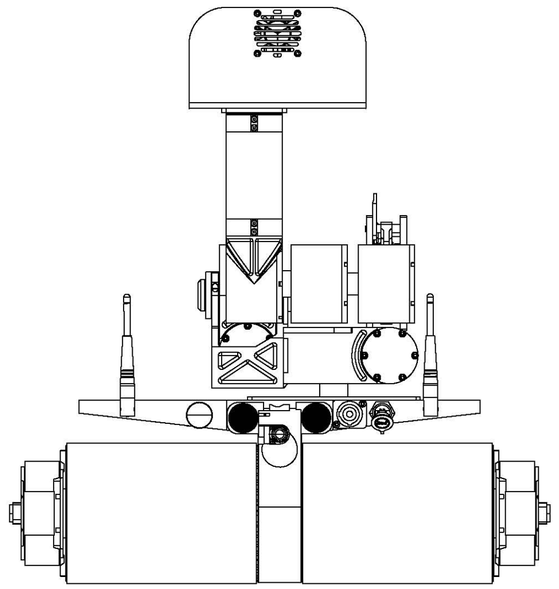

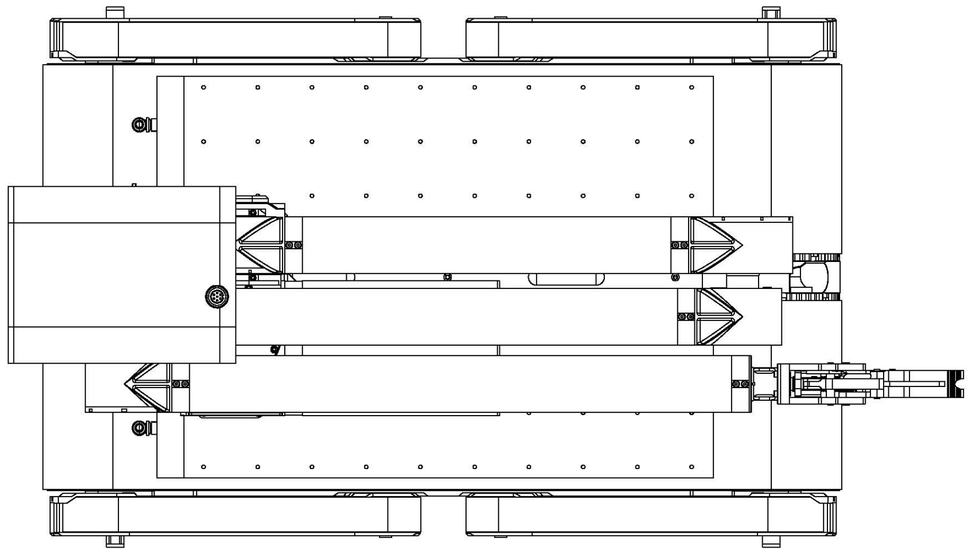

UNLESS OTHERWISE SPECIFIED: DIMENSIONS ARE IN MILLIMETERS SURFACE FINISH: TOLERANCES: LINEAR: ANGULAR:		FINISH:			DEBUR AND BREAK SHARP EDGES	DO NOT SCALE DRAWING	REVISION
	NAME	SIGNATURE	DATE			TITLE:	
DRAWN							
CHK'D							
APPV'D							
MFG							
Q.A				MATERIAL:		DWG NO.	A2
						Complete Skeleton Assembly	
				WEIGHT:		SCALE:1:4	SHEET 1 OF 1

SolidWorks Student Edition.
For Academic Use Only.

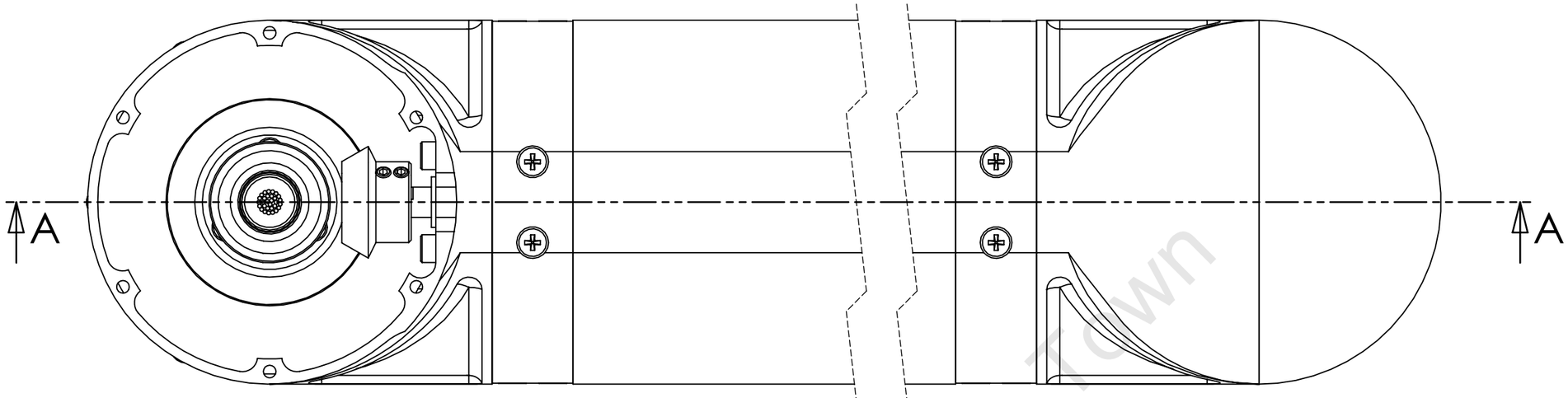

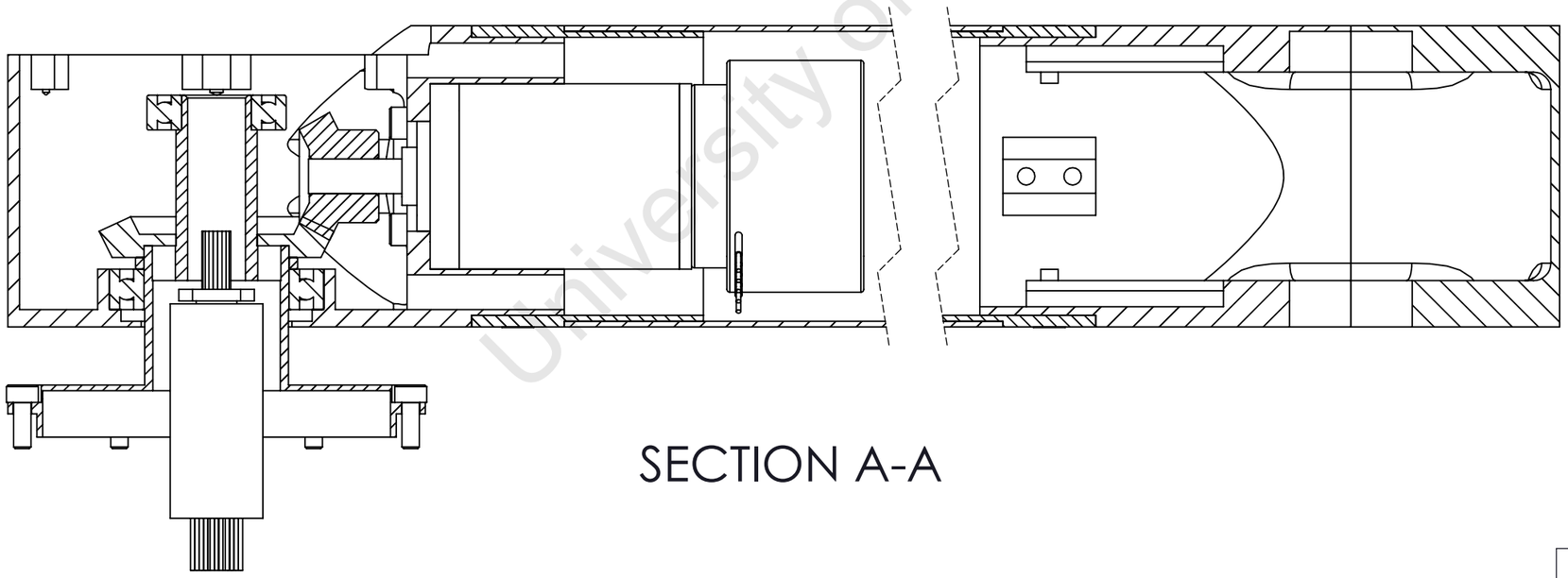

SECTION A-A

A3 Landscape	University of Cape Town Department of Mechanical Engineering			
	Title: Mid Section Sub Assembly			
Assembly Drawing	Scale: 1:1	Date: 04/05/2011	Sheet 1	of 1
	Drawn By: Peter Henson RARL Mech. Eng.		Drawing Number E7	

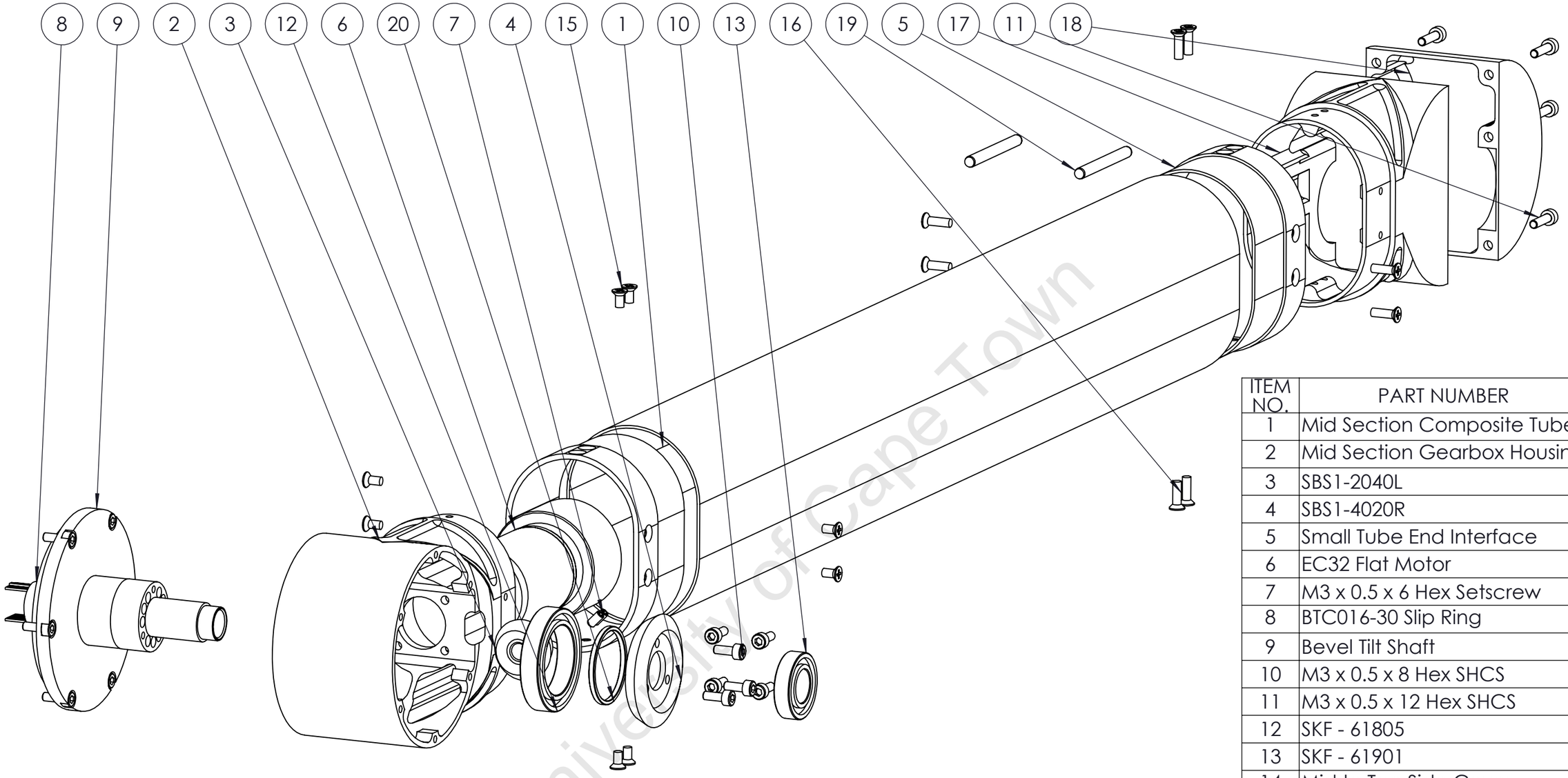

ITEM NO.	PART NUMBER	QTY.
1	Mid Section Composite Tube	1
2	Mid Section Gearbox Housing	1
3	SBS1-2040L	1
4	SBS1-4020R	1
5	Small Tube End Interface	2
6	EC32 Flat Motor	1
7	M3 x 0.5 x 6 Hex Setscrew	2
8	BTC016-30 Slip Ring	1
9	Bevel Tilt Shaft	1
10	M3 x 0.5 x 8 Hex SHCS	13
11	M3 x 0.5 x 12 Hex SHCS	6
12	SKF - 61805	1
13	SKF - 61901	1
14	Mid to Top Side Cover	1
15	M3 x 0.5 x 6 Counter Sunk	8
16	M3 x 0.5 x 10 Counter Sunk	8
17	Bottom to Mid Clamp 1	1
18	Bottom to Mid Clamp 2	1
19	Parallel Pin 4 x 40	2
20	Mid Section Bearing Spacer	1

A3 Landscape	University of Cape Town Department of Mechanical Engineering			
	Title: Mid Section Sub Assembly			
Assembly Drawing	Scale: 1:1.5	Date: 04/05/2011	Sheet 1	of 1
	Drawn By: Peter Henson RARL Mech. Eng.		Drawing Number E6	

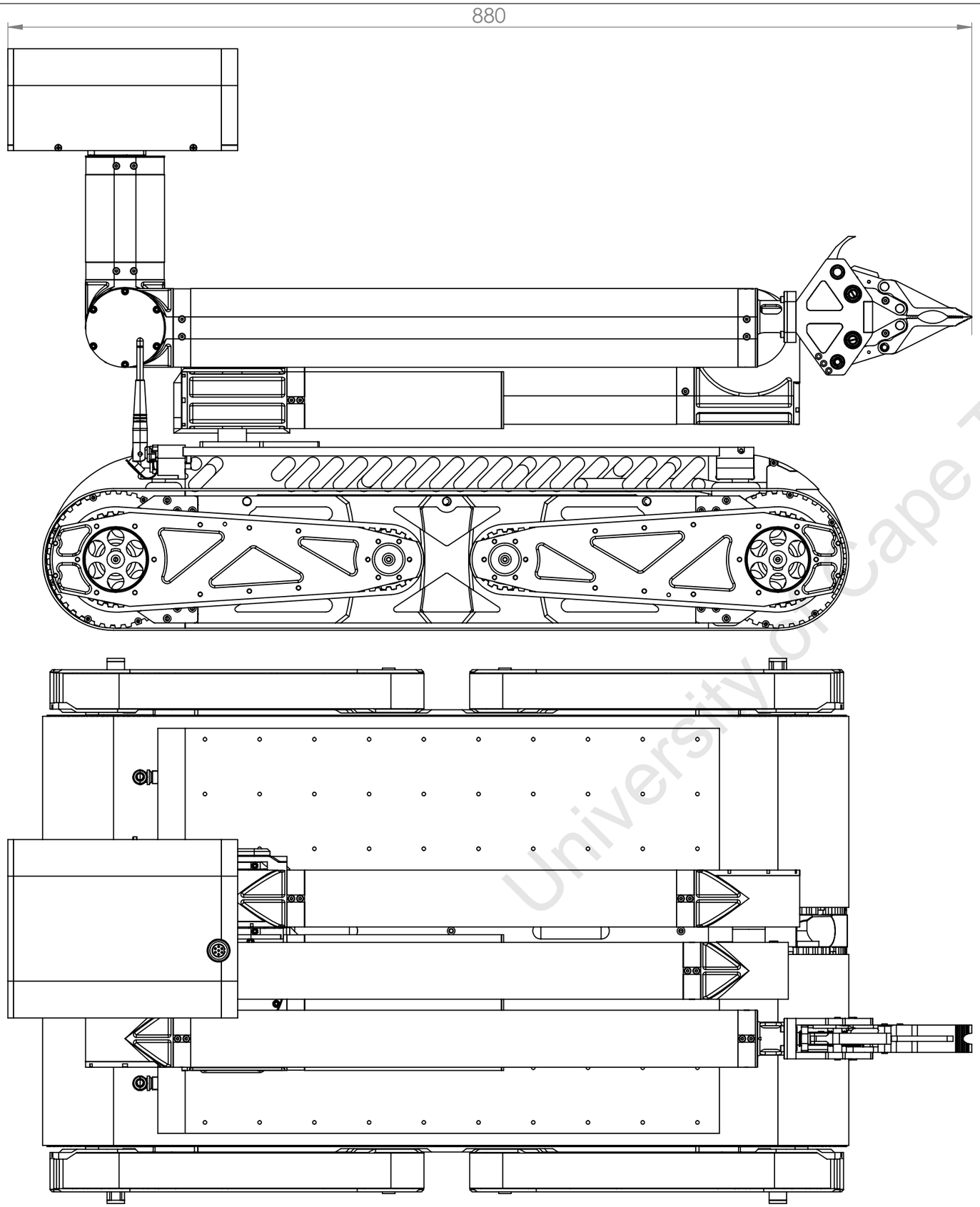

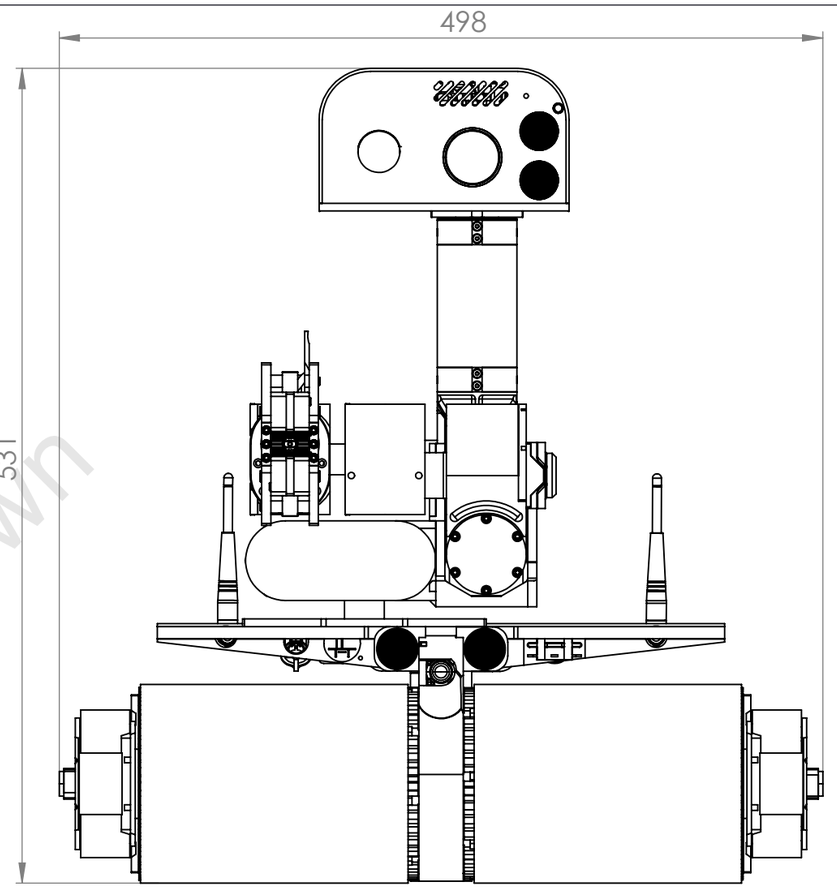

A3 Landscape	University of Cape Town Department of Mechanical Engineering			
	Title: Overall System Assembly			
Assembly Drawing	Scale: 1:4	Date: 19/09/2011	Sheet 1	of 1
	Drawn By: Peter Henson RARL Mech. Eng.		Drawing Number E1	

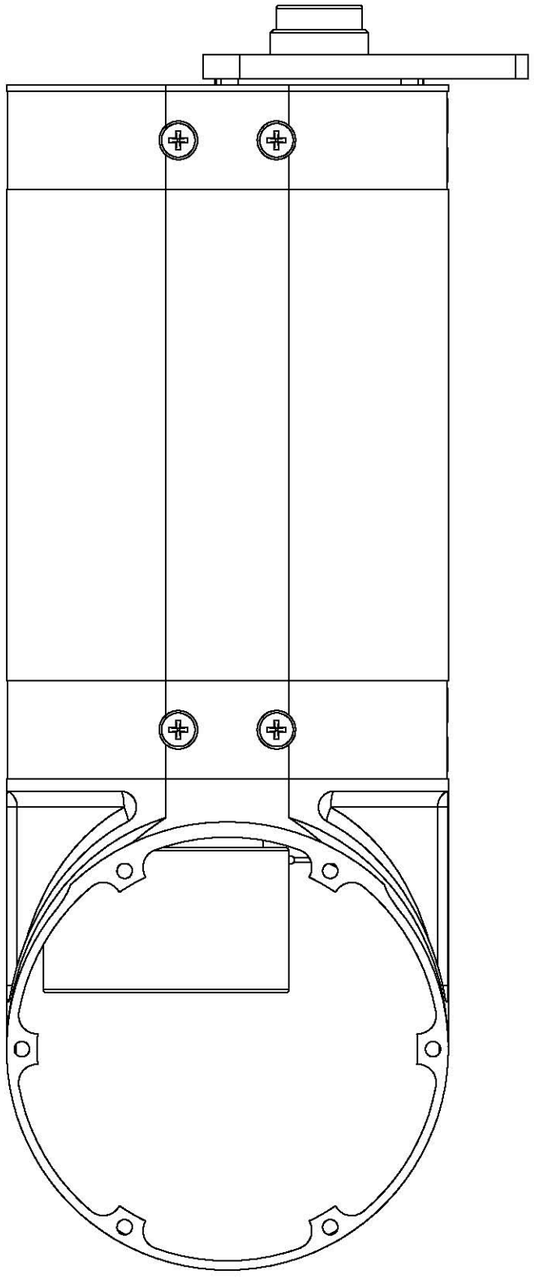

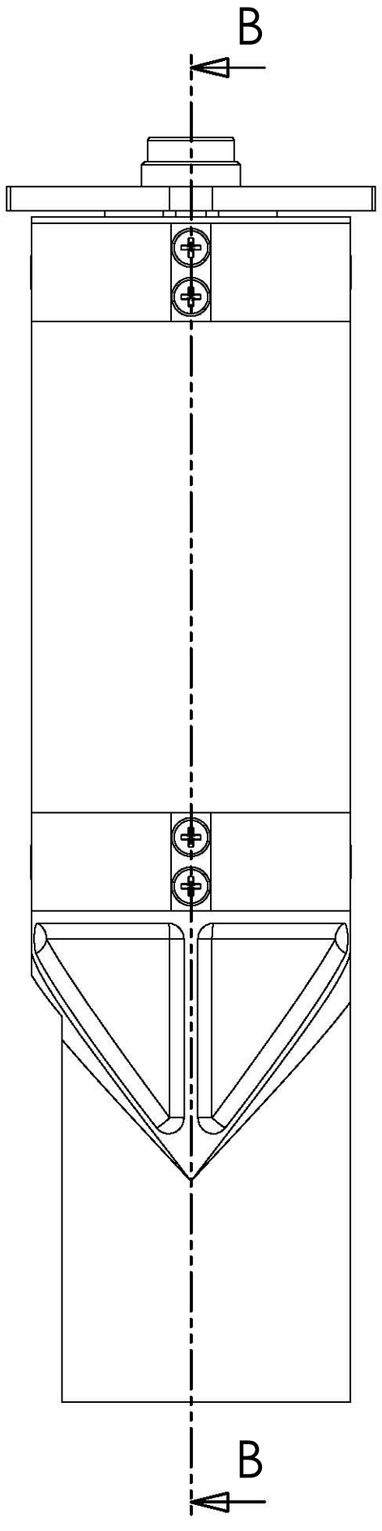

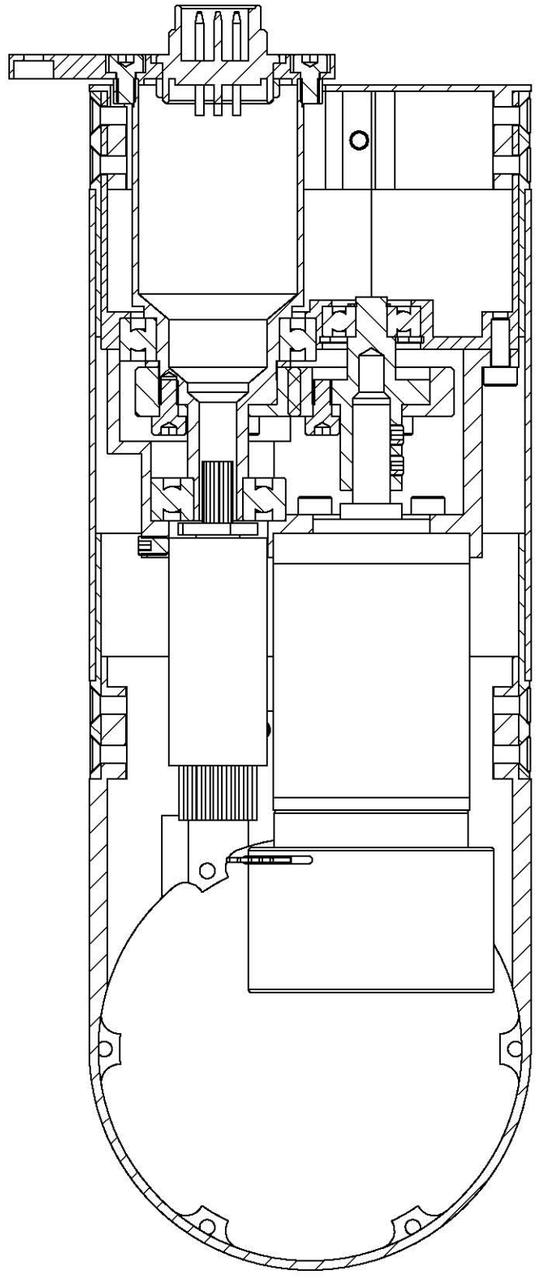

SECTION B-B

A3 Landscape	University of Cape Town Department of Mechanical Engineering			
	Title: Pan-tilt Section Sub Assembly			
Assembly Drawing	Scale: 1:1	Date: 13/05/2011	Sheet 1	of 1
	Drawn By: Peter Henson RARL Mech. Eng.		Drawing Number E11	

ITEM NO.	PART NUMBER	QTY.
1	Pan-Tilt Composite Tube	1
2	Small Tube End Interface	2
3	Pan Motor Housing	1
4	EC32 Flat- GP32 Pan-Tilt Motor	1
5	Pan Shaft	1
6	KHG1-25L	1
7	KHG1-25R	1
8	Motor Helical Mount Shaft	1
9	SKF - 625	1
10	SKF - 608	1
11	SKF - 61804	1
12	M3 x 0.5 x 6 Hex SHCS	6
13	M3 x 0.5 x 8 Hex SHCS	7
14	M3 x 0.5 x 5 Hex SHCS	2
15	BTC016-30 Slip Ring	2
16	Pan Gear Bearing housing	1
17	Pan Motor Bearing Housing	1
18	M3 x 0.5 x 6 Countersunk	16
19	Pan-Section Bearing Spacer	1
20	M16 Internal Circlip	1
21	M5 External Circlip	1
22	7 Pin Inline Plug Male	1
23	7 Pin Inline Plug Male Nut	1
24	Pan Section End Cover	1
25	M3 x 0.5 x 5 Hex Set Screw	3
26	Pan Tilt to Sensor Payload Interface 2	1

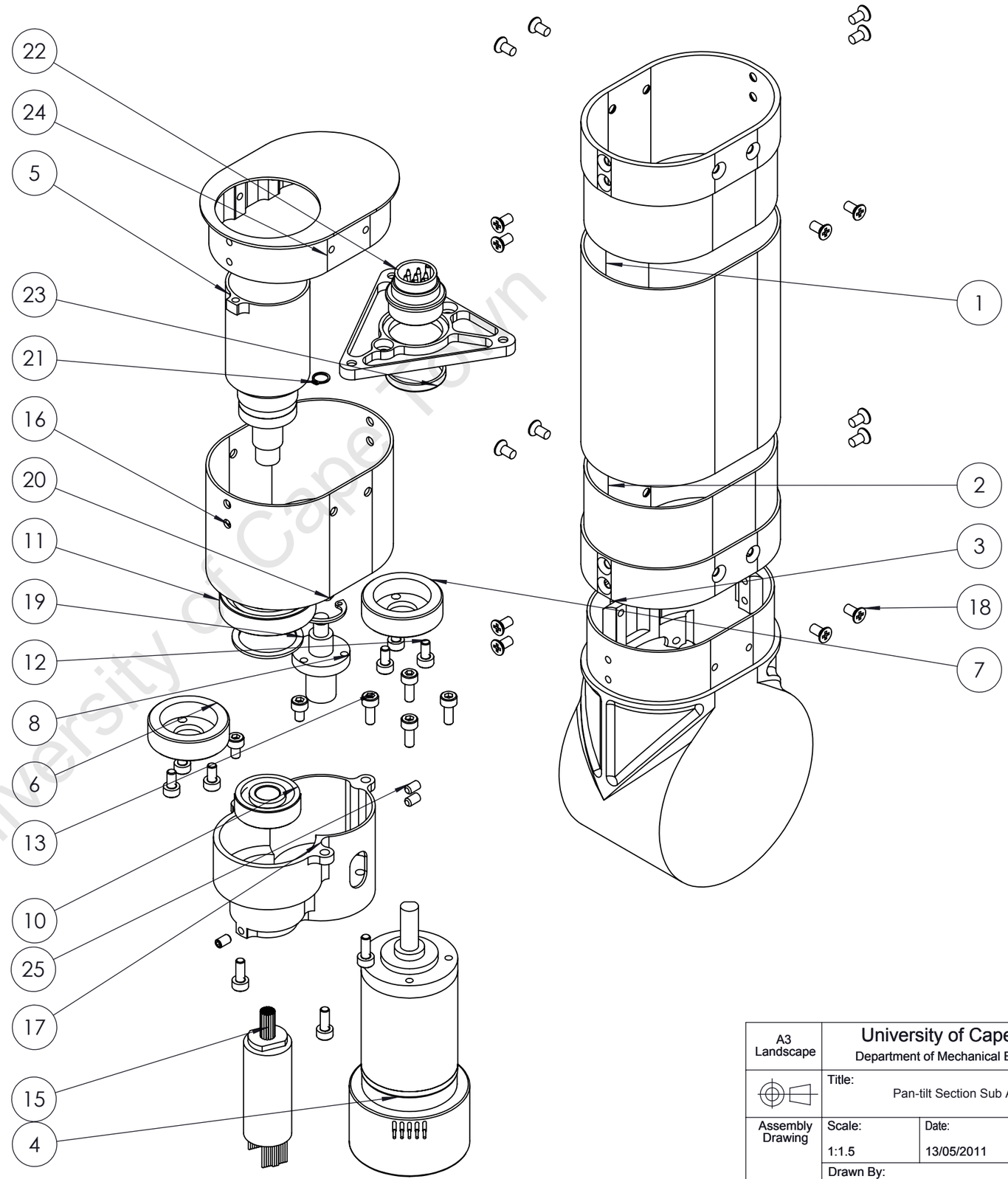

A3 Landscape	University of Cape Town Department of Mechanical Engineering			
	Title: Pan-tilt Section Sub Assembly			
Assembly Drawing	Scale: 1:1.5	Date: 13/05/2011	Sheet 1	of 1
	Drawn By: Peter Henson RARL Mech. Eng.		Drawing Number E10	

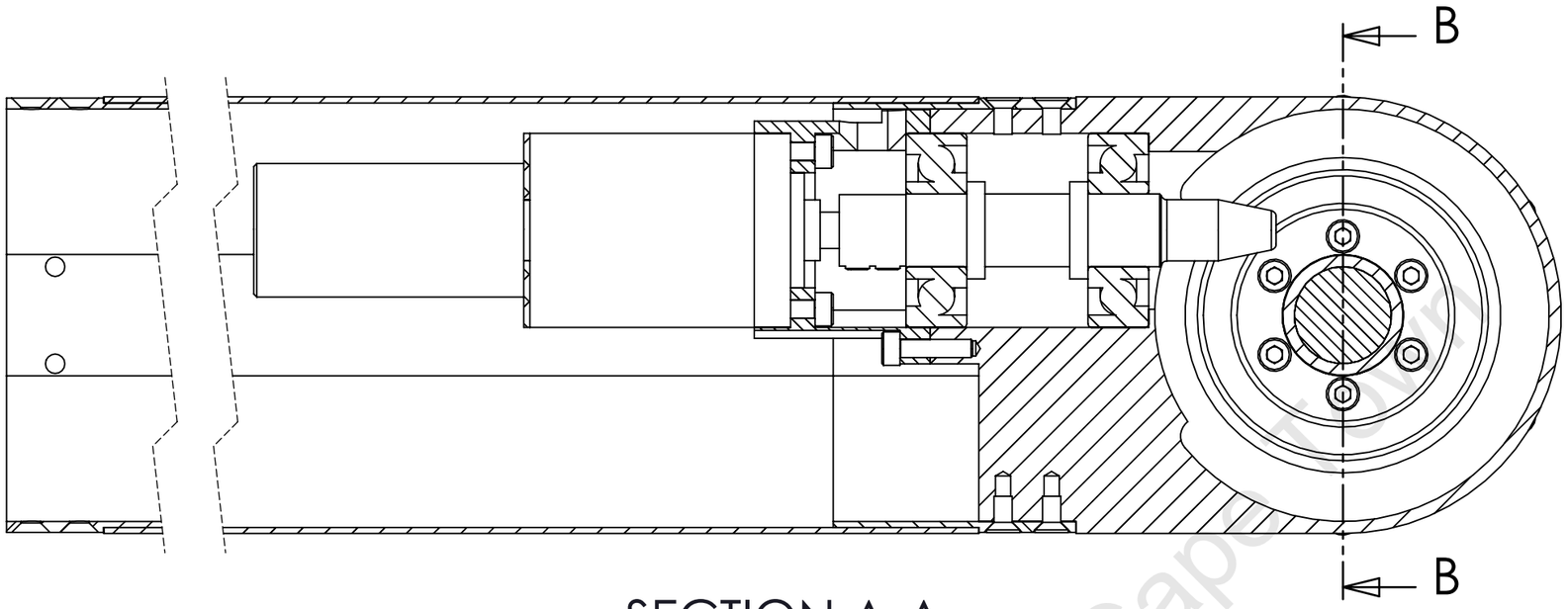

SECTION A-A

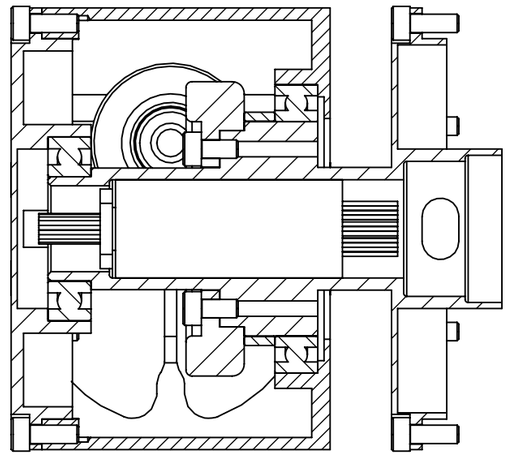

SECTION B-B

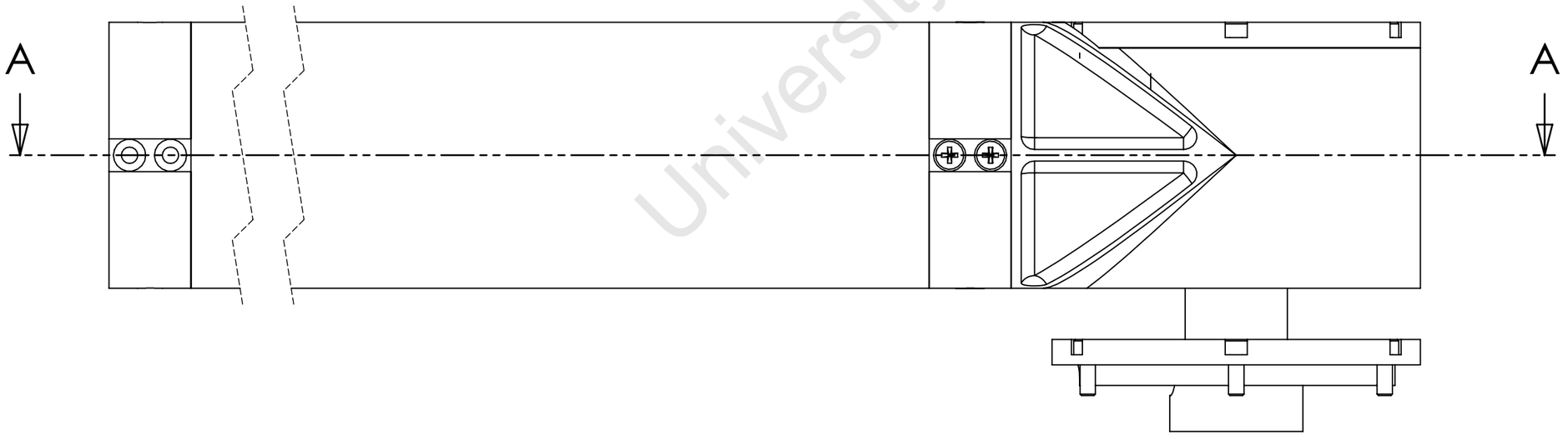

A3 Landscape	University of Cape Town Department of Mechanical Engineering			
	Title: Top Section Sub Assembly			
Assembly Drawing	Scale: 1:1	Date: 04/05/2011	Sheet 1	of 1
	Drawn By: Peter Henson RARL Mech. Eng.		Drawing Number E9	

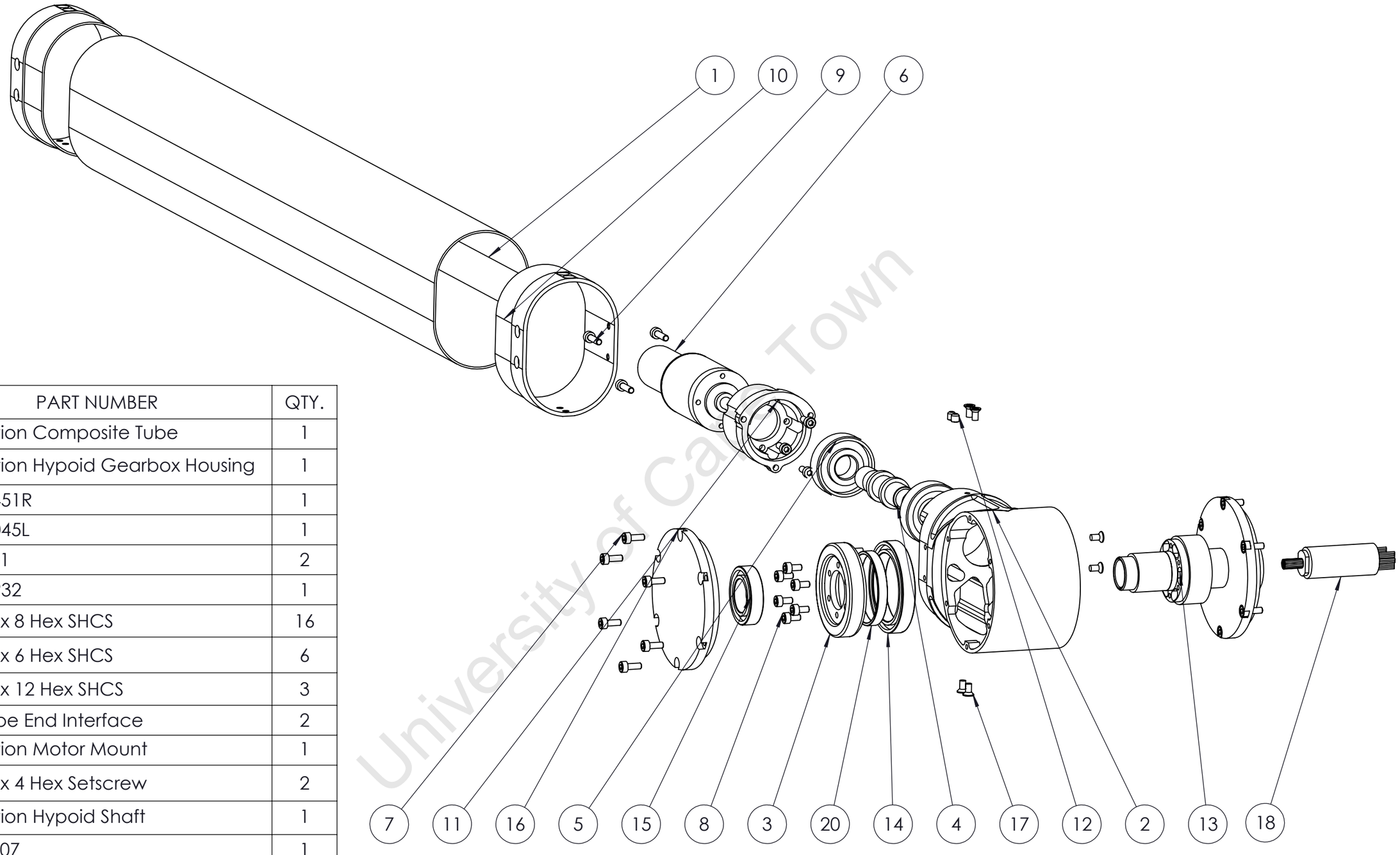

ITEM NO.	PART NUMBER	QTY.
1	Top Section Composite Tube	1
2	Top Section Hypoid Gearbox Housing	1
3	MHP1-0451R	1
4	MHP1-1045L	1
5	SKF - 6201	2
6	EC22 GP32	1
7	M3 x 0.5 x 8 Hex SHCS	16
8	M3 x 0.5 x 6 Hex SHCS	6
9	M3 x 0.5 x 12 Hex SHCS	3
10	Small Tube End Interface	2
11	Top Section Motor Mount	1
12	M4 x 0.7 x 4 Hex Setscrew	2
13	Top Section Hypoid Shaft	1
14	SKF - 61807	1
15	SKF - 61903	1
16	Top Section Hypoid End Cover	1
17	M3 x 0.5 x 6 Counter Sunk	8
18	BTC016-30 Slip Ring	1
19	Mid to Top Side Cover	1
20	Top Section Bearing Spacer	1

A3 Landscape	University of Cape Town Department of Mechanical Engineering			
	Title: Top Section Sub Assembly			
Assembly Drawing	Scale: 1:2	Date: 04/05/2011	Sheet 1	of 1
	Drawn By: Peter Henson RARL Mech. Eng.		Drawing Number E8	

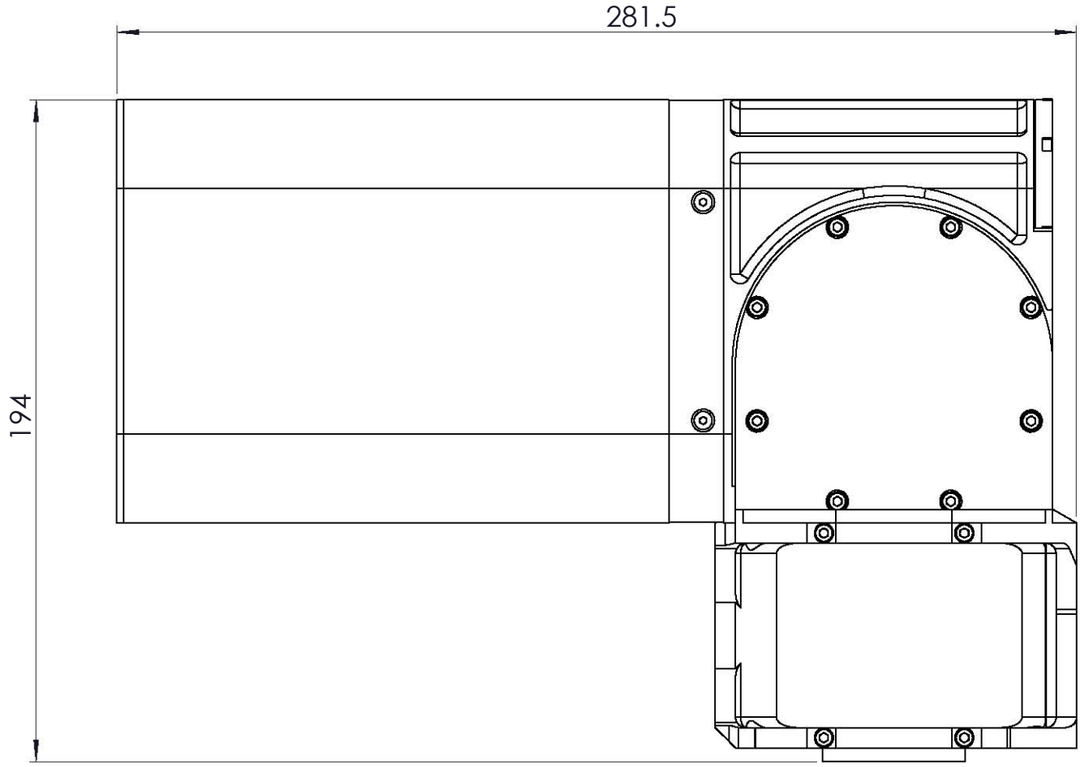

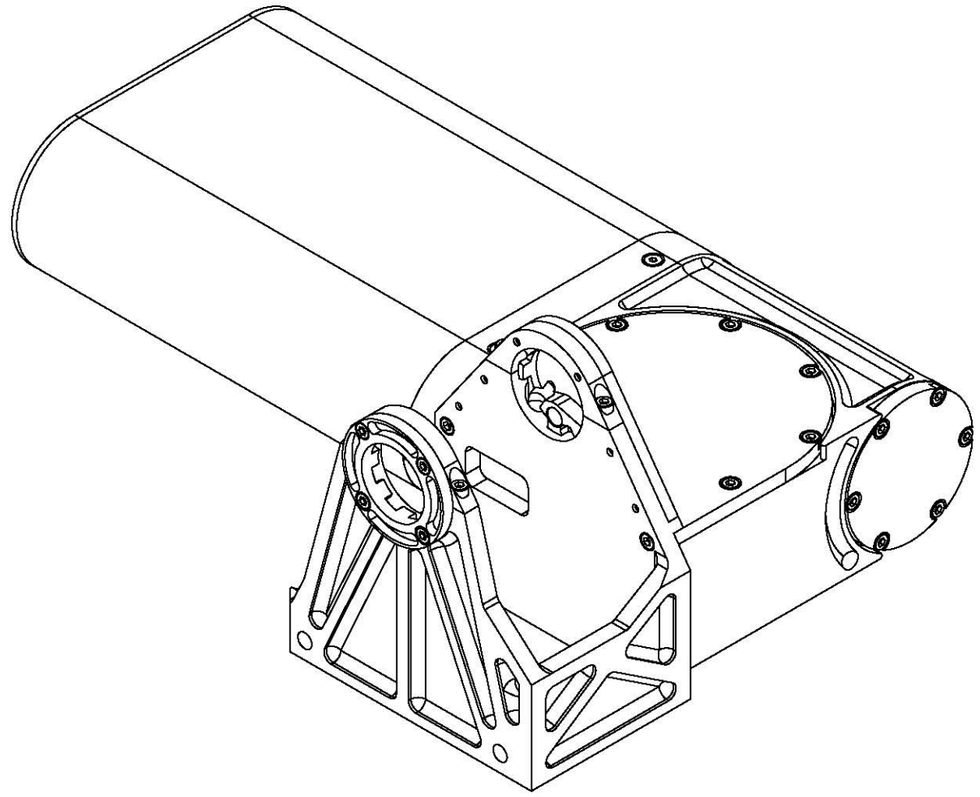

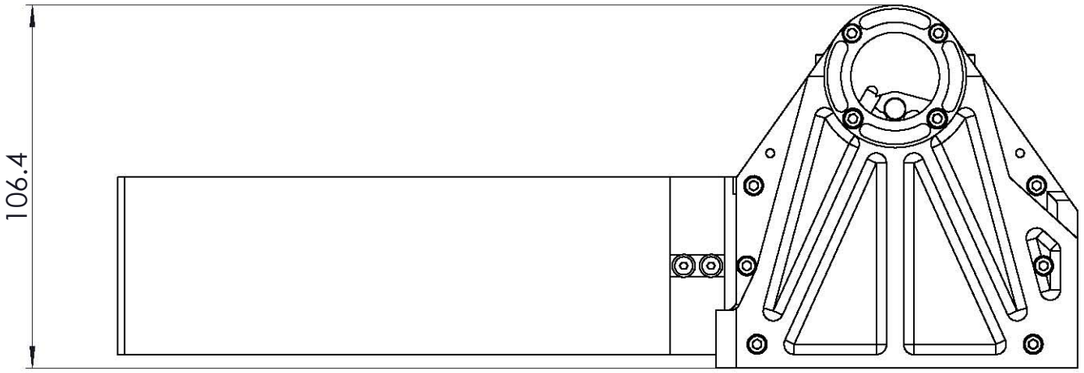

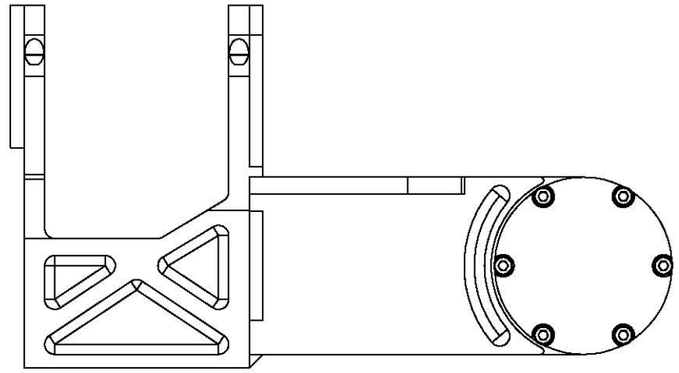

A3 Landscape	University of Cape Town Department of Mechanical Engineering			
	Title: Turntable Section Sub Assembly			
Assembly Drawing	Scale: 1:1.8	Date: 20/09/2011	Sheet 1	of 1
	Drawn By: Peter Henson RARL Mech. Eng.		Drawing Number E3	

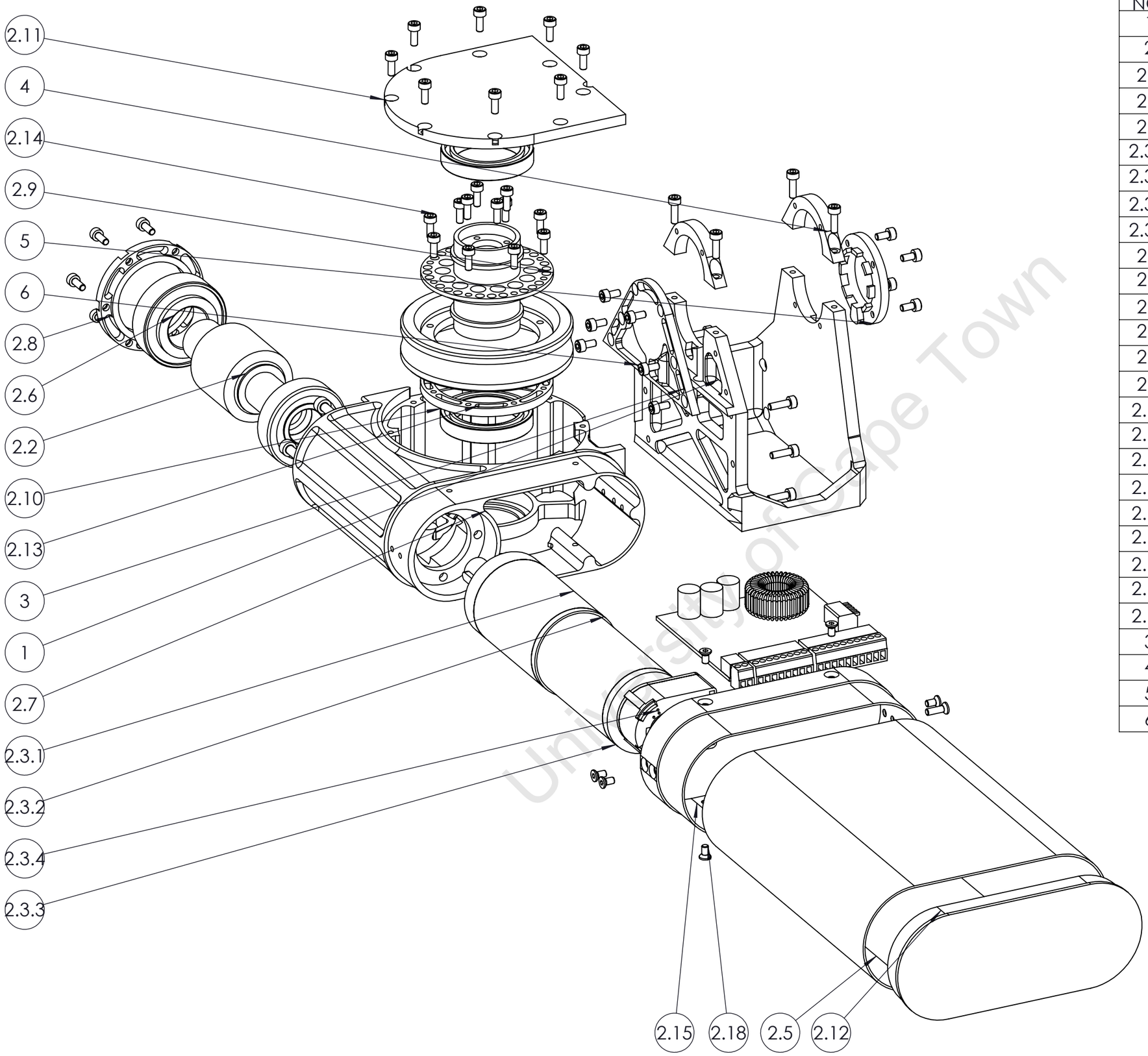

ITEM NO.	PART NUMBER	QTY.
1	Turntable to Bottom Yoke	1
2	Gear Housing Sub Assembly Turntable	1
2.1	AGDL2-36R1_edited	1
2.2	KWGDLS2-R1_edited	1
2.3	ec40ass	1
2.3.1	GP-42 3 stage	1
2.3.2	gearbox_adaptor	1
2.3.3	ec40-120w	1
2.3.4	heds-5540	1
2.4	DECV 505	1
2.5	Large Composite Tube	1
2.6	SKF - 30203	2
2.7	Gearbox housing A	1
2.8	Worm Bearing End Cover	1
2.9	Turntable shaft	1
2.10	SKF - 61806	2
2.11	Wormgear Bearing Side Cover	1
2.12	Large Tube End Cap	1
2.13	Worm Gear Shaft Nut	1
2.14	M4 x 0.7 x 10 Hex SHCS	30
2.15	Large Tube End Interface	1
2.16	Arm to Base Interface	1
2.17	BTC016-30 Slip Ring	1
2.18	M3 x 0.5 x 10 Socket FCHS	8
3	Inside Yoke Cover	1
4	Yoke Top Clamp	2
5	Outside Yoke Cover	1
6	M3 x 0.5 x 10 Hex SHCS	20

A3 Landscape	University of Cape Town Department of Mechanical Engineering			
	Title: Turntable Section Sub Assembly			
Assembly Drawing	Scale: 1:1.8	Date: 19/09/2011	Sheet 1	of 1
	Drawn By: Peter Henson RARL Mech. Eng.		Drawing Number E2	

Appendix A

Literature Survey

Table of Contents

List of Figures

List of Tables

A1. Introduction

This literature survey covers the design options that have been used on manipulator arms in industry and in other research projects. Manipulators designed for many environments and for a diverse set of tasks were considered. A wide variety of sizes were also looked at; from small single-function arms to larger 7-function automobile manufacturing robots and mining excavators. Design aspects from all were regarded, with an aim to learn the optimum arm configuration, and to learn from other arm's short-comings. An example of an industrial solution, the *iRobot Packbot*, of a Search and Rescue Robot fitted with a manipulator arm can be seen in Figure 1-1 below.

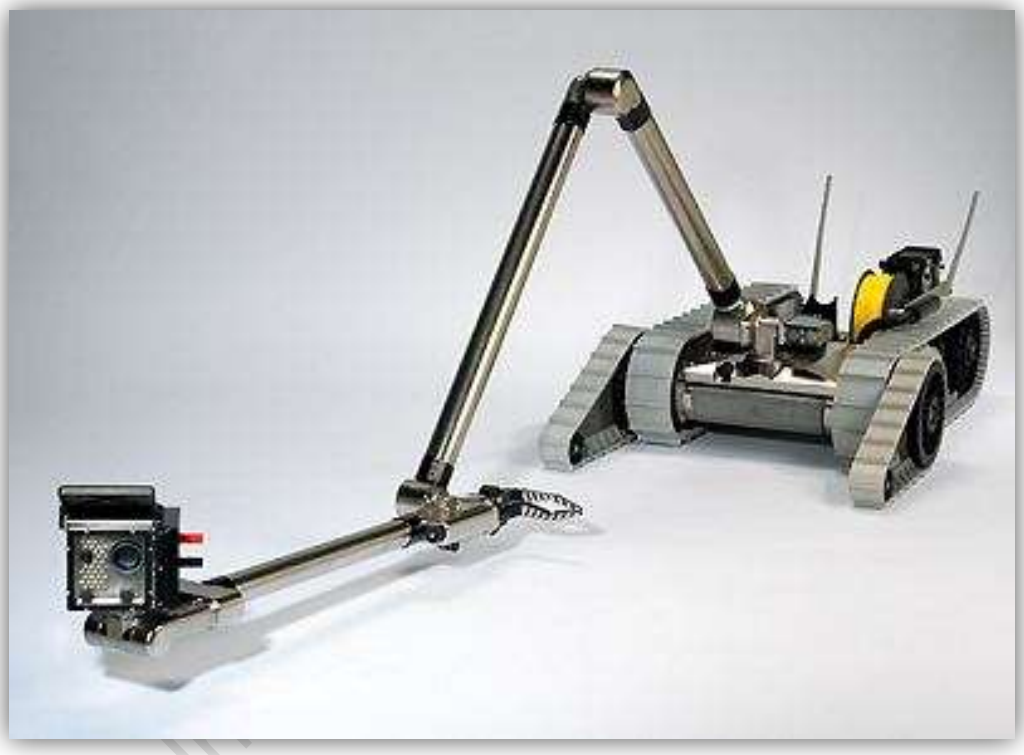

Figure 1-1: Picture of iRobot Packbot EOD showing Manipulator Arm Extended [1]

This survey starts with gaining a thorough understanding of the environment in which the arm will operate and be tested. Other competing robots and industrial options are then reviewed, studied and reported on. It will go into greater depth on the successful options and analyse their winning characteristics.

The survey then goes into depth on arm design with a specific focus on arm layout, constraints and degrees of freedom, all of which directly influence the work envelope. Actuator and joint designs are then looked at, and various options of gearing are also studied. It then explores the existing methods of gripping, cutting and tool manipulation, which fall under the heading of end-effectors.

Finally, literature on control systems and operator interfaces of various types is surveyed and existing industrial solutions are examined.

A2. The Search and Rescue Environment

In order to design a successful solution, it is necessary to develop a good understanding of the various environments in which the robot will be functioning. This section serves to investigate those environments.

A2.1 Post Earthquake Environment

Figure 2-1 Aftermath of New Zealand Earthquake [2]

The terrain of a post earthquake environment is extremely rugged as seen in the picture above. The robots are often underground, or in collapsed buildings. It is therefore often dark. There are also many obstructions; not just on the floor, but also obstructions that limit ‚headroom'. Other obstacles include closed doors and windows. These might require opening by the turning of a handle or knob, or may require sliding. There may be water puddles on the floor, as well as oil leaks. The underground cavities may also be filled with flammable gases, such as household gas. The environment is prone to being dusty, and aftershocks are also a very real hazard.

An arm operating in this environment will therefore be required to fold into a small amount of space. It will need to carry lighting. It will be preferable to have shielded or internal wiring

as there are also many sharp protrusions the may catch on or cut exposed wiring. It will need to be long enough and dexterous enough to open doors and windows, as well as move various obstructions. Its design will have to be relatively dust proof, and it must not create sparks. It will also need to withstand vibrations as the robot will be negotiating rough terrain.

A2.2 Bomb Disposal Environment

Figure 2-2 iRobot Packbot used for Bomb Disposal [1]

An iRobot Packbot can be seen in Figure 2-2 approaching an explosive. Bomb disposal requires a steady touch. It is required both outdoors and indoors and can therefore involve rain, dust, and wind. The terrain is normally stable however, and is generally a normal town environment. It can be imagined that there may be „trip-wires' or explosive cord which need to be cut.

An arm operating in this type of environment should therefore have minimal free-play to ensure steadiness. It will also require smooth operation and control, as opposed to a „jumpy' and erratic operation. The arm will need to operate in the elements, and should therefore restrict ingress of dust and water as much as possible. It should also feature a cutting device.

A2.3 The Mining Environment

Deep underground mines pose several environmental challenges. These include high temperature and humidity. Mines have air conditioning that maintains a slightly more comfortable environment for humans. However in the case of an emergency or malfunction, the robots should be capable of operating without air-conditioning. Rugged rocky terrain can also be expected along with darkness.

The robot will therefore need to have similar requirements as those asked by the post earthquake environment, with the addition of being to operate under relatively high temperatures.

A2.4 The Testing Ground – RoboCup Rescue Blue Arena

The Blue Arena is the arena within the RoboCup Rescue which specifically tests the ‚pick and place' ability of the manipulators. The following has been taken out of the rules for 2009:

The purpose of introducing pick and place tasks in the arena is to encourage development of Cartesian controlled mobile manipulators with inverse kinematics that can perform grasping and precision placement of items at different levels (0, 50, 100 cm) and reaches (30, 60 cm) while working in complex terrains (initially 15° ramps). Wood blocks (10 cm cubes covered in duct tape) provide a relatively lightweight object to manipulate. Addition of a single eye-bolt screwed into one side allows simplified grasping, hooking, or carrying and delivering on a rod. The eye-bolt is roughly 2 cm diameter. This can be considered a sensor, communications repeater, or other useful object that is adapted for easy handling by a robot. There are also full water bottles (500 ml) and small radios that can be grasped and manipulated to encourage more generalized approaches needed to retrieve samples in the field. The goal is to place one of these three objects inside a found victim box to score an additional 20 points - the same incentive as the mapping capability. Two items can be carried in as a payload on the robot from the initial mission start point. But additional items must be retrieved from the Blue arena shelves. Teams may choose which items to have available and in which orientation they will be placed on the shelving targets. [3]

Figure 2-3 shows a SolidWorks rendering of the Blue Arena. The requirements of the Blue Arena can therefore be summarized as follows:

- An L-shaped reach of 100 x 60 cm (can use base to assist in reach)
- Jaw bite of greater than 10 cm
- Ability to lift 500ml of water at full reach

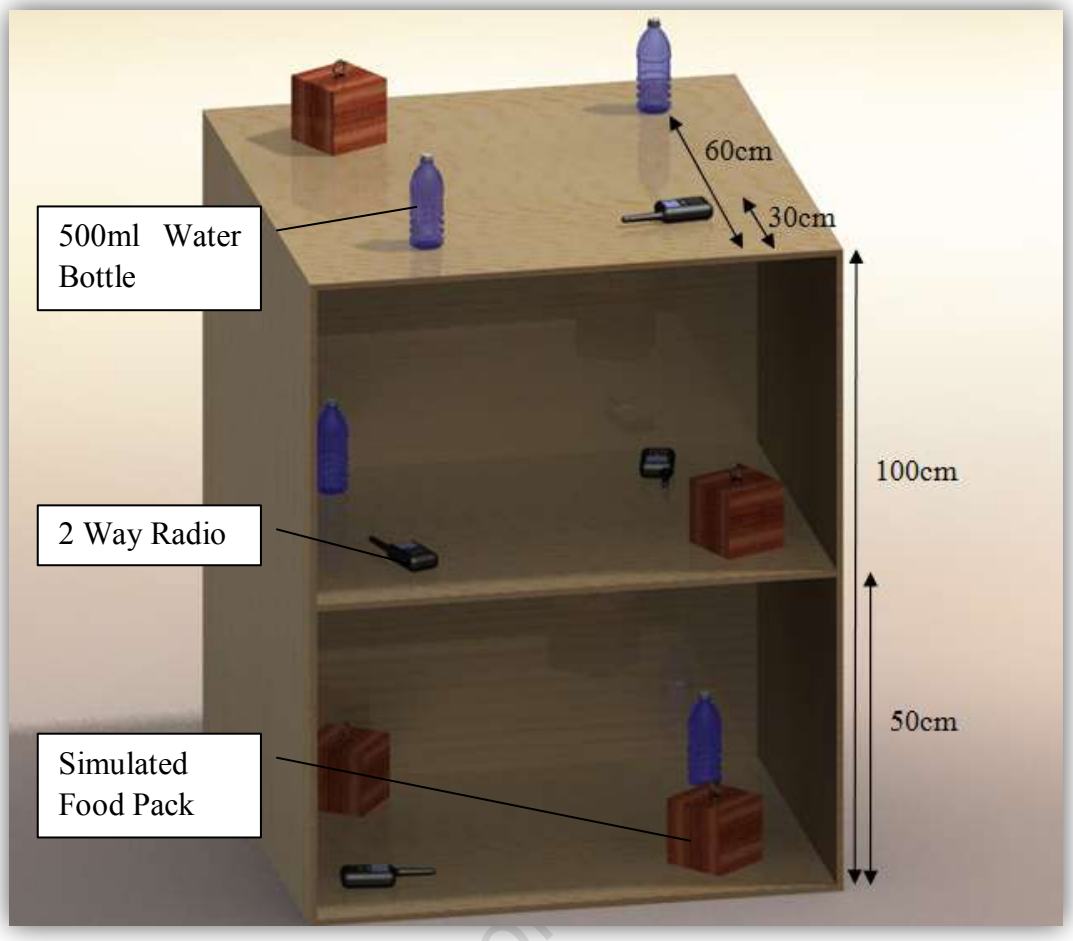

Figure 2-3: SolidWorks Rendering of Mock-Up of the Blue Arena

An addition to the rules which was agreed on in the „Rule Discussion Notes (2010)', which has an effect on the requirements of the manipulator arm, is to:

> *Use barrels open to top to contain simulated victims to challenge reach for ground robots and low hover, visual acuity, and thermal payloads for aerials.* [4]

Essentially, barrels will be used to conceal victims requiring the manipulator to move the sensor payload over the open top, so as to see inside. Manipulating the sensor pack will be one of the manipulator's primary functions throughout the Rescue Arena, as the simulated victims will be behind holes, or in hard to reach places.

A3. Existing Designs

A3.1 iRobot 510 PackBot Manipulator 1.0

An industrial solution on the market which is very good and readily available is the iRobot Packbot. It comes with an option of 2 different arms; the *Manipulator 1.0* and the *Small Arm Manipulator*. These two options are shown below.

Figure 3-1: Picture of 510 PackBot with Small Arm Manipulator [5]

Figure 3-2: Picture of 510 PackBot fitted with the Manipulator 1.0 [5]

As the Manipulator 1.0 is a more advanced arm than the Small Arm Manipulator, and is more relevant to this project, this survey will go into depth on this arm only. The Manipulator 1.0 boasts the following specifications:

- 6 Degrees of freedom plus Pan and Tilt of the camera, making 8 DOF
- Full extension of the camera of 73.5” (1.87m)
- Full extension of gripper of about 54” (1.37m)
- Lifting capacity of 10 lbs (4.53kg) at full extension
- Lifting capacity of 30 lbs (13.6kg) at close-in position

- Continuous rotation on base turntable, wrist and head
- 220° of rotation at shoulder pivot
- 340° of rotation at first and second elbows
- 180° of rotation at gripper
- 220° of head tilt
- Mass of 20.5 lbs (9.3kg)

This arm is very successful, and is therefore a good starting point when researching solutions for the purpose of designing a new arm. From the look of the housings, it can be assumed that hypoid gears are be used in the joint actuators. It can be assumed that slip rings are being used in joints with continuous rotation.

The arm is very streamline, with internal wiring and attachment points for accessories to be added. All the joints are water tight, and the PackBot can operate in all weather conditions. It can be concluded that it is an excellent solution, which is well tested and robust. The only downside of this system is the cost, which is prohibitive for many rescue teams.

A3.2 RoboCup Rescue Competitors

Competitor robots from RoboCup Rescue that include manipulator arms were studied and their specifications and performance are summarized in Table 3-1 below. All the below information was taken from *Team Description Papers* (TDP's) and videos/photos referenced to in the TDP's. The two good solutions are analysed in detail in the following sub sections. The poor solutions all suffered from severe backlash, poor control and low functionality.

Table 3-1: Table Summarizing Competitors Manipulators

	DOF	Base Rotation	Actuator Type	Gripper Type	Wiring	Control Method	Performance
Australia CASualty	1	No	Servomotor	None	External Loom	Position Control	Poor [6]
China NuBotRES	3	No	DC Motor/ Servomotor	Angular	External Wiring	Speed Control	Unknown [7]
England Warwick	3	Yes	DC Motor/ Worm Gear	None	External Loom	Unknown	Above Average [8]
Germany	3	Yes	Hub Motors	None	External	Position Control	Unknown [9]
Iran MRL	5	Yes	Unknown	Parallel	Unknown	Unknown	Unknown [10]
Iran Pars	1	No	DC Motor	None	External	Position Control	Poor [11]
Iran Pasagrad	3	No	DC Motor	Angular	External Loom	Master Slave	Unknown [12]
Iran YRA	5	Yes	DC Motor	None	Internal	Position Control	Above Average [13]
Japan C-Rescue	2	Yes	Servomotor	None	External Loom	Position Control	Average [14]
Japan Niit Blue	1	No	Servomotor	None	Unknown	Position Control	Poor [15]
Japan	3	Yes	DC Hub	None	External	Master	Good [16]

Pelican Utd			Motor		Looms	Slave	
Malaysia Iran Ariana Ava	2	No	Servomotor	None	External Loom	Position Control	Above Average [17]
Mexico Ixnamiki	4	No	Servomotor	None	External Wires	Position Control	Above Average [18]
Pakistan Saviour	1	No	Servomotor	None	External Wires	Position Control	Poor [19]
Thailand Irap Pro	5	Yes	DC Motor	Angular	External Loom	Position Control	Good [20]
Thailand KNUTNB	4	Yes	DC Motor	None	External Loom	Speed Control	Above Average [21]
Thailand Success	6	Yes	DC Motor	Angular	Energy Chain	Speed Control	Above Average [22]

A3.2.1 Japan Pelican United

The Japanese Pelican United manipulator arm won the „Best in Class Manipulator' award at the Singapore 2010 RoboCup. Their advanced control, which used a master-slave system, meant that the full potential of their arm could be utilized. This can be seen on the left Figure 3-3 below. The arm responds quickly to the master controller and makes its operation very user friendly.

Figure 3-3: Pelican United's Manipulator Arm and Master Slave Controller [23]

Their arm has 3 degrees of freedom, as well as camera pan-tilt. Each joint is rotary; it does not have any linearly extending sections. In the video referenced by the picture, it can be seen that it has a relatively high level of free play. It does not have continuous rotation as the wiring on it restricts each joint's range.

A3.2.2 Thailand IRAP Pro

The IRAP Pro's manipulator arm is rate controlled by a *play station* type controller. This means that they do not implement position control. This requires more operator training than the Pelican United's solution. Furthermore, it is not using inverse kinematics, but instead each joint is being driven independently. The manipulator arm as shown in Figure 3-4 has 5 degrees of freedom.

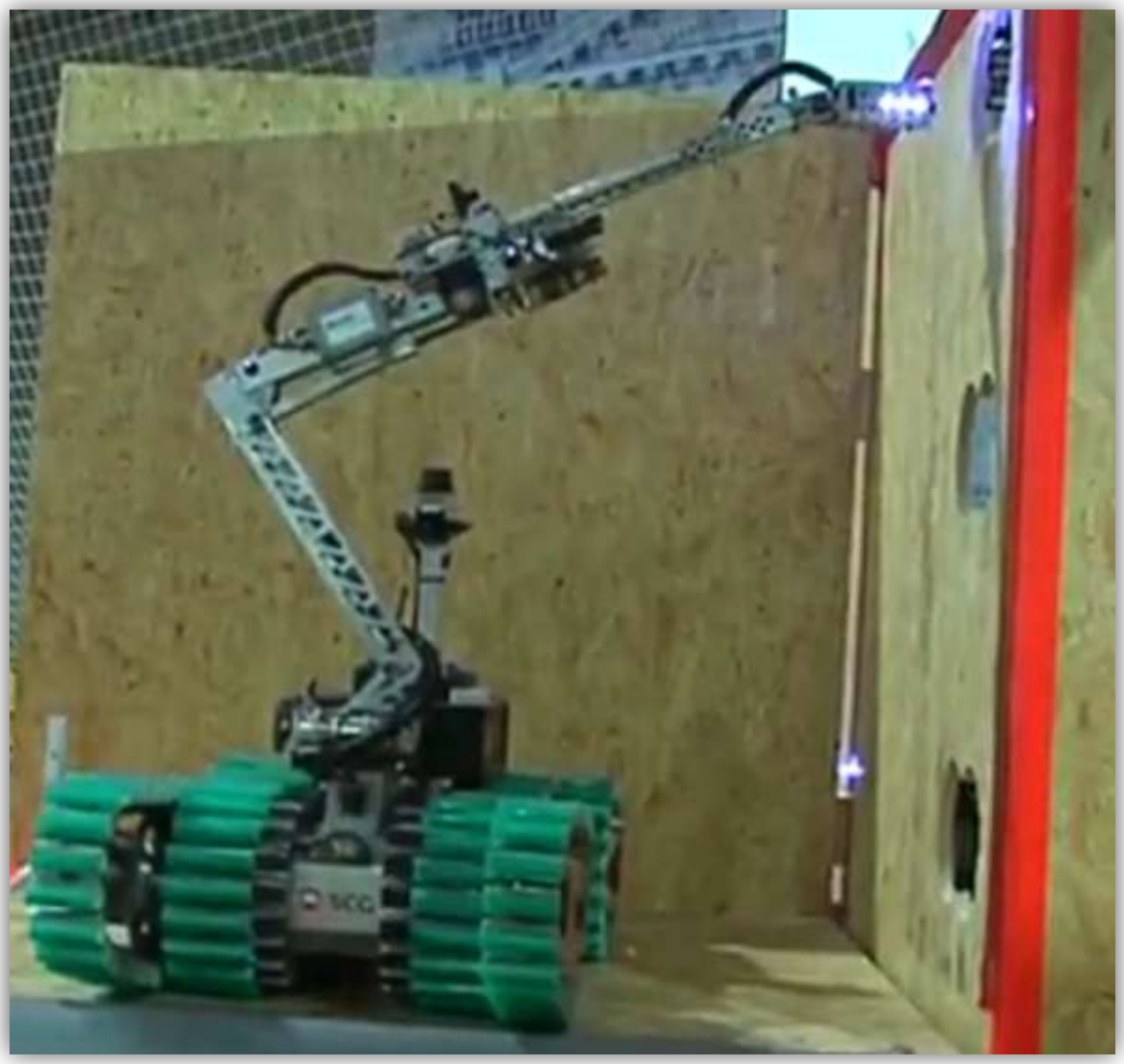

Figure 3-4: IRAP Pro with Manipulator Arm Extended [24]

The last section of the arm is has extending functionality; the rest are rotary joints. The high level of mobility provided by the 5 degrees of freedom makes this arm highly functional, and allows the camera to look into hard to reach holes. The gripper however is located at the end of the second arm section, not at the end of the extending section. This may be because the arm will not be strong enough to lift the 500ml water bottle with the gripper at that lever arm. This is speculation however and not a certain deduction. This placement of the gripper does limit their reach capabilities.

Their joints seem to be operated by linear actuators, like that on industrial mining excavators. This provides a good moment arm on the actuator and allows for a smaller motor. It does however greatly reduce the work envelope, and is generally slower than geared joints.

The arm is simple in its design, and is therefore light, not cumbersome and quick to repair. It can also be assumed that it has a low power requirement on the base. It does however have a large amount of free play and looks untidy with external wiring. This is not ideal, as it can catch on the rugged terrain, or potentially get pinched between the arm and the environment.

A4. Work Envelope

The work envelope is defined as "*the three dimensional volume of space in which the robot manipulator is capable of working*" [25]. A side view of the work envelope for the commercial *Lynxmotion 5-axis Robotic Arm* can be seen in the diagram below.

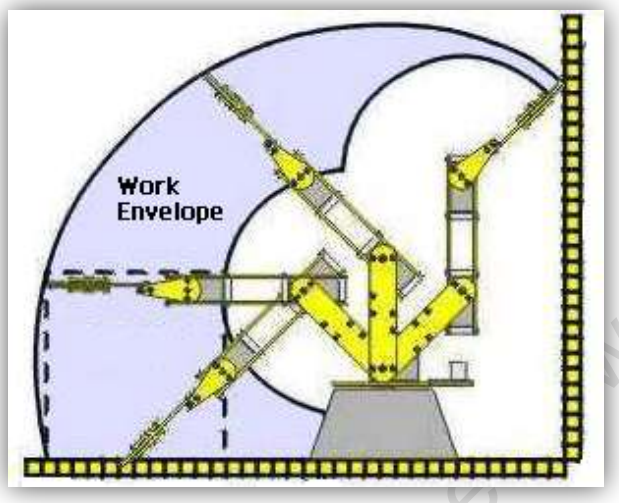

Figure 4-1: Lynxmotion 5-axis Robotic Arm Work Envelope [26]

This robot can be defined as a jointed arm robot. There are several robot arm configurations, and these are listed below.

A4.1 Rectangular Coordinate Robotic Arms

These robots move in a translational motion; they do not rotate. They have a box shaped work envelope. They are very precise and are easy to control [25]. The schematic can be seen in Figure 4-2

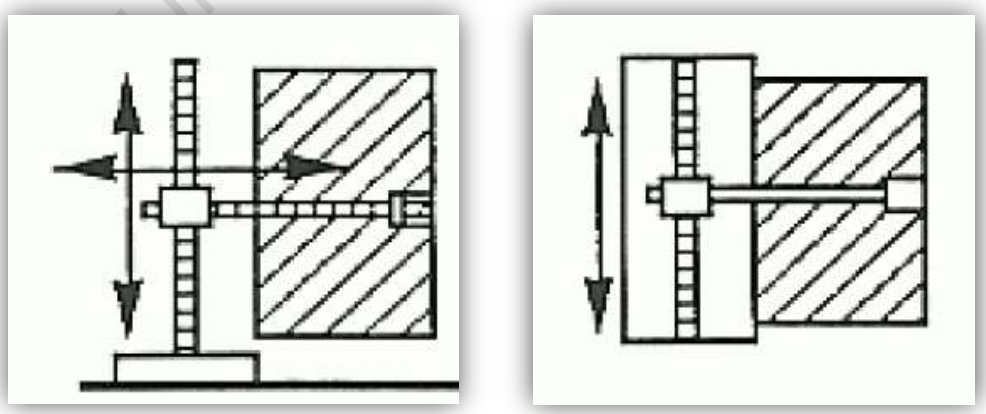

Figure 4-2: Rectangular Coordinate Robot Work Envelope a) Side View, b) Top View [25]

A4.1 Cylindrical Coordinate Robotic Arms

These robotic arms have a mixture of translational motion and rotational motion. Figure 4-3 shows an arm that rotates in the X-Y plane and moves translationally up and down the Z-axis and in and out on the X-axis. These arms are slightly more compact as it can be seen that they take up no space in the Y-axis. This makes them useful in more constrained environments [25].

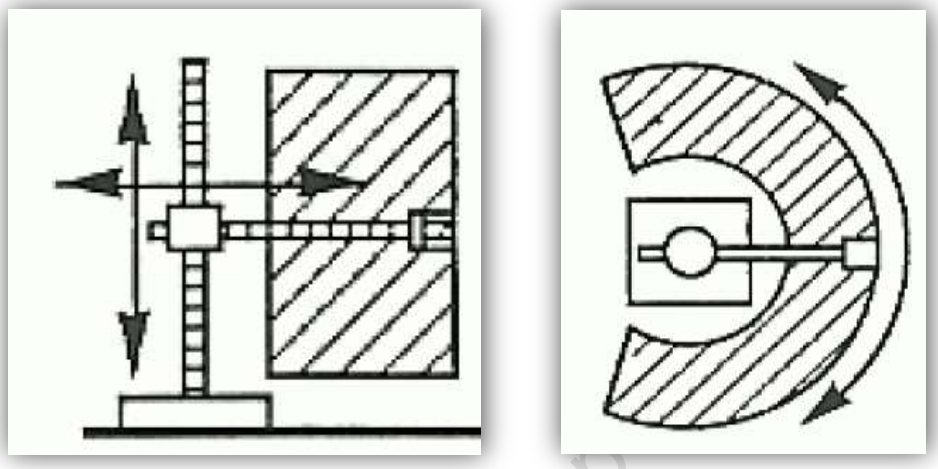

Figure 4-3: Cylindrical Coordinate Robot Work Envelope a) Side View, b) Top View [25]

A4.2 Spherical Coordinate Robotic Arms

This arm configuration is constrained to only move rotationally. The resulting work envelope is part of a sphere. A translational movement can be added, as in Figure 4-4, which expands the work envelope to a ‚thick-walled sphere', with the thickness being determined by the amount of translational travel. This configuration is useful for picking up and moving items and is very compact, allowing for picking and placing of items close to the base [25].

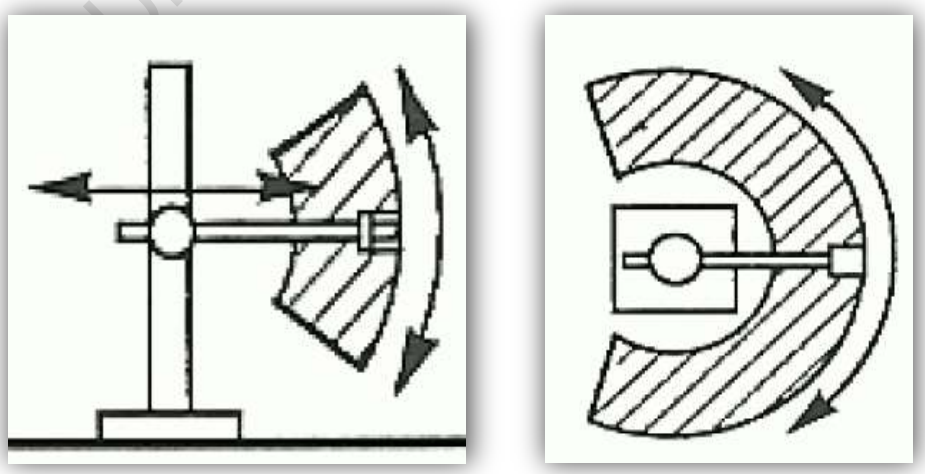

Figure 4-4: Spherical Coordinate Robot Envelope a) Side View, b) Top View [25]

A4.3 Jointed Robotic Arms

These arms have a complexly shaped work envelope due to the action of the joints. It closely resembles a human arm and therefore the joints are usually named shoulder, elbow and wrist. These configurations have good reach both above and below themselves, and because of their ability to fold in on themselves, their work envelope can come relatively close to their base, as can be seen in the figure below. This arrangement is the most commonly used configuration in industry because of its flexibility and strength, despite requiring a more complicated control system [25].

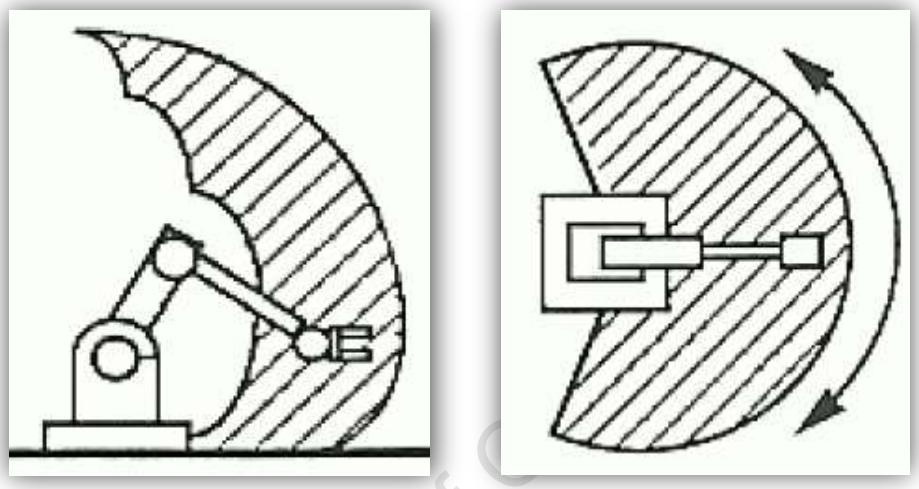

Figure 4-5: Jointed Arm Robot Work Envelope a) Side View, b) Top View [25]

A4.4 Spine Type Robotic Arms

This ‚snake like' design has extraordinary flexibly and has the most complete work envelope of all the configurations, as shown in Figure 4-6. It also has the ability to approach the target with the end-effector at varying angles. This becomes useful with tasks such as spray painting. However, it is does not have the same lifting ability as the other types and it is significantly more expensive, and more complex to control [25].

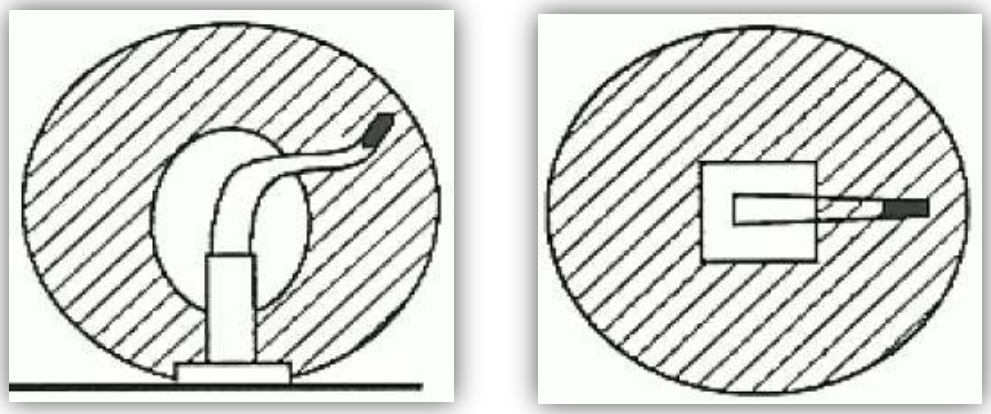

Figure 4-6: Spine Robot Work Envelope a) Side View, b) Top View [25]

A5. Actuator and Joint Design

A5.1 Hydraulic vs. Pneumatic vs. Electric

Three main types of robotic actuators exist; namely hydraulics, pneumatics and electrical. There are also steam, internal combustion, and others, but these are not common. The table below shows a summary of the characteristics of each when compared with each other.

Table 5-1: Table Showing Summary of Hydraulics, Pneumatics and Electric Actuators

	Power	Weight	Speed	Cost	Power Source	Control
Hydraulic	High	High	Low	High	Hydraulic Pump	Good
Pneumatic	Medium	Low	High	High	Compressor	Difficult
Electric	Low	Low	Medium	Low	Batteries	Excellent

All of the RoboCup Rescue teams so far have utilized electric actuators in their robots. This is because of their relatively low weight, and good control, but mainly because electricity is readily available from the batteries on the robot. Both of the other options, despite their superior strength, require an extra step in the conversion of electrical potential energy (stored in the battery) to mechanical energy; this being either a compressor or a hydraulic pump. These are both heavy and add to the power losses due to the added inefficiencies of the extra stage. The result is that they have a low *energy density*, i.e. low energy to weight ratio when compared to the electrical option. Electrically operated actuators are therefore the obvious choice in robotics.

A5.2 Linear Actuator vs. Rotary Actuator

All three of the above methods of power actuation can produce both a linear actuation and a rotary actuation. In the following figures, both pneumatic and electrical *linear* actuators are shown as well as their *rotary* actuators.

Figure 5-1: Festo Pneumatic Cylinder [27] Tolomatic Pneumatic Rotary Actuators [28]

Figure 5-2: Maxon Spindle Drive Electrical Linear Actuator and Rotary Actuator [29]

There are advantages and disadvantages for both options, and a compromise has to be made in order to achieve the highest priority specifications. Both types were used among the robots studied that competed in the Robocup Rescue 2010.

Linear actuators normally have a strength advantage as they apply the force at a greater distance from the pivot and therefore apply a larger torque. They also exhibit less backlash and more overall stability in the arm, as they secure the arm in two places as opposed to just the one of a rotary joint.

However the disadvantages of a linear actuator are many. They move slower than rotary actuators, and the arm does not move at a constant angular speed throughout its range due to the geometry of the joint. The main disadvantage however is that a linear actuator cannot perform 360° continuous rotation, due to the necessary linkages used to convert the linear motion to an angular motion. They can at best achieve 180° of rotation, but more commonly achieve between 45° and 135°. Electrical linear actuators such as the spindle drive seen in Figure 5-2 are further disadvantaged as the spindle shaft cannot retract like those of its hydraulic and pneumatic counterparts. This obstructs the arm as it opens and closes and poses great spatial challenges to the designer.

Rotary actuators apply less torque as they are applying the force very close to the pivot. They are however faster, and provide continuous rotation, and operate the movement at a constant angular velocity throughout the range of actuation. Rotary actuators are also significantly more compact and take up less space than their linear counterparts.

Rotary actuators often require gearing of some sort in order to increase the torque, or in order to transmit power through 90°.

A5.3 Bevel Gear vs. Worm Gear

There are two main gear types for transmitting torque though 90°; *worm gears* and *bevel gears*. A worm gear speed reducer can be seen in Figure 5-3 and a bevel gearbox in Figure

5-4. Both gear arrangements effectively transmit power through 90°, but they are used in different applications as they have different characteristics.

Worm gears have a larger ratio for the equivalent overall size, and therefore slow the output (worm gear) speed significantly, while increasing the output torque by the same factor. The bevel gear however is significantly more efficient (90+ %), than the worm gear (40% - 50%) but cannot achieve such high ratios [30].

Figure 5-3: Cutaway of a Worm Gearbox Showing Gear and Bearing Arrangement [31]

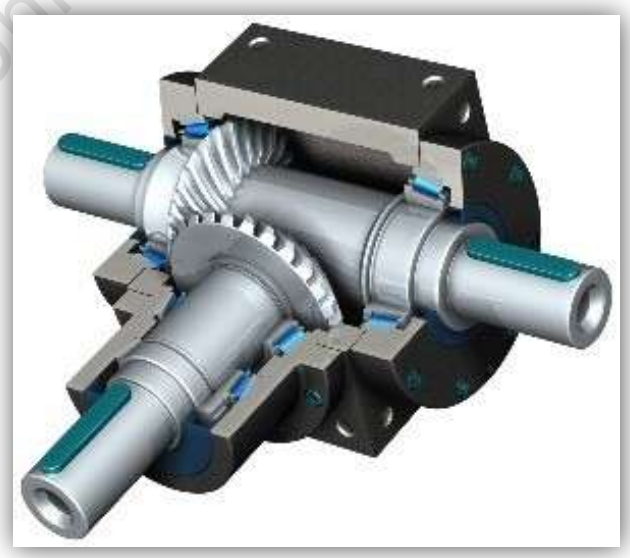

Figure 5-4: Cutaway of Bevel Gearbox Showing Gear and Bearing Arrangement [32]

A5.4 Low Backlash Worm Gear Review

A problem noticed with many of the competing teams that were researched is a large quantity of backlash (free-play) in all of the manipulator joints. This causes the sensor pack to judder about while the robot moves around, and creates a shaky picture and erroneous laser mapping.

"Backlash in gears is generally defined as the play between mating teeth. For purposes of measurement and calculation, backlash is defined as the amount by which a gear tooth space exceeds the thickness of the engaging worm thread on the pitch circle of the gear. Or, stated another way, backlash is the movement at the pitch line of the gear (in millimetres) or as rotational movement of the gear (in degrees or arc minutes) with the worm locked." [33]

Several different worm gear designs were researched and are listed below.

A5.4.1 Single vs. Double Enveloping Worm Set

The choices that one faces in worm design are many. There are regular Lego type worm and gear combinations where both the worm and worm wheel (gear) are regular cylinders. They can be likened to a worm gear running on a helical gear. These do not have good wearing characteristics, as the contact area is relatively small, and therefore generates a large pressure.

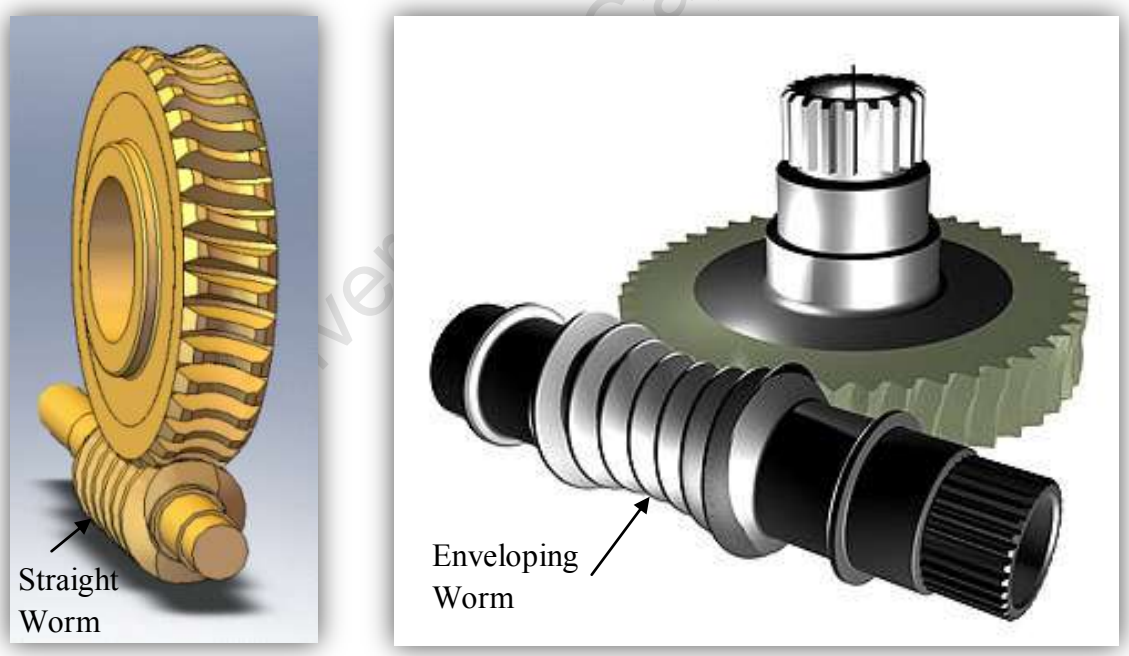

Figure 5-5: a) Single Enveloping Worm Gear [34] b) Double Enveloping Worm Gear [35]

Most industrial gears are single enveloping gears, in which only the worm is a regular cylinder, whilst the worm gear envelopes the worm, creating a greater contact area, and a better life span. The next level of complexity is double enveloping worm gear sets. These typically have between three and eleven teeth in contact continually [33]. They also increase the contact area per tooth, by having two „lines' in contact on the tooth's surface for most of

the stoke (except when the two lines converge mid-stroke) [33]. This makes these gears capable of transferring significantly more torque, up to 80% increase. The increased complexity unfortunately means higher manufacture cost, and small sized gears are not made because of the increased intricacy. Diagrams comparing the two technologies are shown above in Figure 5-5.

A5.4.2 Duplex Worms

Duplex worms are worms that are designed to accommodate wear throughout the life span, whilst maintaining minimal backlash. They achieve this characteristic by increasing the tooth thickness on the screw from one end of the worm to the other whilst maintaining the pitch. The designer then allows the worm to be moved axially along its shaft every so often to re-tighten the worm and eliminate the backlash. It is also useful when initially installing the gears, as manufacturing errors in the centre distance between the gears can be accounted for. A diagram showing the duplex gear and how it operates can be seen in Figure 5-6.

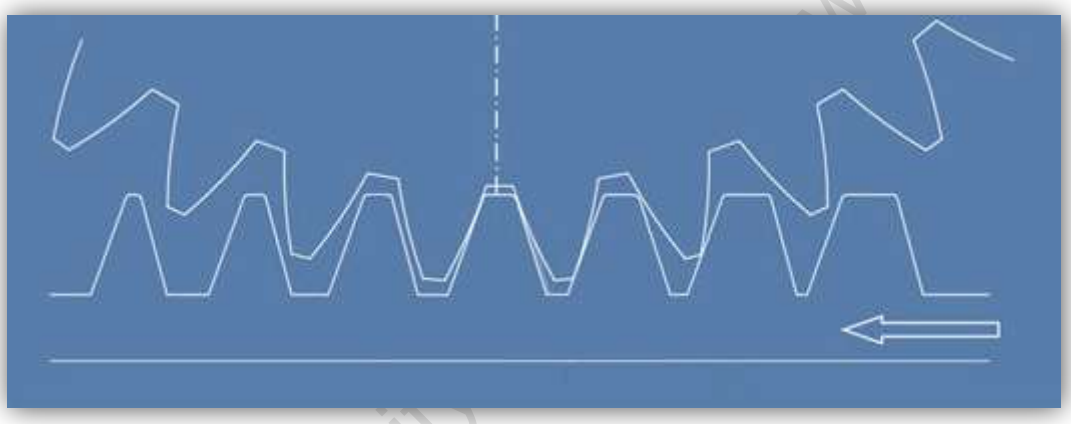

Figure 5-6: Diagram Showing Duplex Worm Gear Eliminating Backlash [36]

A5.4.3 Cone Drive Absolute Zero Backlash Worm Gears

Cone Drive is an American gear manufacturer who sells off the shelf zero backlash gear sets. The following is the product description, as given on their website. No images were available.

"Absolute zero backlash worm gearsets have a two-piece worm, quilled together at the axial center of the worm thread. One segment of the worm is fixed in its bearing set, while the other segment is positioned laterally by adjustable-force pre-load disks, maintaining a consistent clamping force on both sides of the gear thus removing all backlash. In this self-adjusting design, half of the power input worm contacts the drive side of the gear while the other half of the worm makes continuous contact with the opposing side of the gear" [33]

The shortfall of this design is that only half of the worm (the driving half) is carrying the load. This means gears twice as strong need to be selected. Another problem is that because of the clamping force provided by the *adjustable-force pre-load disks* the friction is greatly

increased, and so the power and torque requirements are much greater. Wear rate will also greatly increase. These are therefore not suitable for application in the arm.

A5.4.4 OTT Zero Backlash Solution [37]

OTT Gear Technology is a German company who have patented a zero-backlash worm gear set. This design boasts several new and uncommon changes in the design of the worm and worm wheel. It has several similarities to the Cone Drive design above, in that it comprises of two worm halves; a *shafted worm* and a *hollow worm*. It also has essentially one half worm driving the worm wheel for each direction. This means that each half worm has a working flank and a rear flank (which is not in contact), as seen in Figure 5-7 and Figure 5-8 below. However, it is not spring loaded but rather preset to zero, and fixed in this position, and so the OTT concept does not experience the increased frictional losses of the previous design.

Figure 5-7: Picture showing OTT Worm and Wheel; a) Disassembled b) Assembled [37]

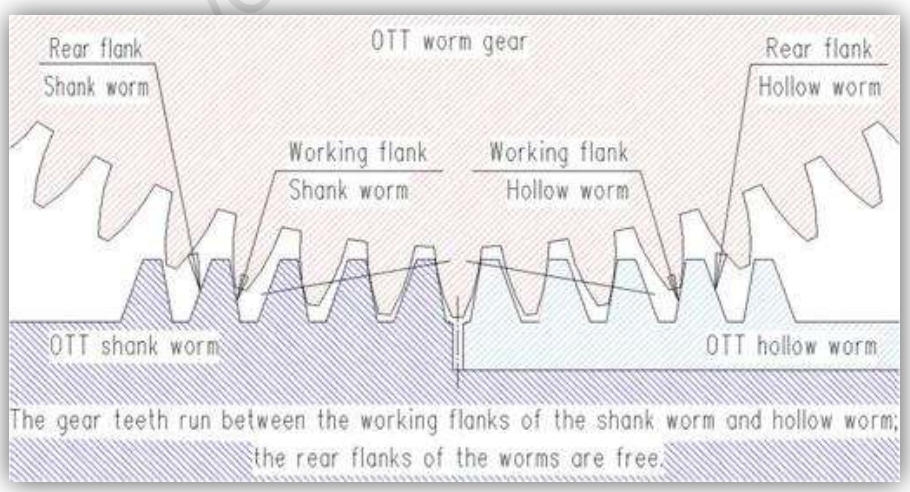

Figure 5-8: Diagram showing Concept behind OTT Zero Backlash Worm Gear [37]

The shafted and hollow worms are always fully mated, and backlash is eliminated by rotating one with respect to the other until the teeth fill the gap. This rotational offset is then locked and this ensures zero backlash while maintaining close to normal friction levels. Because

only one flank of the worm is in contact, the rear flank can be designed to offer increased strength to the tooth. The duplex design previously mentioned is suseptable to tooth expension with heat, and therefore increased friction. However, because the OTT design has only one flank in contact, heat does not affect or increase friction.

As seen in Figure 5-8 above, the teeth in the OTT design are ‚taller' (around 4 times the module), meaning that more teeth than normal are in contact at any one time. This also means that the low strength disadvantage of using half the worm is negated. However, it does require that the worm wheel has a large tooth number. The smallest centre distance available is therefore 50mm. The rotational locking device to secure the two half worms is also very bulky and so the required housing is larger than that of a conventional worm.

A5.4.5 Steering Box Designs

As the manipulator arm to be designed is to have a fairly long reach, and will have to pick up relatively heavy objects, the torque on its joints is going to be considerably large. It is also desired for the arm to have minimal backlash. The author therefore looked for a system that was already implemented and working successfully and one which displayed these desired characteristics. Steering boxes used in motor vehicles display these qualities, both in high torque and minimal backlash. Several steering options are available. The design below shows the simplest type of steering box. It is not commonly used however as it is not very efficient.

Figure 5-9: Worm and Sector Steering Box [38]

The next design, shown in Figure 5-10, is the system most commonly used in modern vehicles. The rolling elements convert the friction experienced from a high sliding friction to a comparatively lower rolling friction. The system also eliminates backlash and it allows the parts to all be made of steel, rather than bronze, which allows greater torque and a longer life.

Figure 5-10: Worm and Nut (Ball Worm) Steering Box [38]

A quick calculation assuming a human pulls up to 10kg on a steering wheel (without power assistance) at a radius of 200mm gives an input torque of 20Nm. Multiplied by the reduction ratio of about 18:1 gives an output torque of 360Nm. (This is a very high torque, and explains how a person can twist a rubber tire on tar, despite the fact it is supporting a car weighing over a tonne.) Furthermore, because of the consequences of failure of a vehicle's steering, it can be assumed that it has a large safety factor designed into it. It can be assumed that the output can handle up to 700Nm. This is a considerably high torque, and proves this system's worth in torque transfer.

The complication however with this system, as seen in Figure 5-10, is that it is not designed to perform continuous rotations. While adapting it to perform continuously like a normal worm is not impossible, it becomes very difficult to manufacture. Several patents with such designs already exist [39].

A6. End-Effectors

An end-effector is the tool or gripper attached to the wrist of a robotic arm. The end-effector is not considered as part of the *arm*; it is not considered as a degree of freedom or an axis as it does not contribute to the work envelope [40].

It is preferable to have a flexible and dexterous end-effecter, as the process of returning the SRR back to the operator in order to change the end-effecter and then re-entering the SRR into the *danger zone* is time consuming and expensive on battery power. This is particularly necessary for multi-task operations (Those missions which require more than just observation) [41].

A6.1 Grippers

A6.1.1 Methods of Gripping

Gripping can be achieved three separate ways:

1. *Friction:* The normal force, as in the diagram below, of the gripper provides a sufficient frictional force to hold the object. This requires a sufficiently high coefficient of friction, and hence many frictional grippers have rubber coated jaws [40].

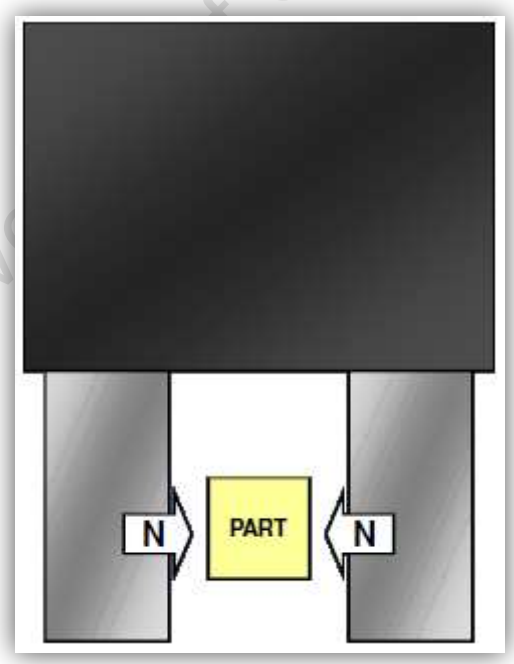

Figure 6-1: Picture showing part to be held by frictional constraint [40]

2. *Geometrical Shape:* The gripper is shaped according to the object it wants to pick up, as seen in Figure 6-2 below. For example, a gripper used for picking up eggs might have two cup shaped jaws. Often serrated jaws will be used for picking up irregular

objects and can use a combination of gripping by friction and gripping on geometrical shape [40].

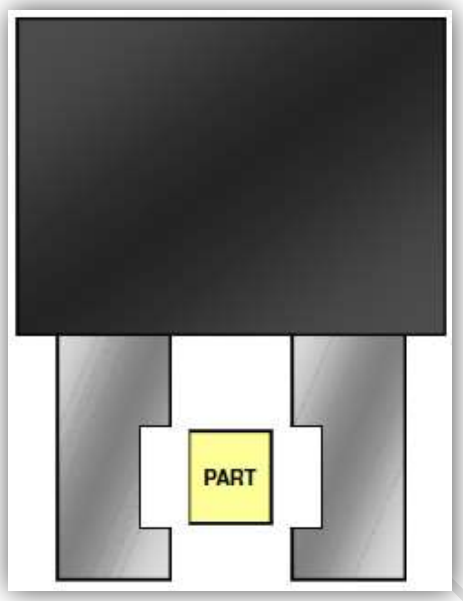

Figure 6-2: Picture showing part to be held by geometrical constraint [40]

3. *Attraction:* This includes magnetism, suction, „Velcro', electro-static attraction, etc. This is not a common gripping method used on multi-task manipulators [40].

A6.1.2 Two Jaw vs. Three Jaw Grippers

Grippers come with varying amounts of jaws, but normally with two or three. Three jaw grippers have the benefit of being able to pick up close-to-spherical shapes. Two jaw grippers are preferred when dealing with cylindrical shaped objects, such as pipes. Examples of 2 and 3 jaw grippers done on 3D CAD programs can be seen in the two pictures below.

Figure 6-3: Two Jaw Angular Gripper [42]

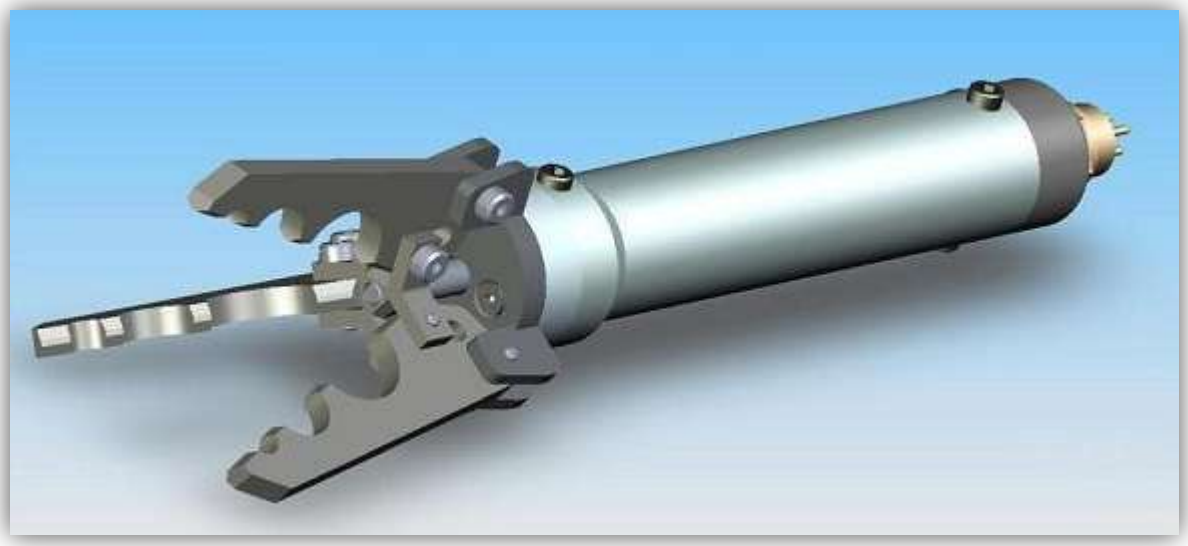

Figure 6-4: Three Jaw Angular Gripper [43]

The actuation of each type is the same, and therefore the cost and simplicity of each is similar. It is therefore a matter of which type of function is desired of the arm. It can be noted that on manipulators with several degrees of freedom (but especially wrist rotation), that the two jaw gripper is preferred as it can be rotated to approach the object at any angle. On single function manipulators, the three jaw option is normally preferred.

A6.1.3 Angular versus Parallel Grippers

The 2 pictures above show *angular grippers*, also known as *bird's beak grippers*. These grippers are hinged at one end in a rotational type constraint. Schematics of an angular gripper can be seen below.

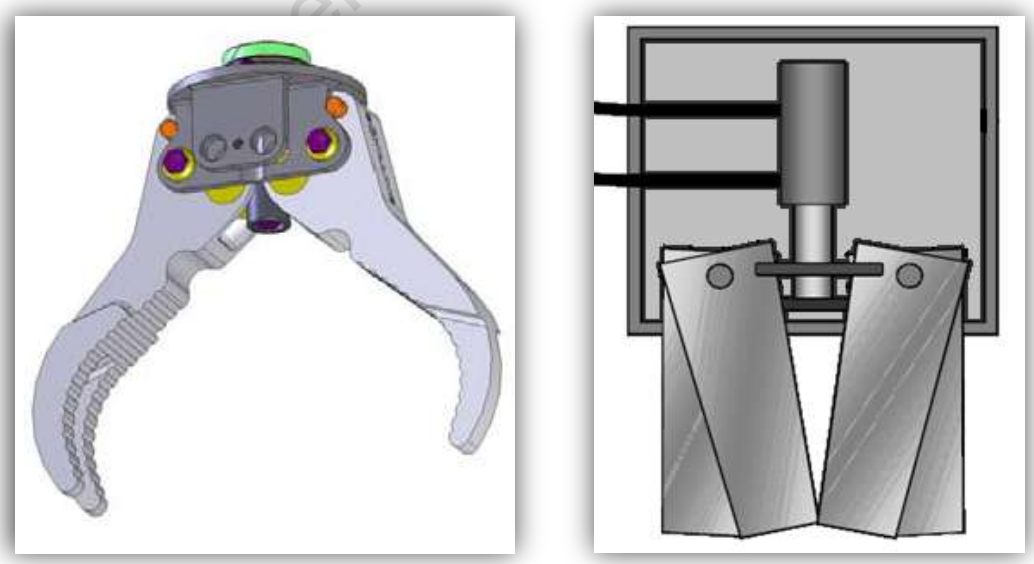

Figure 6-5: a) Schilling Angular Gripper [44], b) Angular Action Gripper Schematic [40]

Another method is to use *parallel grippers*. These use equal length arms, constrained at equal distances on both the jaws and the wrist. A schematic of a parallel action gripper can be seen in the following figures.

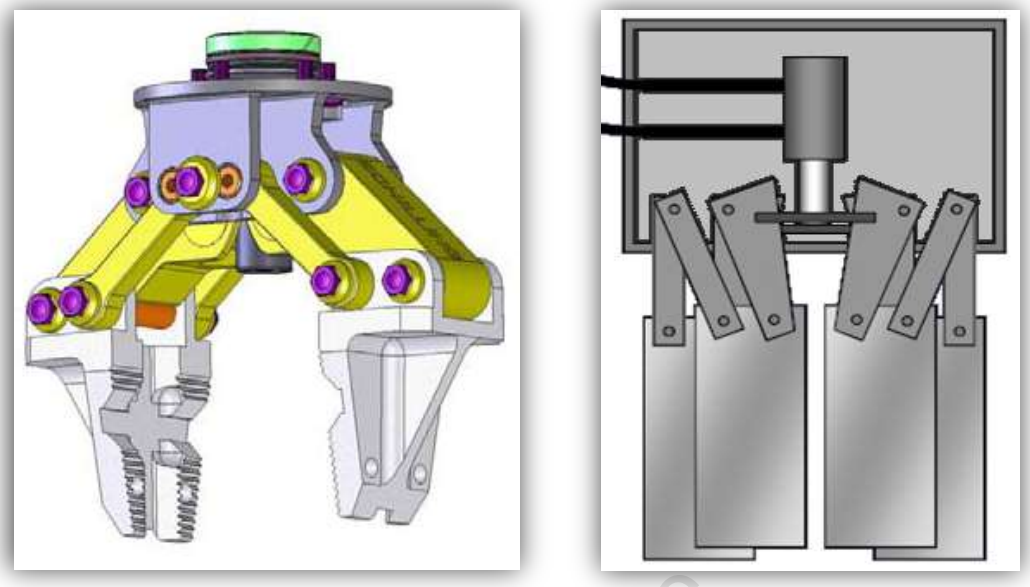

Figure 6-6: a) Shilling Parallel Gripper 3D [44], b) Parallel Action Gripper Schematic [40]

While parallel action grippers can be advantageous, especially when approaching objects with parallel sides, such as hexagonal nuts and bolts, boxes etc, they are more complex than angular action grippers. When irregular shaped objects need to be picked up, the simpler angular action grippers are preferred [40].

There is a method of incorporating both the simplicity of the angular type gripper, and the usefulness of parallel jaws, and this is achieved by using L-shaped jaws. The base of the L closes in an angular fashion, and the tips in a parallel fashion. This can be seen utilised by the Packbot in Figure 6-7.

Figure 6-7: a) Packbot with Adjustable Jaws [45], b) Packbot with Fixed Jaws [46]

Self-aligning grippers are another hybrid of both parallel and angular grippers. As the schematic below shows, the main jaws are constrained as angular jaws, and the „finger-tips' are free to align to the shape of the object. These are not practical for picking up cylindrical objects, as they can both tilt outwards and squeeze the object out of the jaws.

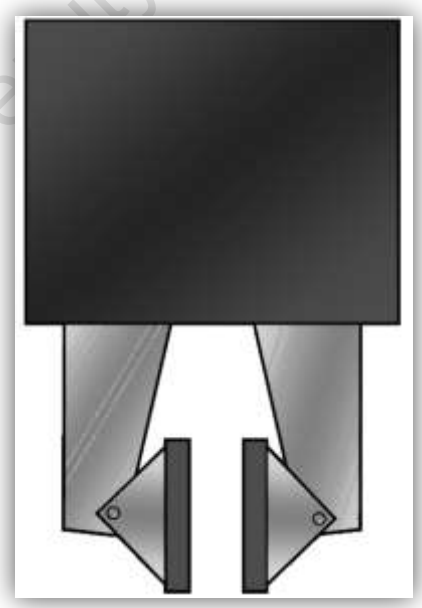

Figure 6-8: Self-Aligning Gripper [40]

A6.2 Cutters

Several industrial multi-purpose grippers come with a cutter incorporated into the design. Two of these existing designs, the first from Sea View Systems and the second from Hydro-lek, are shown below. In both designs, the gripper operates with the retraction of the actuator and the cutter operates with the extension of the actuator. That is, as the gripper opens, the cutter closes, and vice versa.

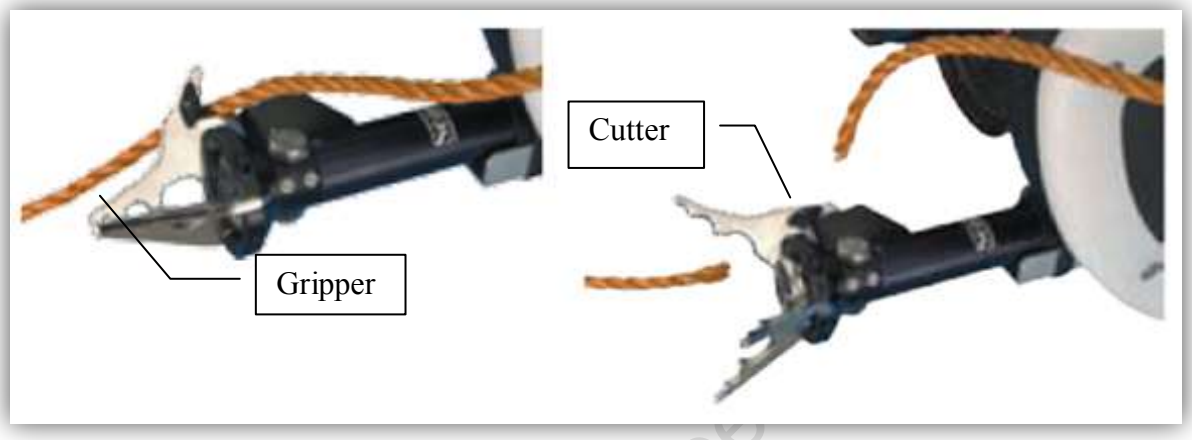

Figure 6-9: Sea View Systems' Gripper-Cutter Combination [47]

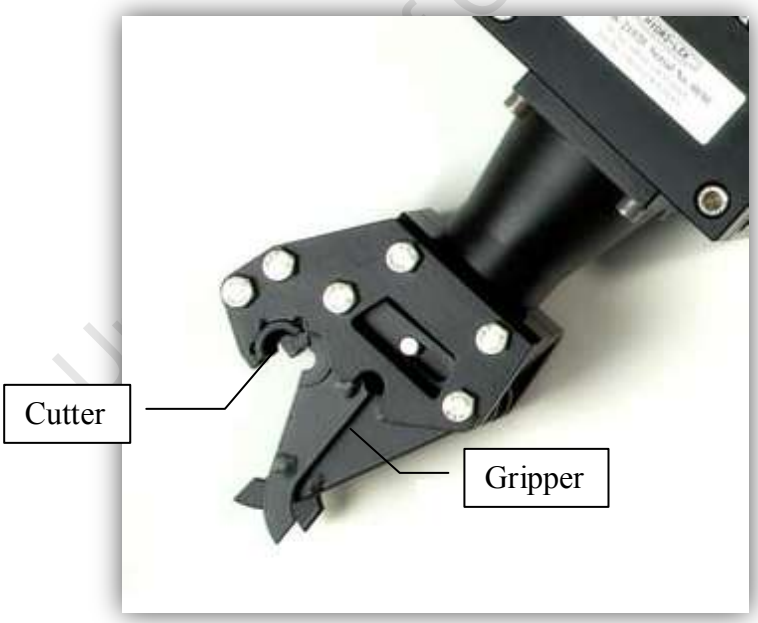

Figure 6-10: Hydro-lek's Gripper-Cutter Combination [48]

Another method of incorporating a cutter and gripper is to have the cutter closer to the hinge than the gripper, and so it both cuts and grips on the closing stroke, and how you handle the material depends on where you place it in the gripper-cutter combination. Most pliers use this arrangement, and the layout can be seen in the Leatherman shown in Figure 6-11.

Figure 6-11: Leatherman Juice XE6 Showing Gripper-Cutter Combination [49]

While this solution is simpler, it is limited to a very small diameter target, such as thin wire. When trying to cut larger objects, the gripper closes on the object, and this prevents the cutter from being able to completely slice through the object. This second method also requires some type of holding force to keep the object in the cutters whilst cutting, as the cutters have a tendency to force the object out of the cutter. An improvement to this is the system used by garden secateurs. As can be seen in Figure 6-12, they utilize a curved blade, with the sharper, thinner blade being convex, and as the object is forced to slide down the blade, the thinner blade puts a backwards rolling moment on the object, which stops it from sliding out. During this process, it cuts the object from several angles.

Figure 6-12: Felco 2 Secateurs [50]

A7. Wiring

From research into the other teams at the RoboCup Rescue, it is evident that wiring poses a significant challenge. Very few of the teams managed to have orderly neat wiring that was protected from potential damage. The PackBot does not however have this problem, as all of its wiring is internal. While detailed designs of the PackBot are unavailable, it is believed that they employ the use of *Slip Rings*. These allow continuous rotation of an arm joint, and prevent wires from twisting.

A7.1 Slip Rings

Slip rings basically consist of conductive brushes running on rings. There are other options such as that employed by Mercotac in which liquid mercury is used as the conductor between two rings [51]. Most systems however utilise brushes running on rings. The material used in both the conductor and the brushes defines the signal and power transfer quality. High current, low noise (and expensive) slip rings will utilize precious metals such as gold on their brushes and rings. Other high quality designs use multi-stranded metal fibres, ensuring that there is always contact [52]. The slip ring by MOOG seen below employs multi-fibre technology.

Slip rings may be of two types; through-bore or non through-bore (capsule) type. Often a shaft travels through the centre of a joint, and the thorough-bore option would be used in these cases. Capsule slip rings are smaller but require clever design as they cannot accommodate a through shaft. The motor in these instances cannot be mounted axially with the joint, but must operate the joint through a set of gears or something similar. Capsule type slip rings are normally used in the bore of a hollow shaft.

Figure 7-1: Picture of MOOG Capsule Slip Ring [52]

A8. Control of Robotic Arms

There is a large variety of industrial solutions for manipulator control. These range from simple toggle switches to state-of-the-art master slave controllers such as the Kraft Raptor's controller. Figure 8-1 shows this solution. Tele-operation using a master/slave system is the most commonly used control system [41].

Figure 8-1: Kraft Raptor Manipulator Master Slave Control Station [53]

The complexity of the arm generally governs which controller can be chosen for each arm. Single function arms normally have a toggle on-off switch, and manipulators with more functions typically have master/slave controllers.

Both position control and speed control are used on manipulator arms. The Orion 7 series manipulator arms for instance comes in both the 7R, which is *rate-controlled*, and the 7P, which is *position controlled* [54]. Position-control controllers are laid out as in the option seen above, where a replica version of the arm can be manipulated by hand and the actual arm replicates the miniatures position. It is known as master-slave control. This is achieved by using angular sensors on each of the joints on both the arm and the controller.

Rate-control controllers usually have joysticks, and the speed of the arm is governed by how far out of the neutral position the joystick is moved. This option as seen below, is used in mining diggers, and is a quicker method of operation but requires a significant level of operator skill.

Figure 8-2: JCB Excavator Cabin showing the Rate Control Joysticks [55]

A9. Concluding Remarks

It can be seen that a multi-jointed arm gives the best work envelope for a relatively low degree of complexity. A two jaw gripper will best suit a multi-jointed arm, especially if it includes a rotating wrist joint. Given the electrical power available and the weight and size limitations, electrical actuators are the only choice. Worm gear arrangements like that of the University of Warwick's (see below), will be most suitable to produce the required amount of torque and holding torque. It will be preferable to have more degrees of freedom however, and to incorporate a gripper/cutter on the arm.

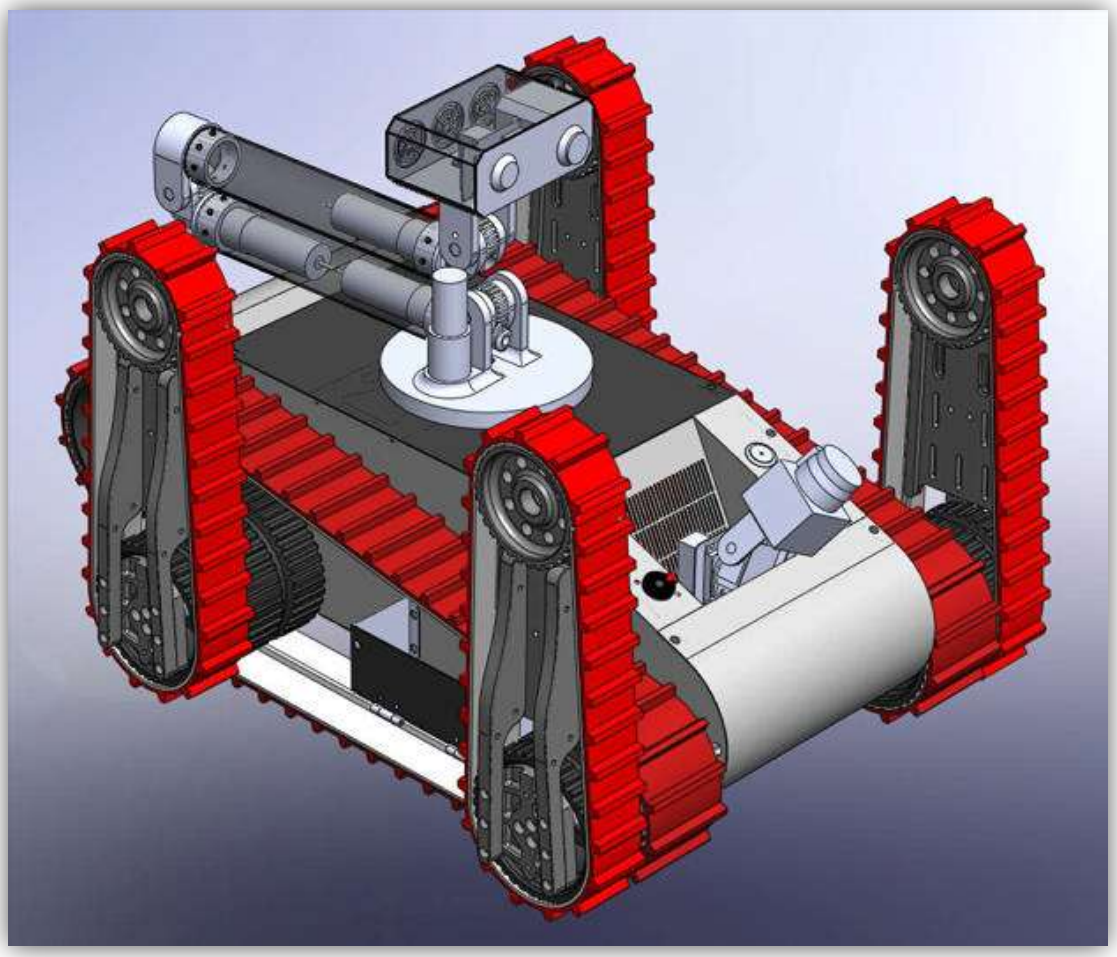

Figure 9-1: Warwick Mobile Robotics SolidWorks Model showing Worm Joints [56]

Elimination of backlash (free-play) is also desirable but will depend on the availability and cost of rare worm gear designs such as the duplex worm or the double enveloping worm.

Control can be performed by either position control or rate control. As joystick devices are readily available, and cost effective, they are a favourable choice. However, it will be preferable if they could operate on inverse kinematics, allowing the operator to just manipulate the end-effector. If a master-slave type controller is chosen, it will have to be custom built for the arm.

A10. References

[1] Military Suppliers & News, "Irobot - PackBot EOD Unmanned Tactical Mobile Robot," [Online]. Available: http://www.armedforces-int.com/upload/image_files/articles/images/companies/1249/IRobotImage3.jpg. [Accessed 9 8 2010].

[2] [Online]. Available: http://1.bp.blogspot.com/-mSw0zAX2BgA/TWN81pdQfyI/AAAAAAAAC4A/etFZkHCNBw8/s1600/nzeq.jpg. [Accessed 26 August 2011].

[3] NIST, "RoboCupRescue Robot League Rules 2009.1," 2009. [Online]. Available: http://robotarenas.nist.gov/2010/RoboCupRescueRobotLeagueRules(v2009.1D)pdf.pdf . [Accessed 10 04 2010].

[4] NIST, "Rules Discussion Notes," International Rescue Robot Workshop, 2010.

[5] "510 PackBot," [Online]. Available: http://www.irobot.com/gi/ground/510_PackBot. [Accessed 28 Jan 2012].

[6] CASualty, "RCR2010_(Australia_CASualty)_TDP," 2010.

[7] NuBotRES, "RCR2010_(China_NuBotRESQ)_TDP," 2010.

[8] Warwick, "RCR2010_(ENGLAND_wawrick_mobile_robotics)_TDP," 2010.

[9] Resko, "RCR2010_(Germany_Resko)_TDP," 2010.

[10] MRL, "RCR2010_(IRAN_MRL Rescue Robot)_TDP," 2010.

[11] PARS, "RCR2010_(Iran_Pars)_TDP," 2010.

[12] Pasagrad, "RCR2010_(IRAN_Pasargad)_TDP," 2010.

[13] YRA, "RCR2010_(IRAN_YRA)_TDP," 2010.

[14] C-Rescue, "RCR2010_(JAPAN_C-Rescue)_TDP," 2010.

[15] NIITBLUE, "RCR2010_(JAPAN_NIITBLUE)_TDP," 2010.

[16] Pelican Utd, "RCR2010_(JAPAN_PelicanUnited)_TDP," 2010.

[17] Ariana Ava, "RCR2010_(Malaysia_Iran_AriAnA_AVA)_TDP," 2010.

[18] Ixnamiki, "RCR2010_(Mexico_IxnamikiTeam)_TDP," 2010.

[19] Saviour, "RCR2010_(Pakistan_Saviour)_TDP," 2010.

[20] IRAP Pro, "RCR2010_(Thailand_IRAP_PRO)_TDP," 2010.

[21] KNUTNB, "RCR2010_(Thailand_KMUTNB)_TDP," 2010.

[22] Success, "RCR2010_(Thailand_SUCCESS)_TDP," 2010.

[23] [Online]. Available: http://www.youtube.com/watch?v=ajuRNegB0O8. [Accessed 27 January 2012].

[24] [Online]. Available: http://www.youtube.com/watch?v=vPWxbTOpg10&feature=related. [Accessed 27 January 2012].

[25] H. H. Nazer, "Robots: Applications and Fundementals," 2003. [Online]. Available: http://sharif.ir/~cedra/files/slide/Robotic2.pdf.

[26] E. M. Gallofin, M. L. G. Fernandez and C. M. Oppus, "Design and Construction of a Computer-Controlled Robotic Arm".

[27] Festo, [Online]. Available: http://www.festo.com/pnf/en-gb_gb/products/catalog?action=search&key=dsnu. [Accessed 21 October 2010].

[28] Tolomatic, "Tolomatic VRX Vane Rotary Actuators," [Online]. Available: http://www.tolomatic.com/files/image/products/large/VRX_Cover_CRW_4308-400w.jpg. [Accessed 22 October 2010].

[29] Maxon Motor, "Maxon Motors," [Online]. Available: http://www.maxonmotor.com/. [Accessed 25 October 2010].

[30] W. P. Crosher, Design and Application of the Worm Gear, New York: ASME Press, 2002.

[31] Hangzhou Yushen Speed Reducer Co., Ltd., [Online]. Available: http://img.alibaba.com/img/imagerepos/hz/yu/hzyushen/1271652507773_hz_myalibaba_web10_953.jpg. [Accessed 21 October 2010].

[32] Neeter Drive, "Neeter Drive," [Online]. Available: http://www.engnet.co.za/images/showcase/bigpic/POW015_mi_bevel_gearboxes.jpg. [Accessed 22 October 2010].

[33] Cone Drive, "Double Enveloping Technology," [Online]. Available: http://www.conedrive.com/doublenvelopingtechnology.php. [Accessed 26 October

2010].

[34] MITCalc, [Online]. Available: http://www.mitcalc.com/images/wormgear1.gif. [Accessed 26 October 2010].

[35] Zakgear, "Globoid Technology from ZAKGEAR," [Online]. Available: http://www.zakgear.com/Wormoid.html. [Accessed 26 October 2010].

[36] Allytech, "OTT Dual Lead Concept - Duplex Design," [Online]. Available: http://www.allytech.eu/index_fichiers/DualLeadwormgearswithoutbacklah.htm. [Accessed 26 October 2010].

[37] "OTT Worm Gears," [Online]. Available: http://www.allytech.eu/index_fichiers/Backlashfreewormandwormwheel.htm. [Accessed 14 January 2012].

[38] C. Longhurst, "The Steering Bible," [Online]. Available: http://www.carbibles.com/steering_bible.html. [Accessed 26 October 2010].

[39] R. K. Sedgwick and J. J. Hughes, "Recirculating Ball Worm Drive". USA Patent 3,468,179, 23 September 1969.

[40] B. Nelson, "Introduction to Robotics," 2009. [Online]. Available: http://www.iris.ethz.ch/msrl/education/iris_intro/.

[41] J. Yuh, "Design and Control of Autonomous Underwater Robots: A Survey," in *Autonomous Robots 8*, Netherlands, Kluwer Academic Publishers, 2000, p. 7–24.

[42] Silver Crest Submarines, [Online]. Available: http://www.silvercrestsubmarines.co.uk/images/Image6.gif. [Accessed 30 September 2009].

[43] Solidworks, [Online]. Available: http://i.d.com.com/i/dl/media/dlimage/31/43/1/31431_large.jpeg. [Accessed 1 October 2009].

[44] Schilling Robotics, "Parallel and Intermeshing Jaw Upgrade Kit," 2009. [Online]. Available: www.schilling.com/support/Documents/jawupgrade.pdf.

[45] TCMnet, "iRobot_PackBot_510_with_FasTac_Kit_side," [Online]. Available: http://blog.tmcnet.com/blog/greg-galitzine/iRobot_PackBot_510_with_FasTac_Kit_side.jpg. [Accessed 9 8 2010].

[46] Defense Review, "iRobotPackbotEODBrochure-SpecSheet_1," [Online]. Available: http://www.defensereview.com/1_31_2004/iRobotPackbotEODBrochure-

SpecSheet_1.jpg. [Accessed 9 8 2010].

[47] Sea View Systems, "Single Function Manipulator and Rope Cutter," [Online]. Available: www.seaviewsystems.com/wp.../Single-Function-Manipulator.pdf.

[48] Hydro-lek, "5 Function Manipulator - Mini - HLK-43000," [Online]. Available: http://www.hydro-lek.com/images/HLK-43000_Screen.jpg. [Accessed 3 October 2009].

[49] Leatherman, "pronomadgear," [Online]. Available: http://pronomadgear.com.au/images/categories/leatherman_juice_xe6S.jpg. [Accessed 16 Oct 2009].

[50] Felco Secateurs, [Online]. Available: http://www.dyg.ie/files/plants/Felco%202%20secateurs.jpg. [Accessed 2009 October 21].

[51] Mercotac, "Using Slip Rings," [Online]. Available: http://www.mercotac.com/?gclid=CI7Z5eSC9KQCFQlm7AodBiIyhQ. [Accessed 2010 October 27].

[52] MOOG Components Group, "Technical Information," [Online]. Available: http://www.moog.com/literature/MCG/fiberbrush.pdf. [Accessed 21 October 2010].

[53] Kraft TeleRobotics Inc., "Raptor Force Feedback Manipulator," USA, 2005.

[54] Schilling Robotics, "Orion Series," 2009. [Online]. Available: www.schilling.com/products/manipulators/pages/orion.aspx.

[55] JCB, [Online]. Available: http://img.directindustry.com/images_di/photo-g/crawler-excavator-40942.jpg. [Accessed 2009 October 22].

[56] University of Warwick, "Team Description Paper," 2010.

[57] J. K. Nisbett and R. G. Budynas, Shigley's Mechanical Engineering Design, New York: McGraw-Hil, 2008.

Appendix B

Specifications

Table of Contents

List of Figures

List of Tables

B1. Introduction

This appendix looks at each of the required specifications, and details the justifications of each of the specifications. It starts by presenting a summary list, and then expands on each of the requirements, justifying that specification. The summary list is shown in the main body together with the achieved specifications.

B2. List of Specifications

Table 2-1: List of Specifications

No.	D/W	Requirements	Desired	Location
1.	**Arm Performance Specifications**			
1.1.	D	Minimum Shelf Reach	1m High and 650mm Deep	B3.1.1
1.2.	D	Minimum Lift at Full Reach	1kg	B3.1.2
1.3.	D	Ability to Support Sensor Pack	2kg	B3.1.3
1.4.	D	Minimum Joint Rotation Speed	20°/s	B3.1.5
1.5.	D	Maximum Joint Backlash	0.2°	B3.1.6
1.6.	D	Internal Wiring	Yes	B3.1.7
2.	**End Effector Performance Specifications**			
2.1.	D	Minimum Gripper Bite Size	142mm	B3.2.1
2.2.	D	Continuous Wrist Rotation	Yes	B3.2.2
2.3.	D	Cutting Ability	Yes	B3.2.3
2.4.	D	Ability to Use Tools	Yes	B3.2.4
3.	**Physical Specifications**			
3.1.	D	Fit Through *Fireman's Triangle*	Yes	B3.3.1
3.2.	D	Ability to Fit into Standard Pelican Type Box	Yes	B3.3.2
3.3.	D	Maximum Weight Excluding Sensor Pack	10kg	B3.3.3
4.	**Control System Specifications**			
4.1.	D	Master-Slave Controller	Yes	B3.4.1
4.2.	D	Inverse Kinematic Control	Yes	B3.4.2
5.	**Power Specifications**			
5.1.	D	Operate Off 36V Supply Batteries	Yes	B3.5.1
5.2.	D	Maximum Current Draw	10A	B3.5.2
6.	**Budget Specifications**			
6.1.	D	Maximum Cost	R70000	B3.6.1

B3. Justification of Specifications

B3.1 Performance Specifications

B3.1.1 Minimum Shelf Reach

According to the rules for the Blue Arena of the RoboCup Rescue [1], the furthest away object to be grasped will be placed 600mm deep on a shelf that is 1m high, (see figure below). As the block is 100mm deep, an extra 50mm will be required to properly grasp the object. This depth is measured from the inside of the elbow, to the tips of the jaws. For more information, see the section on the Blue Arena in the Literature Survey, Appendix A.

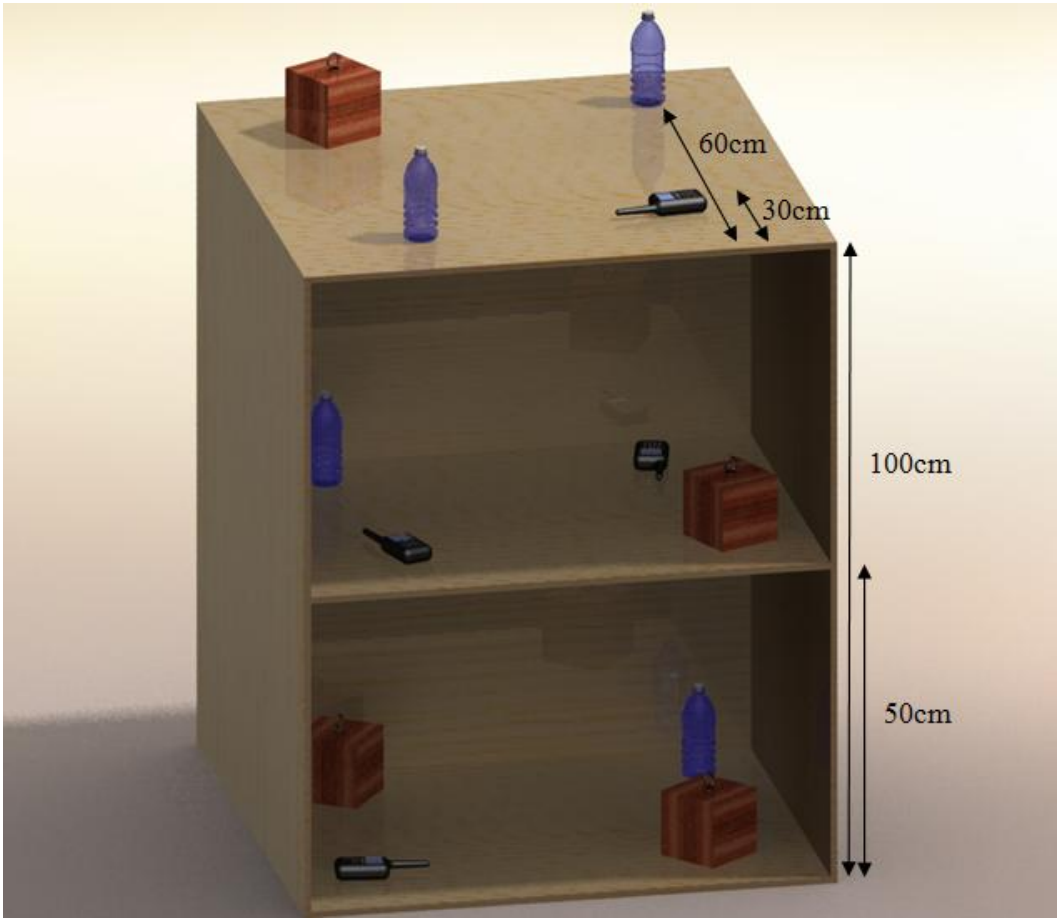

Figure 3-1: SolidWorks Rendering of Mock-Up of the Blue Arena

B3.1.2 Minimum Lift at Full Reach

The heaviest object to be lifted is a 500ml water bottle, which weighs just above 500g. It has however been decided on, in order to have extra functionality, to have the capability of lifting 1kg.

B3.1.3 Ability to Support Sensor Pack

The robot will be equipped with a sensor pack, (that has itself been specified to be less than 2kg), and this sensor pack will be mounted on the arm. The arm is required to carry the pack as well as provide it with power and communications.

B3.1.4 Teleoperation

The entire robot will be teleoperated and therefore so will the arm. This means that the arm will run off the batteries housed in the base, and will communicate using the central TCP-IP being used by the base. For testing the arm should be able to be operated off one Ethernet cable, and a power source.

B3.1.5 Minimum Joint Rotation Speed

The robot must move through the arena in a limited amount of time. This means that a faster operating speed is preferable. A speed of 20°/s was chosen as a good compromise between speed and control. This will allow the arm to unfold from its home position and reach the furthest block on the top shelf in just under 10 seconds.

B3.1.6 Maximum Joint Backlash

Backlash is a negative effect in which the arm can move 'on its own accord'. As this significantly complicates and reduces precision control, as low a backlash as possible is preferable. A tip error of less than 10mm is desirable. If the three arm joints have equal error, then a backlash of less than 0.2° is required on each joint.

B3.1.7 Internal Wiring

For both aesthetics and robustness, the wiring should be internal. This will protect the wiring, and keep the robot streamline, and prevent it from 'snagging' on debris.

B3.2 End Effector Performance Specifications

B3.2.1 Minimum Gripper Bite Size

According to the rules for the Blue Arena of the RoboCup Rescue [1], the object of greatest width is a wooden cube measuring 100mm in length. In order to quickly approach and grip the block, no matter its orientation, a bite size of at least 142mm, (100mm x √2) is necessary. The diagram below shows the block in its worst case scenario.

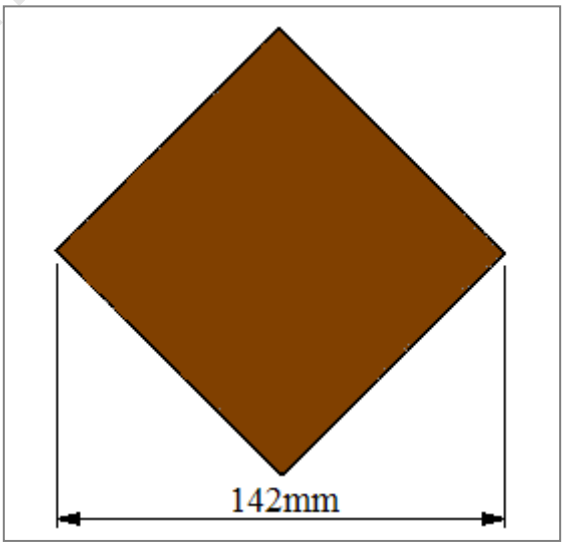

Figure 3-2: Diagram showing Block in Worst Case Scenario

B3.2.2 Continuous Wrist Rotation

As the arm is required to use tools such as screw-drivers, (see Ability to Use Tools below), it will be required to spin them through more than 360° continuously.

B3.2.3 Cutting Ability

To add extra functionality, the end effector is to have an integrated cutter capable of cutting nylon or cotton rope or small diameter metal wire.

B3.2.4 Ability to Use Tools

Also to increase functionally, a tool receptacle will be required. The ability to store the tools onboard and change tools remotely is also required. Typical tools required will be flat and Philip's type screwdrivers, Allan keys, torque keys, etc. The receptacle should be either the standard ¼ inch square socket (male), or the standard ¼ inch hex-socket (female).

B3.3 Physical Specifications

B3.3.1 Fit through *Fireman's Triangle*

As the robot will be used for search and rescue in complicated terrains such as a collapsed building, it needs to navigate though small openings. The test opening that is used in the RoboCup Rescue is an equilateral triangle of 600mm, known as the *Fireman's Triangle*. The entire robot (base, arm and sensor pack) will have to enter through this triangle. As the base occupies the bottom 180mm of the triangle, the arm and sensor pack will have to fit in a smaller, 420mm equilateral triangle.

B3.3.2 Ability to Fit into Standard Pelican Type Box

For secure transportation, the entire robot should fit into a pelican type box, without the need to disassemble.

B3.3.3 Maximum Weight Excluding Sensor Pack

The complete robot should be deployable by two people. The base is specified to be less than 25kg. It has been decided to design the arm to weigh less than 10kg.

B3.4 Control System Specifications

B3.4.1 Master-Slave Controller

A master-slave type controller consists of a small 'replica' of the arm, which is the *master*, and when it is moved, the actual arm (the *slave*) mimics the motion. This allows quick and intuitive control of the arm. The *master* is placed at the operator's station.

B3.4.2 Inverse Kinematic Control

Inverse kinematic control allows the operator to just focus on controlling the end of the arm, while the background programming calculates what the rest of the arm joints should be doing.

B3.5 Power Specifications

B3.5.1 Operate Off 36V Supply Batteries

The base of the robot houses 6 rechargeable 18V Makita Li-ion batteries, of which, some are arranged into pairs providing 36V. The arm should therefore be capable of running off either 18V or 36V or both.

B3.5.2 Maximum Current Draw

Very high current draws may damage the batteries being used. High current draw heats up wiring, slip ring brushes and connectors, and over a sustained period, it may damage them. It is therefore preferable to have as low a current draw as possible. 10A was chosen as a maximum current draw during operation.

B3.6 Budget Specifications

B3.6.1 Maximum Cost

The whole arm project, excluding the sensor pack, should be relatively low cost. This is when compared with commercial options, such as the PackBot.

B4. References

1. **NIST.** RoboCupRescue Robot League Rules 2009.1. *RoboCupRescue.* [Online] 2009. [Cited: 10 04 2010.] http://robotarenas.nist.gov/2010/RoboCupRescueRobotLeagueRules(v2009.1D)pdf.pdf.

Appendix C

Concept Design

Table of Contents

List of Figures

C1. Introduction

This appendix looks at the conceptual design phase of the project. The project started with initial layout concepts. Several options were considered and a winning option was chosen, and then a 3D concept was developed. The *reach* specification as well as the requirement to fit in the *fireman's triangle* were the main driving specifications in the initial stages. Motor and gearbox options were then chosen for the preliminary iteration, and a more detailed concept placing the motors in the arm was developed.

This was then used to run initial design calculations and to choose a more accurate motor-gearbox combination. The *lifting capability* specification was the driving specification in this phase. To satisfy the *low-backlash* specification and the *internal wiring* specification, several gearbox concepts were looked at, and designed.

With the selection of motors and gearboxes, a more detailed concept was developed, after which another iteration of the calculations was done. Once a suitable combination was realised and chosen, the project moved out of the conceptual stage into the detailed design. This appendix will cover in detail all stages barring the final product.

C2. Arm Layout Concepts

Two general layout concepts of the arm were selected. Both could achieve the required reach and both concepts required 6 functions (motors). The schematics can be seen below.

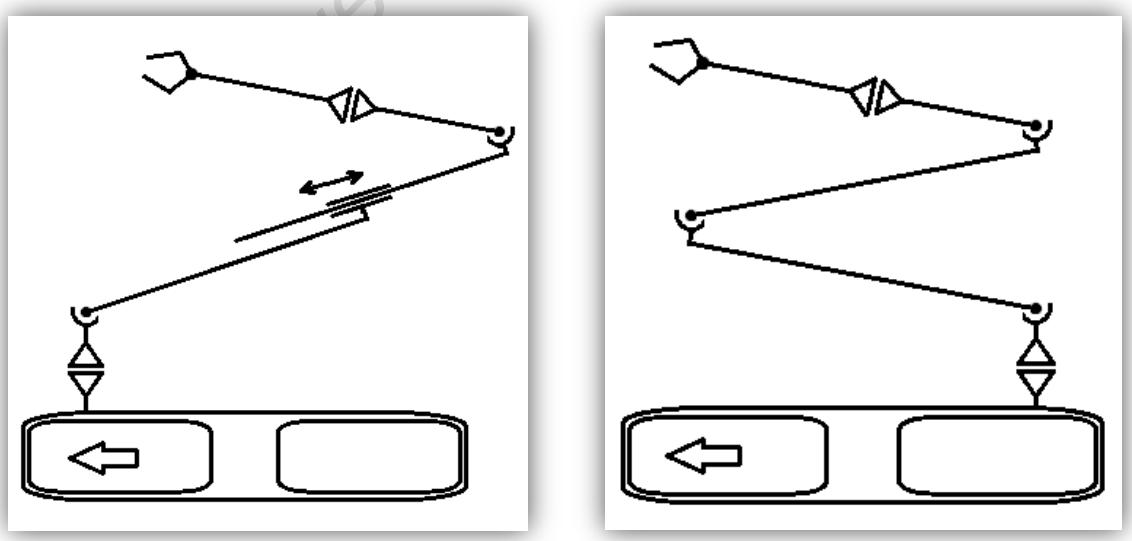

Figure 2-1: Concepts A (left) and B (right) of Manipulator Arm Layouts

There is only a slight difference in functionality between the two concepts. Concept A is slightly easier to operate as the last arm segment does not change angle whilst it is being extended. For Concept B to have this functionality, very advanced control will be required.

Concept B has however been chosen as it is less complicated to design and manufacture, and from past experience, extending arms are problematic. One of the complications making extending arms problematic is that the wiring must extend and retract with the arm. They also do not have the 'reaching over an obstacle' functionality as the arm does not have the extra elbow.

In both concepts the sensor pack will be mounted at the bottom of the top arm segment.

C3. Actuator and Arm Concepts

C3.1 Positioning of Turntable Motor

A basic mock-up of the arm according to Concept A's layout was done and can be seen in Figure 3-1 and Figure 3-2.

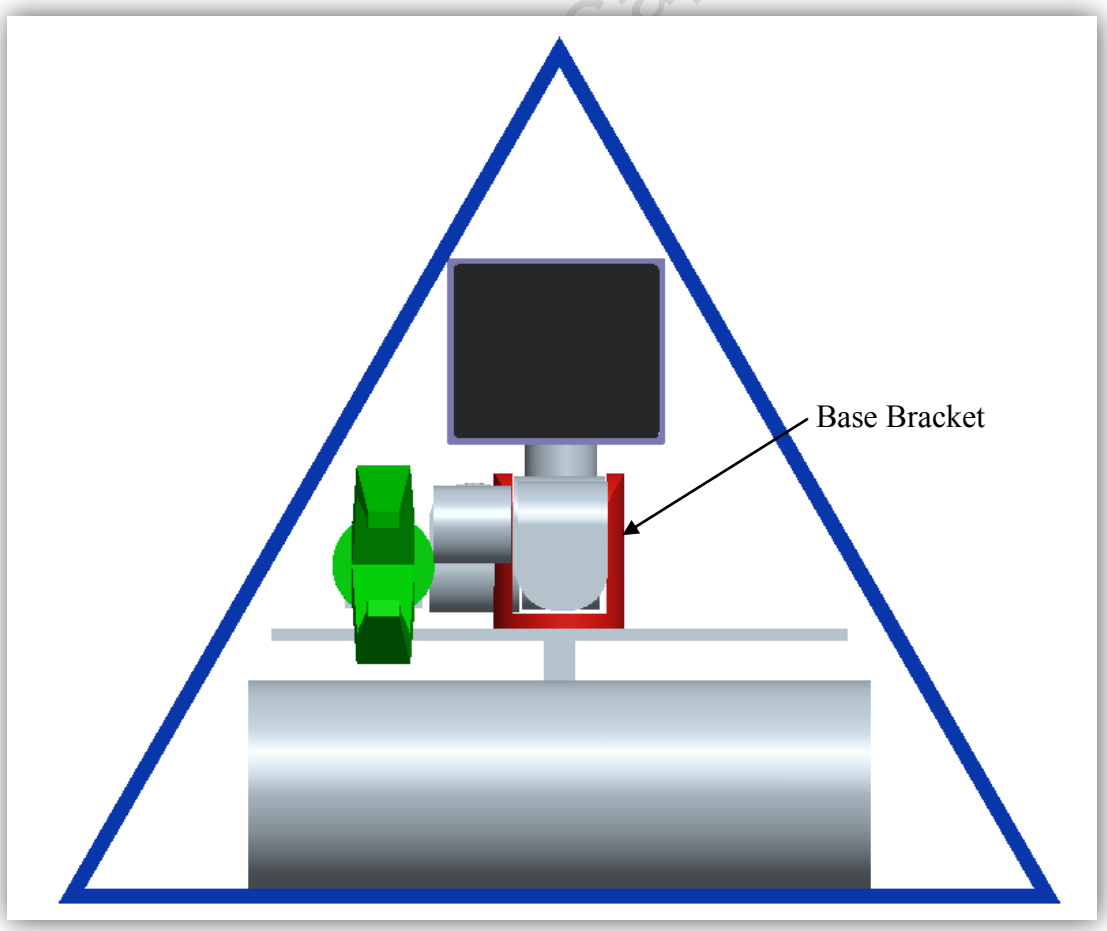

Figure 3-1: Front View of Conceptual Layout Showing Entry Triangle

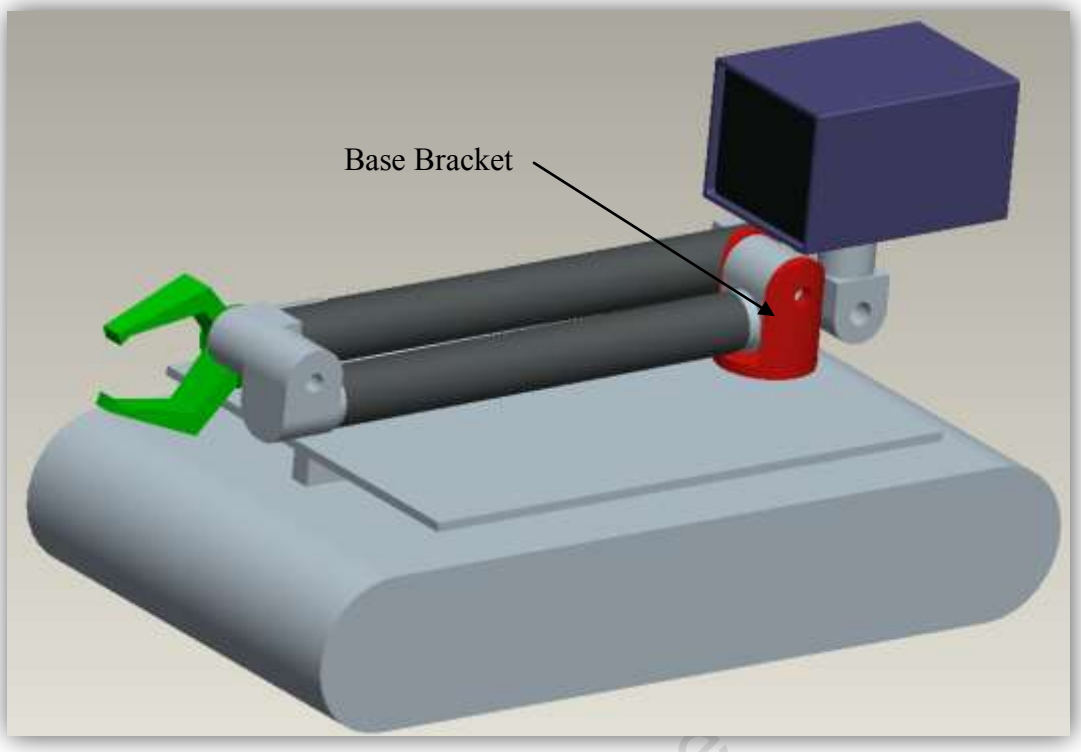

Figure 3-2: 3D View showing Conceptual Layout of Arm and Sensor Pack

The initial turntable concept had the two base motors positioned in a housing that was mounted on top of the base. The benefit of this concept is that both of the motors are not picking themselves up with the arm and it so results in a lighter arm. A sketch of this concept is shown below. However, the requirement for the completed robot to fit through the entry triangle of 600 x 600 x 600 mm caused several problems as this housing pushed everything up and this caused the sensor pack to cut the triangle.

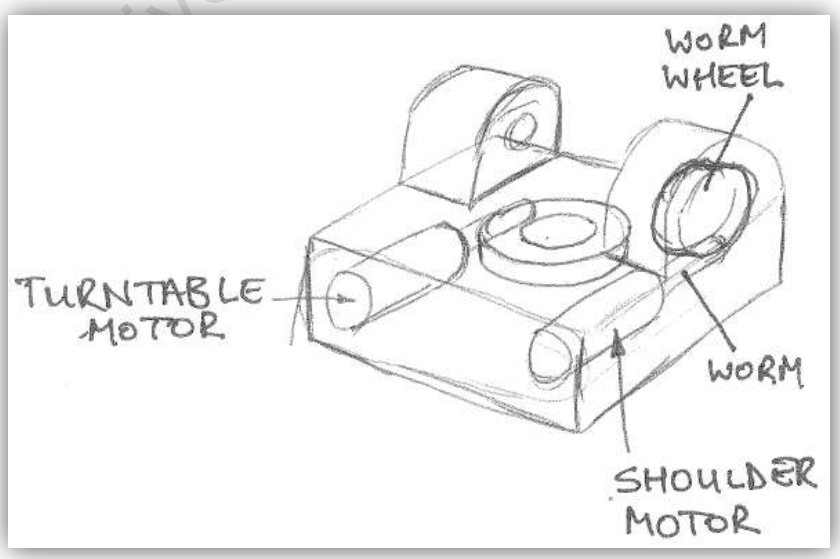

Figure 3-3: Sketch showing Initial Turntable Concept

Two concepts were then generated which do away with this housing. One concept was to house the turntable motor in the base and run a shaft up to the red *base bracket* (seen in Figure 3-1 and Figure 3-2). The other base motor which lifted the arm at the base would be moved into the first section of the arm. The second concept was to have the motor mounted vertically on the side of the *base bracket* and spinning a pinion gear, which turns on the outside of a gear fixed to the base. This can be seen in Figure 3-4 and Figure 3-5.

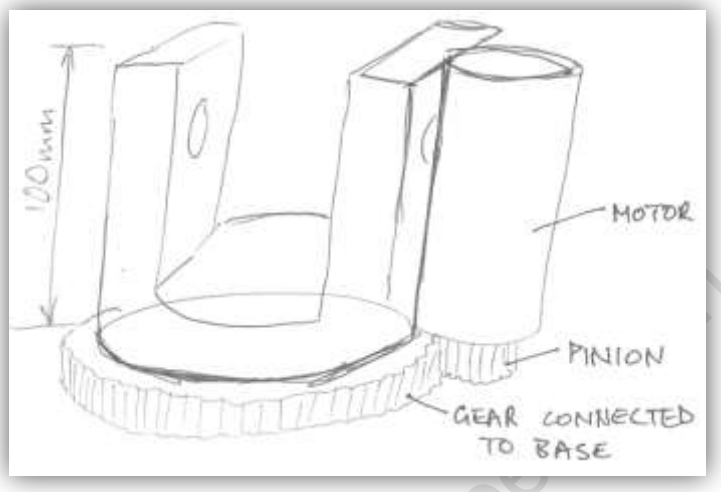

Figure 3-4: Sketch showing Second Turntable Concept

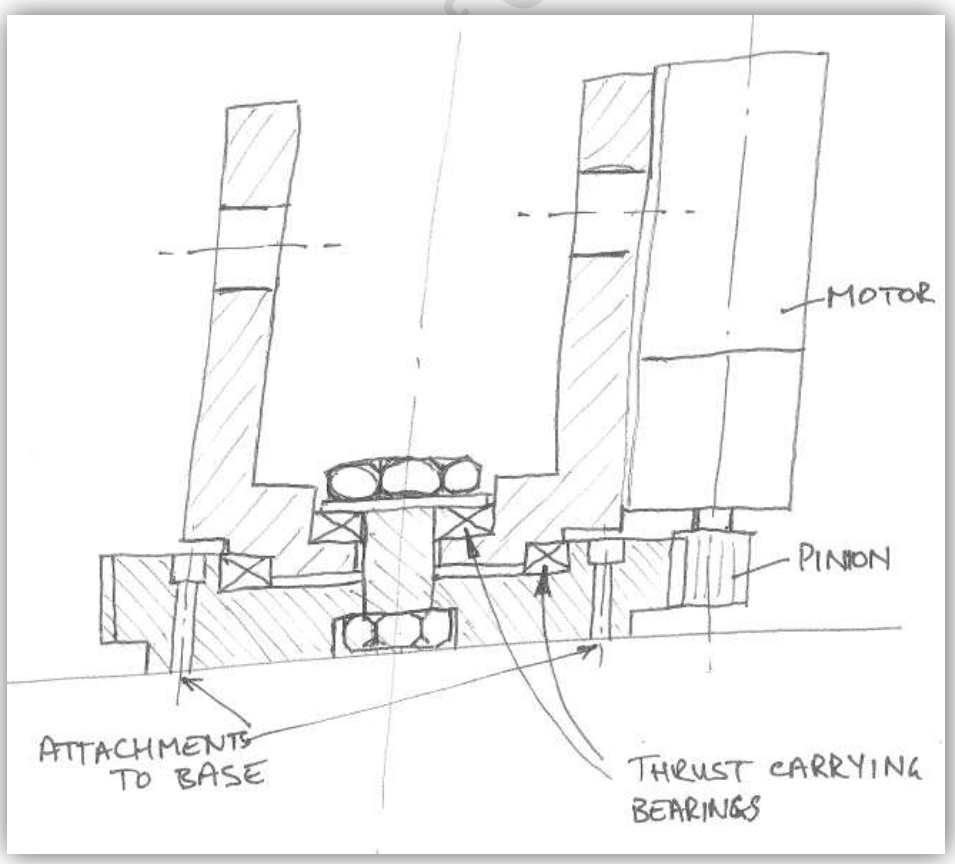

Figure 3-5: Sketch showing Cross-section through Second Turntable Concept

It was ideal to mount the motor rather on the arm, as discussed in the second concept, as it would allow the arm to be modular from the base, and would give it the functionality to be mounted on anything. However, as the motors were decided on, it was discovered that all possible options would be too tall to fit vertically in that space, and would once again push the sensor head up and out of the triangle.

A further concept was then designed, which was a mixture of the initial concepts. The turntable motor would be in a separate housing which meant the arm could operate as a standalone unit, and the first arm motor was put in the arm. Instead of having the turntable motor mounted vertically, and it running a spur gear, it was rotated 90 degrees and run through a worm gear. This was mounted to the side of the red bracket, so as not to push the arm any further upwards. The drawback however is that the rotating axis is offset from the red bracket. The main benefit of this design is that all of the first three actuators have the same motor and gearbox design, making manufacturing simpler, and reducing the number of required spares. This concept was chosen for the final design and can be seen in the sketch below.

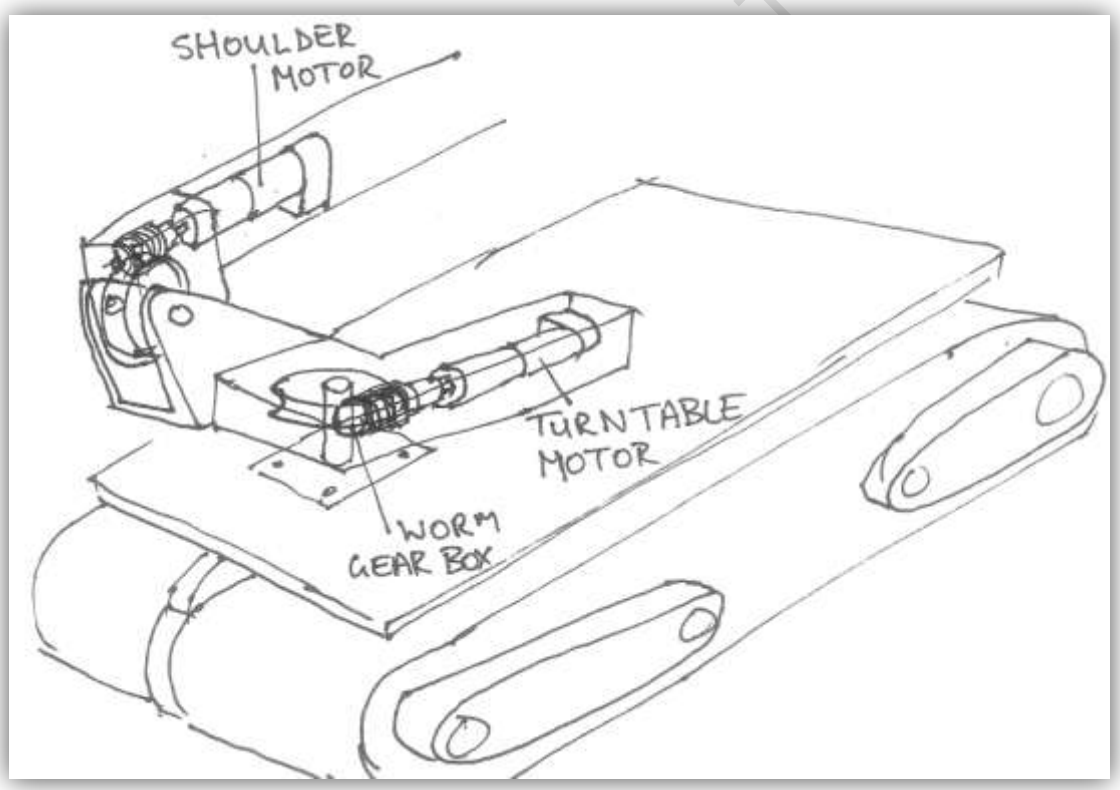

Figure 3-6: Sketch showing Final Turntable Concept

C3.2 Bottom Arm Section

As discussed in the previous section, it was decided to have a standard actuator for all the high torque joints. The turntable motor is likely to have a very low torque requirement, as the bearings will be carrying all of the weight, and the motor will be required to only overcome the rotational inertia. However, if the robot is sitting on an incline of 45 degree to the left for

example, and the arm is required to rotate to the right, the turntable motor will in fact be lifting 0.707 of the shoulder motor's torque. It was therefore decided to include it with the shoulder and first elbow as high torque joints.

Because of the large torque requirements, large reduction ratios were required. On top of this, it was also desirable for the arm to hold its position, even when switched off. *Worm gears* were therefore the obvious choice, as they 'auto-lock' when not being driven, and they allow for large reduction ratios. They are angularly offset by 90° which allows them to be housed in the arm's tube section. This also allows for the wiring to pass through the centre of the rotating axis.

Figure 3-7 shows the bearing arrangement, slip ring positioning and motor mounting of the worm gear housing concept.

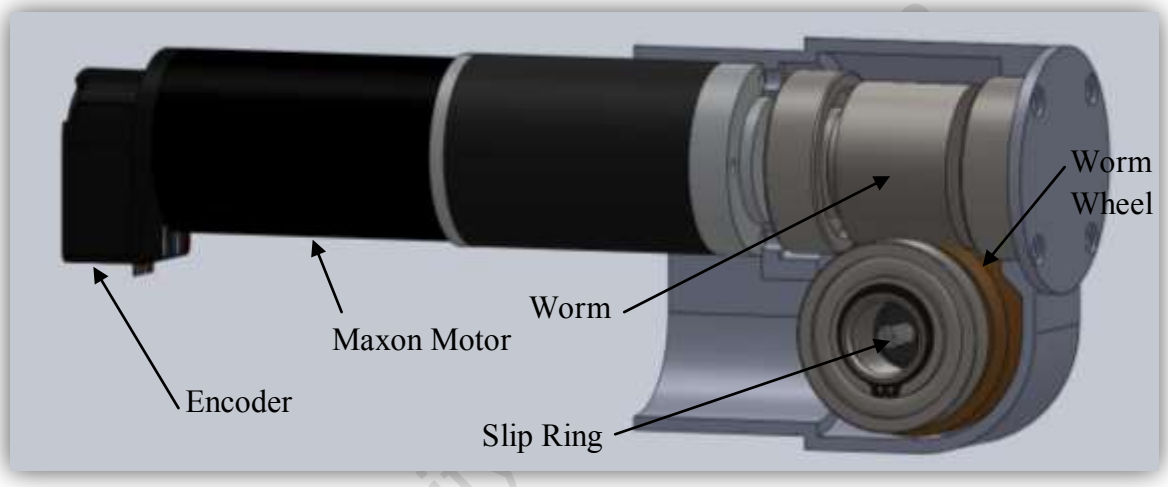

Figure 3-7: Worm Gear Housing Detailed Concept

C3.3 Pan-tilt Concept

The design shown in Figure 3-8 was a concept for the Pan-Tilt system. It required the motors to *not* be axially aligned with the rotating pivot, allowing the slip ring to carry the wires down the centre of rotation. This is achieved by using a bevel gear and an offset spur gear. The disadvantage of the *pan* arrangement was that the entire oval shaped housing rotated around the L-shaped shaft. This meant offsetting it far enough to allow for the housing to pass in the gap. The concept was then developed to have the slip ring stationary with respect to the Sensor Payload, and have the motor stationary with respect to the *tilt* shaft. This resulted in the housing remaining stationary and the sensor payload rotating on top of it. This is seen in the final solution discussed in detail in the main body of the report.

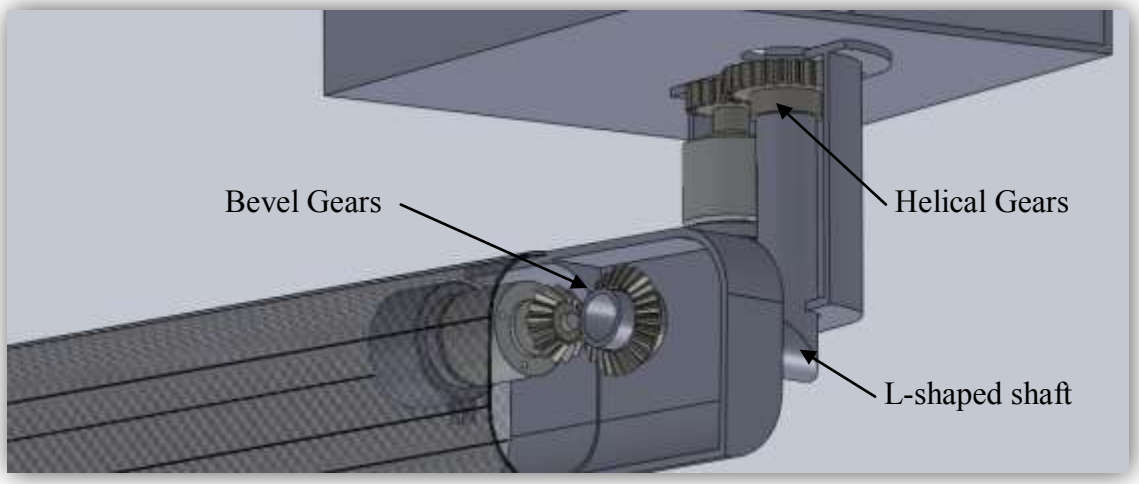

Figure 3-8: Pan-Tilt System that allows Internal Wires

C3.4 End Effector Designs

One of the requirements for the arm is that it has continuous wrist rotation. This is to allow for use of tools such as screwdrivers and sockets etc. The complication is that the gripper is after the wrist, and so the controls, wiring, etc have to pass through the wrist section. The below concept allows all the wiring and motors to remain stationary, and therefore eliminates this problem.

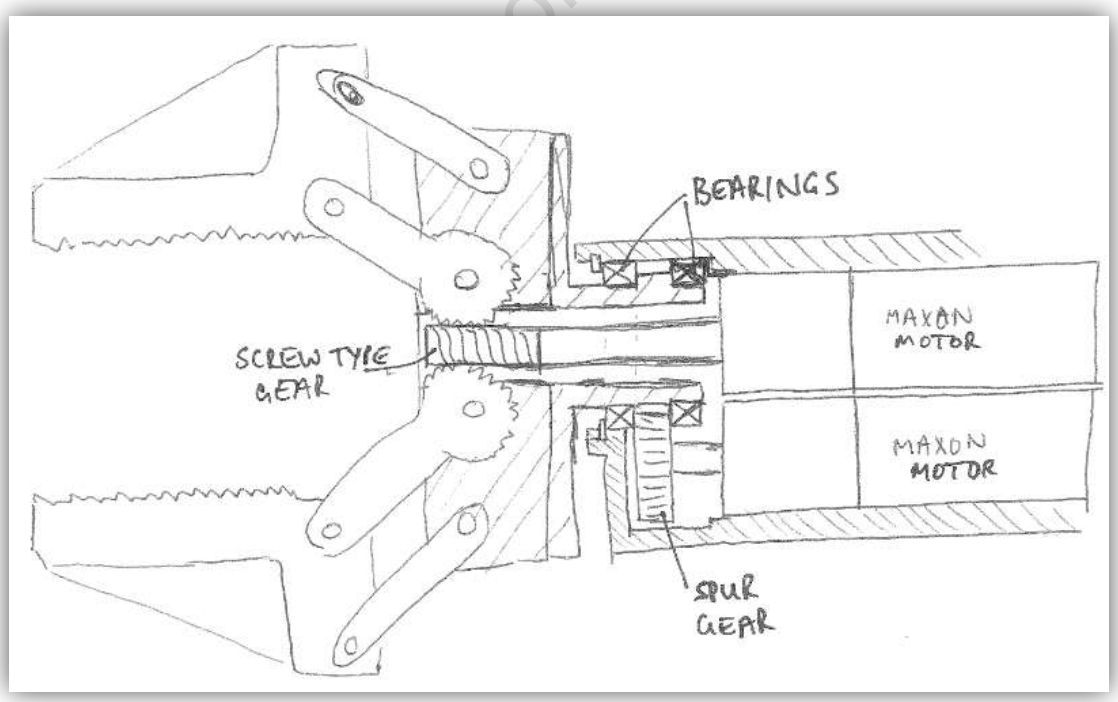

Figure 3-9: Cross Sectional Sketch showing Wrist and Gripper Concept

There are problems however with this design; it will require accurate and complex control as when the wrist rotates, the gripper will be either loosened or tightened, unless it is controlled

to rotate at the exact same speed as the wrist. On top of this, if any touch sensors were to be mounted on the jaws, there is no wiring available to communicate with it.

Undergraduate students, Marten Cross and Terry Scott developed an angular gripper and a parallel gripper respectively, as sub-projects to this project. The final designs of each can be seen below. These grippers were both manufactured and tested. The angular gripper proved to have better functionality, but it did not meet the weight specifications. The parallel gripper proved to be strong, aesthetic and light enough to be used. It will therefore be the gripper used. Masters student Michael Reiger is currently developing the next generation gripper, with touch sensing and better overall functionality. It will also be lighter.

Figure 3-10: Rendering of Angular Action Gripper

Figure 3-11: Rendering of Parallel Action Gripper

C4. Low-Backlash Concepts

One of the main specifications, and one of the key aspects making this arm unique among its competition, is the requirement for *near-zero backlash.* A large amount of research was done into existing low backlash concepts. Research specifically with regards to worm gears was carried out. The report on this research can be found in Appendix A, the Literature Survey.

There was one promising low backlash solution commercially available. It is known as *duplex* worm gears. However, it is rare, and therefore a costly option. It was then decided to design new concepts to cancel the backlash. The below sketches show two such concepts.

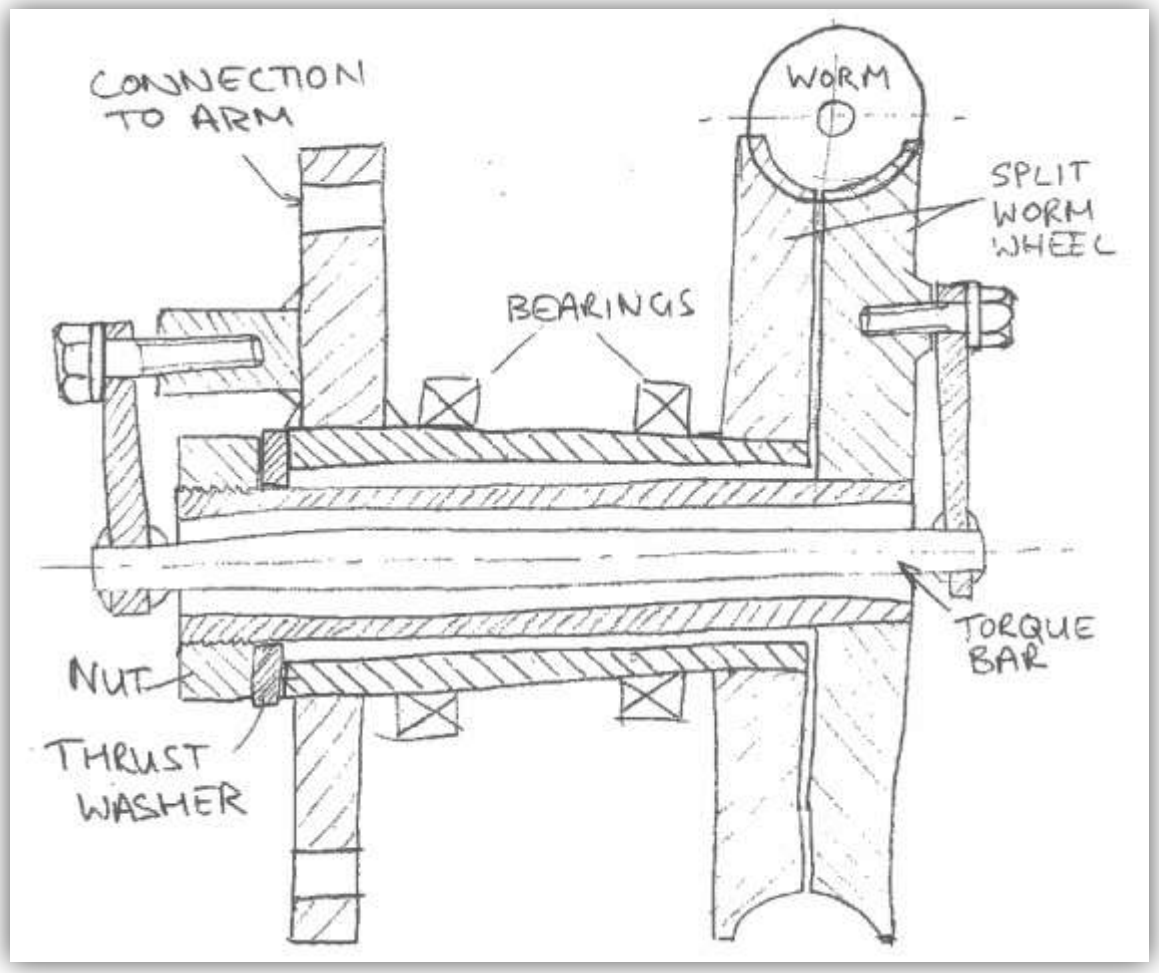

Figure 4-1: Cross Sectional Sketch of Split Worm Wheel Zero Backlash Design

This concept uses a *torque bar* to force open the teeth of each split *worm wheel* half, in order to completely *fill* the gap in the *worm* and thereby remove all backlash. The shortfall of this concept is that only half of the worm (the driving half) is carrying the load. This means that gears twice as strong need to be selected. Another problem is that because of the clamping force provided by the *torque bar, the* friction is greatly increased, and so the power and torque requirements would increase in proportion to the friction increase. The wear rate will also greatly increase as the driving surface area is halved.

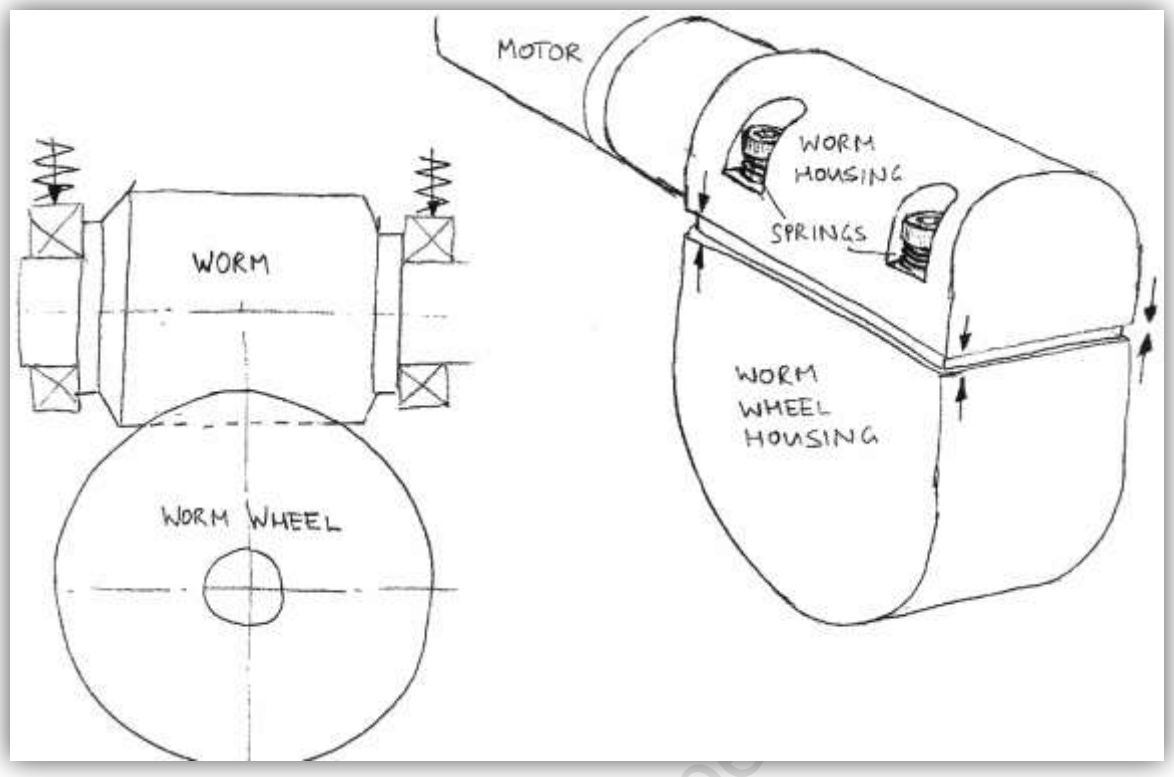

Figure 4-2: Sketch showing Spring Loaded Housing Concept for Zero Backlash

The concept shown above is also a spring loaded type design. It forces the worm into the worm wheel, again removing the backlash. Unlike the previous concept, it uses the entire tooth, and not just half. It does however still have the increased friction problem, requiring more torque and giving a greater wear rate.

This is however not a good solution as worm gears run less efficiently and wear quickly if they are not on their design *centre distance*. [1]

It was therefore decided to go with *duplex* gears. In this design the worm needs to be able to be shifted axially and locked. It was decided that the worm would be preset using cylindrical spacers of different thickness to offset it from the bearings, which would remain stationary in the housing. It is preferable for the bearings to be further apart from each other, to better support the worm.

C5. Gravity Compensation Concepts

After running calculations, it was seen that the base actuator would be required to provide 120 Nm of torque. This is extremely high and posed a problem in worm gear selection. The brass worm gears were not strong enough to handle this torque, and so gears with a large diameter had to be chosen. This unfortunately increased the size of the housing and further increased the weight, causing further problems.

A solution was thought up that reduced the required base torque. It consisted of a torsion spring that would offset the torque due to gravity. The spring strength was decided to be equal to the torque experienced when the arm is in its collapsed position. This would mean, the motors would feel a near-zero (weightless) loading, when the arm is collapsed. This is shown in the graph below.

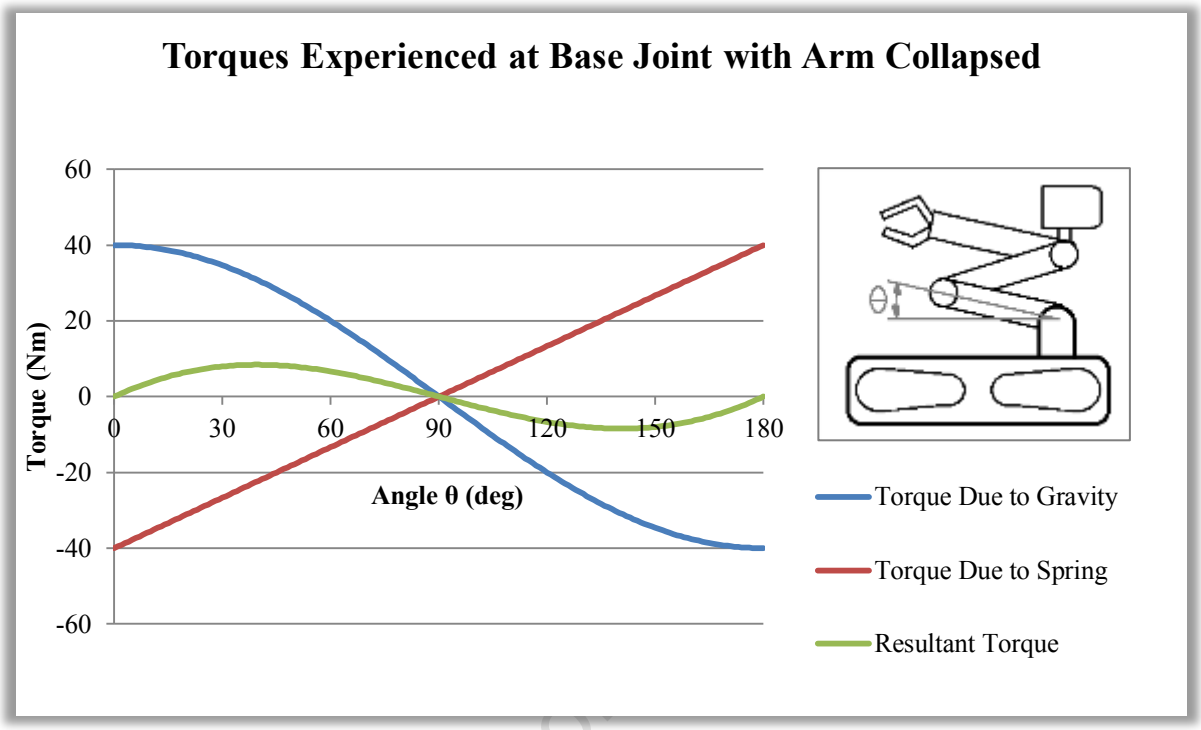

Figure 5-1: Graph Showing Torque Offset due to Spring with Arm Collapsed

The spring is unloaded in the vertical position, and so deflection occurs when the arm moves down in either direction from the vertical. The graph shows that while it is not constantly a zero loading, (due to the fact that the loading due to gravity is a sinusoidal function with respect to change in angle while the spring loading is a directly proportional relationship), it is significantly closer to zero (below 10 Nm), and easier for the motor. When the arm is fully extended and loaded, the maximum loading experienced by the actuator is reduced to just over 80 Nm, as seen in Figure 5-2. This is a considerable saving in required torque, and allows for smaller diameter gears to be chosen.

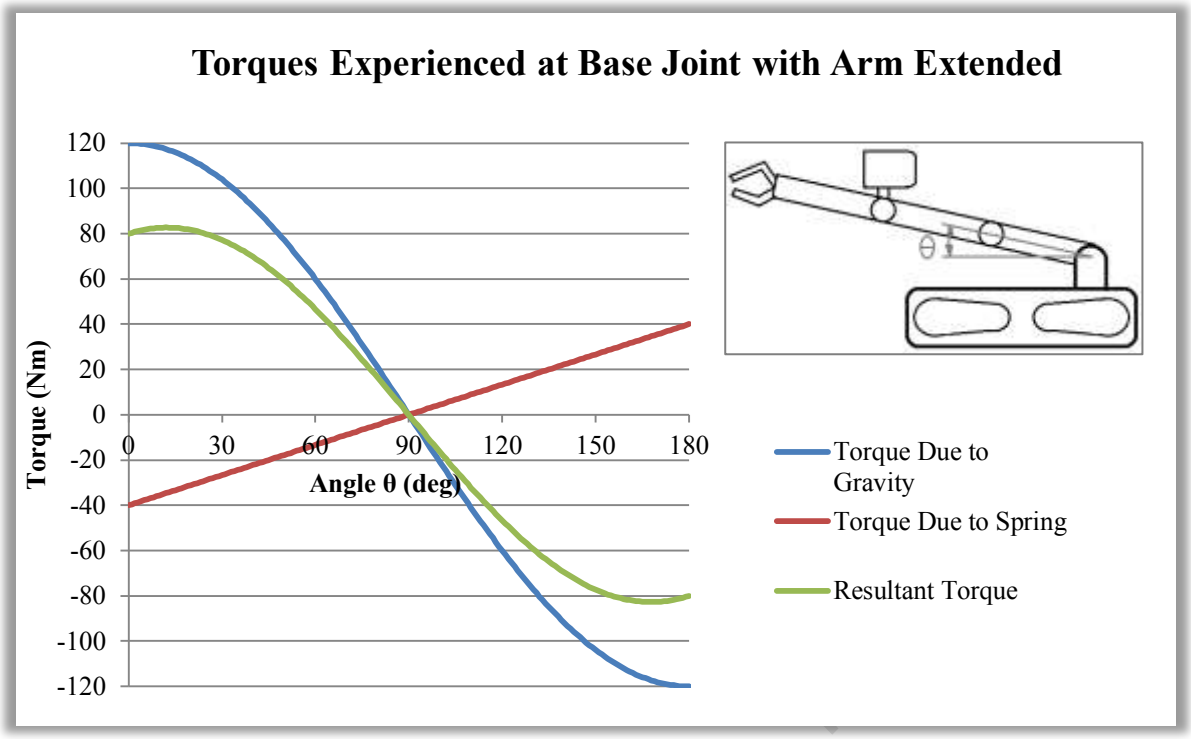

Figure 5-2: Graph Showing Torque Offset due to Spring with Arm Extended

The space available for the torsion spring was very small, and so use of a *torsion bar* instead was investigated. Figure 5-3 shows its use in motor vehicle suspension. Note its very compact nature.

Figure 5-3: Figure Showing Use of Torsion Bar in Vehicle Suspension [2]

However, after running calculations, it was determined that a torsion bar short enough to fit into the required space would not be able to flex through 90 degrees without permanently deforming. Torsion springs were then looked into, and a suitable option was chosen. This is shown in detail in the main body of the report.

C6. Final Concept and Summary

A revised and more detailed concept of the manipulator arm's layout was then developed on Solidworks. This final concept is shown in the four following pictures. The position that it is in, in Figure 6-1, is how it will most likely be when travelling and negotiating terrain. In this position, the main camera should take the place of the *stalk camera*. Figure 6-2 shows Front, Left and Top views of the arm on the base. Figure 6-3 shows the arm in its 'Home' postion with the entry triangle around it, and Figure 6-4 shows the complete system concept, with the angular gripper included. This was not the final design; it was the last coneptual model designed. The detailed design phase was then started, and this is covered in the main body of this report.

Figure 6-1: Rendered 3D View of Robot Arm Concept in Normal "Travelling" Position

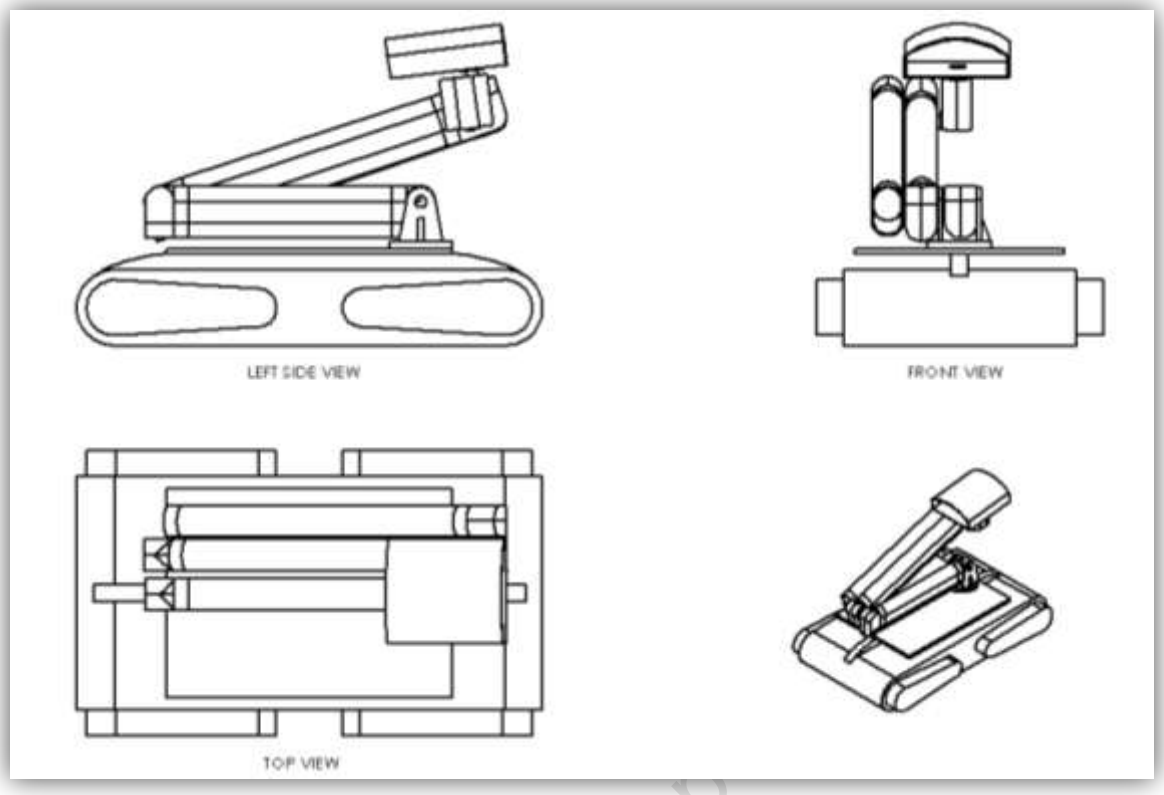

Figure 6-2: Front, Left, Top and Isometric Views of Arm Concept

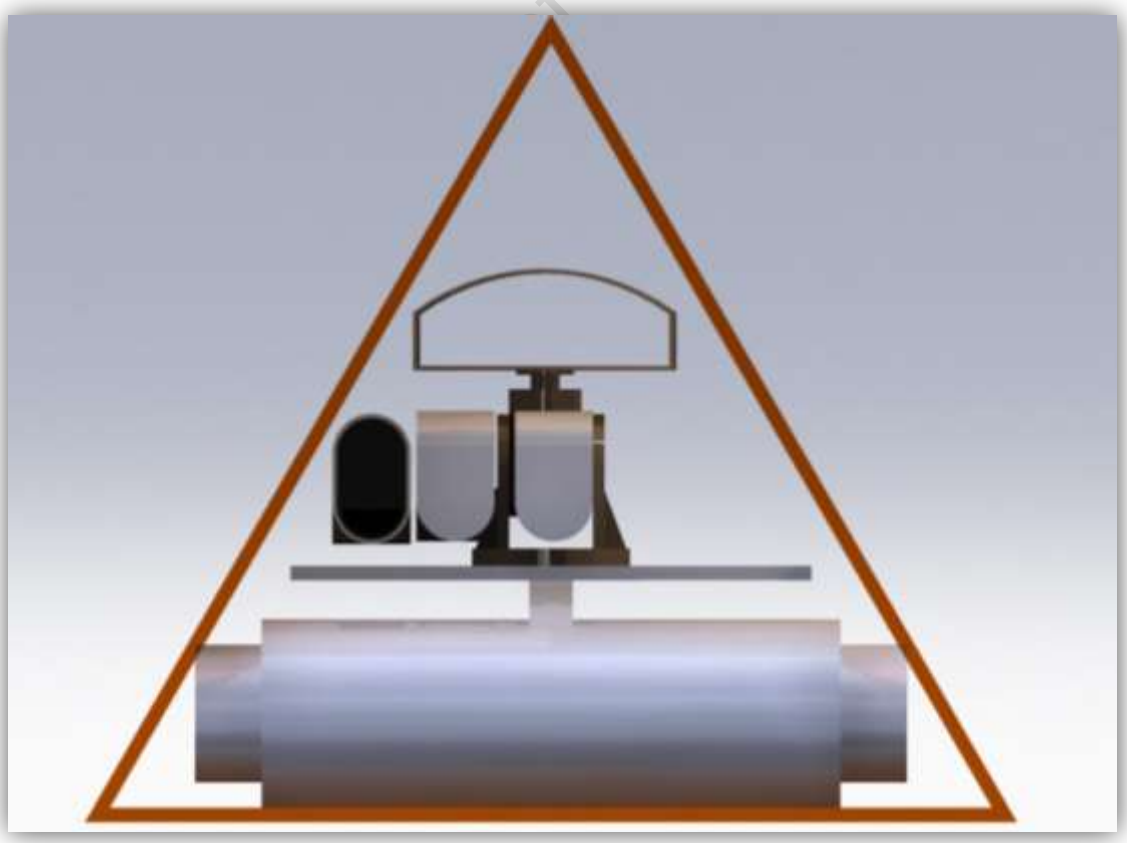

Figure 6-3: Rendered View showing Rescue Robot in Entry Triangle

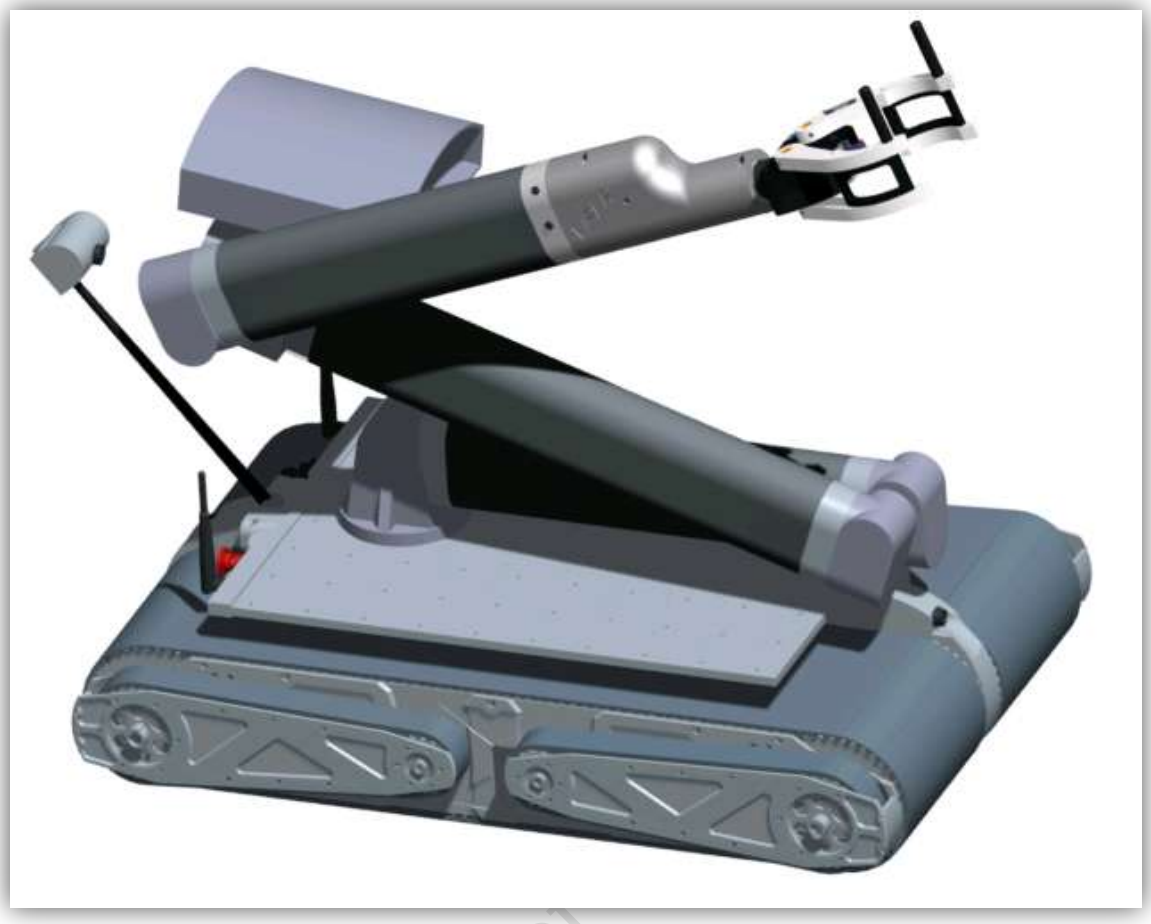

Figure 6-4: Rendering of Complete System Concept with Angular Gripper

C7. References

1. **Crosher, William P.** *Design and Application of the Worm Gear.* New York : ASME Press, 2002. 0-7918-0178-0.

2. Suspension Bible. *Car Bibles.* [Online] [Cited: 22 October 2010.] http://www.carbibles.com/images/longitudinal-torsion-bar.jpg.

Appendix D

Testing Documentation

Table of Contents

List of Figures

List of Tables

D1. Introduction

This appendix lists in detail the testing procedures and documents the results of these tests. It will include photographs were appropriate and will reference videos. Videos referenced to in the results can all be found on the accompanying CD. The specific joints talked about in the testing procedures are shown on the below diagram. The RATEL's manipulator arm has 6 degrees of freedom plus a pan and tilt for the sensor payload, equalling a total of 8 actuators, or joints.

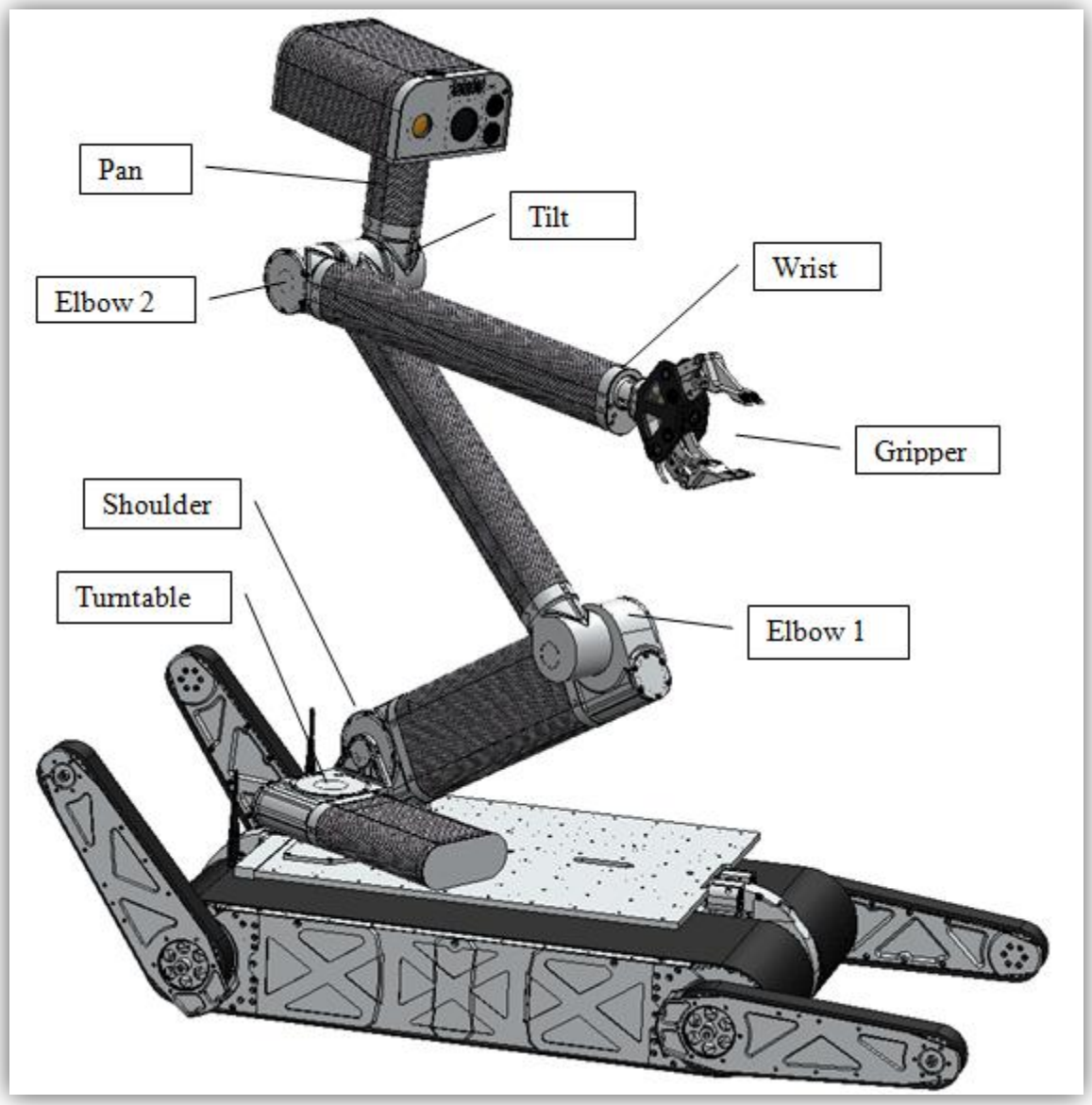

Figure 1-1: Picture of Manipulator Arm showing the Different Joints

D2. Test 1: Testing the Work Envelope

Procedure: With arm fully loaded:

a) Open gripper to maximum
b) Rotate wrist continuously
c) Rotate Elbow 2 continuously
d) Rotate Elbow 1 from clockwise limit to anticlockwise limit
e) Rotate Shoulder from clockwise limit to anticlockwise limit
f) Rotate Turntable continuously
g) Pan Sensor Payload continuously
h) Tilt Sensor Payload from clockwise limit to anticlockwise limit

Measure: Measure the dimensions of the work envelope

Table 2-1: Table of Results for Test 1

Test 1	Joint	Dimension	Speed	Video
a	Gripper	113.3mm	45mm/s	111
b	Wrist	360° Continuous	570°/s	112
c	Elbow 2	360° Continuous	18°/s	110
d	Elbow 1	360°	16.5°/s	115
e	Shoulder	180°	14°/s	115
f	Turntable	360° Continuous	16.5°/s	104
g	Pan	360° Continuous	90°/s	103
h	Tilt	273°	45°/s	105

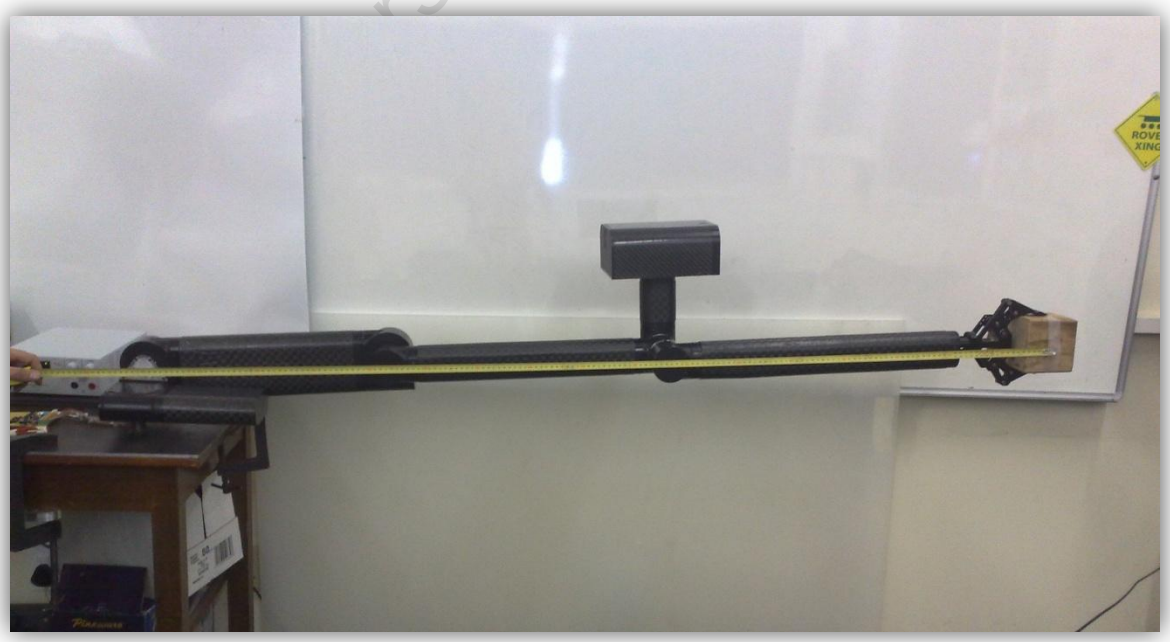

Figure 2-1: Picture showing Measurement of Work Envelope

D3. Test 2: Testing the Loading Capabilities

Procedure: Fully load arm complete with sensor payload, with maximum specified payload of 1kg. Extend arm to its full horizontal reach (worst case scenario)

a) Rotate Elbow 2 joint upwards from horizontal to vertical, return to horizontal
b) Rotate Elbow 1 joint upwards from horizontal to vertical, return to horizontal
c) Rotate Shoulder joint upwards from horizontal to vertical, return to horizontal

Measure: for a-c above

i. Measure the maximum current draw
ii. Measure the time taken to rotate 90deg

Table 3-1: Table of Results for Test 2

Test 2	Joint	Max Current (A)	Time per 90deg (s)	Video
a	Elbow 2	1.2	6	88
b	Elbow 1	2.7	6	95
c	Shoulder	2.9	7	102

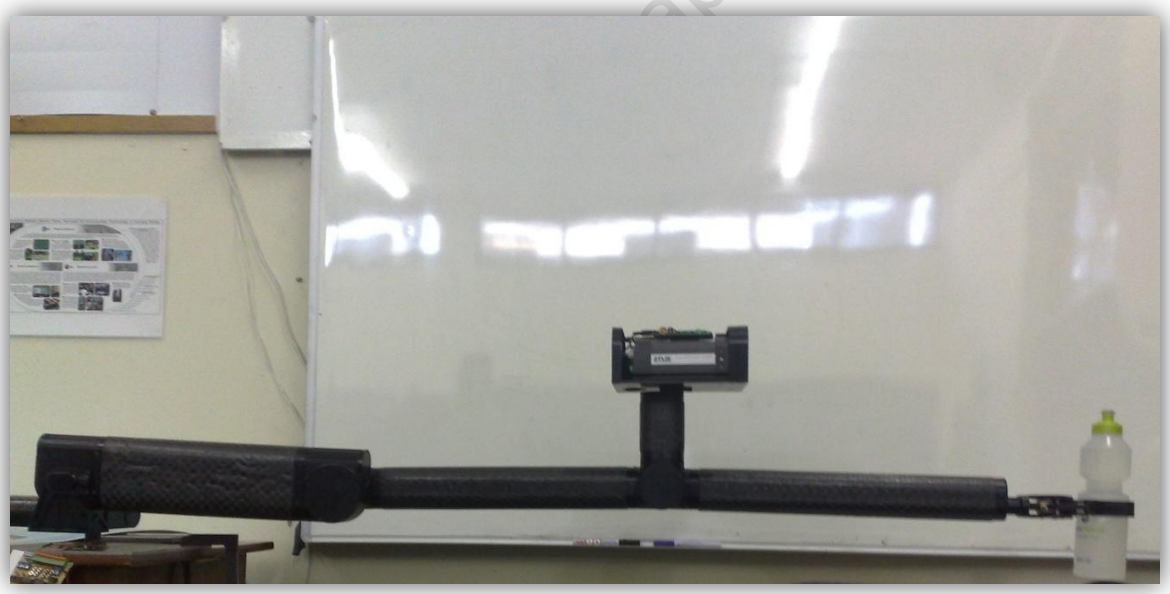

Figure 3-1: Manipulator Arm holding 1kg Water Bottle at full Extension (Start of Test 2c)

D4. Test 3: Testing Overall Mass of the Arm

Procedure: Put entire arm on a scale

a) With Sensor Payload
b) Without Sensor Payload

Measure: Mass of arm

Table 4-1: Table of Results for Test 3

Test 3	Configuration	Mass (kg)	Picture
a	With Sensor Payload	14.5	840
b	Without Sensor Payload	12.5	841

Figure 4-1: Figures showing Test 3: Mass Measurement of a) Complete Arm b) Sensor Payload (Note: 4.2kg mounting plate included in (a))

D5. Test 4: Testing the Blue Arena Capabilities

Procedure: With arm mounted at base height, and stowed in 'home position', extend as fast as possible to pick up a wooden block 600mm deep on a 1m high shelf. Repeat test 4 times.

Measure: Time to complete task

Table 5-1: Table of Results for Test 4

Test 4	Time (s)	Video
a	12.0	121
b	12.0	122
c	11.0	123
d	10.5	124

D6. Test 5: Testing No-Load Backlash

Procedure: With base securely fastened to immovable surface:

a) With Elbow 2 joint in the vertical (no load) position, externally manipulate joint with minimal force in the anticlockwise, then clockwise direction
b) With Elbow 1 joint in the vertical (no load) position, externally manipulate joint with minimal force in the anticlockwise, then clockwise direction
c) With Shoulder joint in the vertical (no load) position, externally manipulate joint with minimal force in the anticlockwise, then clockwise direction
d) With Turntable joint in the vertical (no load) position, externally manipulate joint with minimal force in the anticlockwise, then clockwise direction
e) With Pan joint in the horizontal (no load) position, externally manipulate joint with minimal force in the anticlockwise, then clockwise direction
f) With Tilt joint in the vertical (no load) position, externally manipulate joint with minimal force in the anticlockwise, then clockwise direction

Measure: for a-f above, measure backlash (free play) in degrees.

Table 6-1: Table of Results for Test 5

Test 5	Joint	Angle of Backlash (deg)	Set up Photo	Protractor Photo
a	Elbow 2	0.5	844	845
b	Elbow 1	0~0.1	851	855
c	Shoulder	0~0.1	865	866
d	Turntable	0~0.1	857	859
e	Pan	0.8	861	864
f	Tilt	0.3	847	849

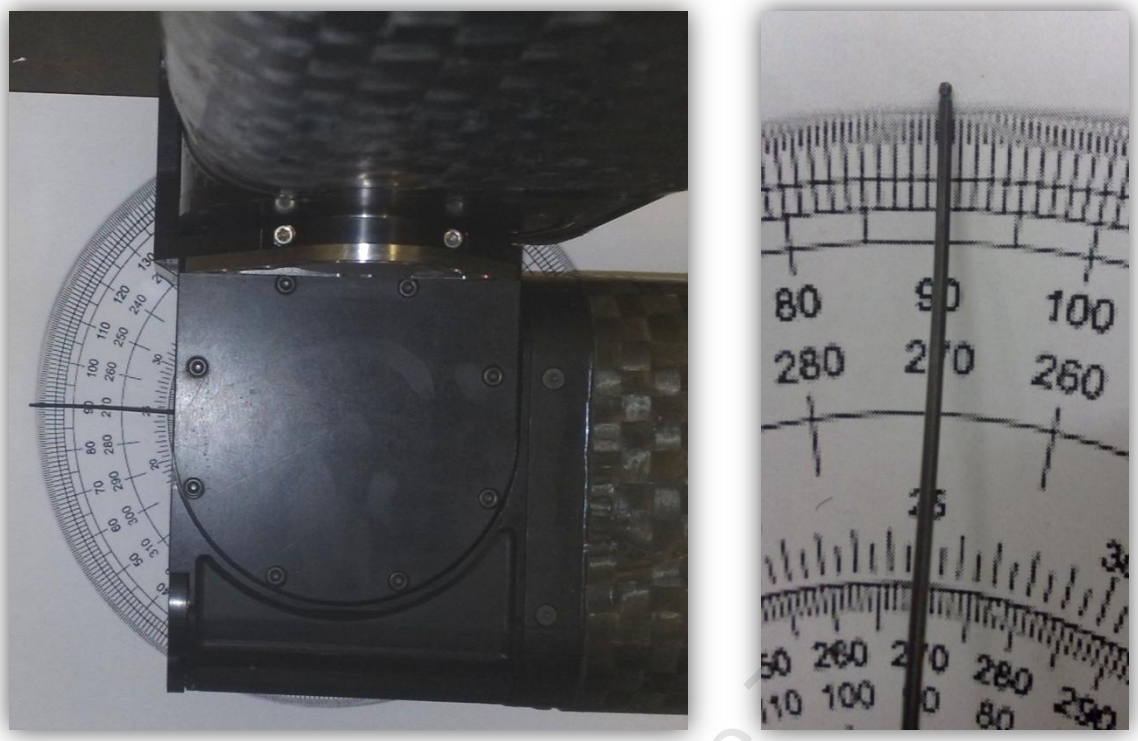

Figure 6-1: Pictures showing Backlash Test on Turntable Joint

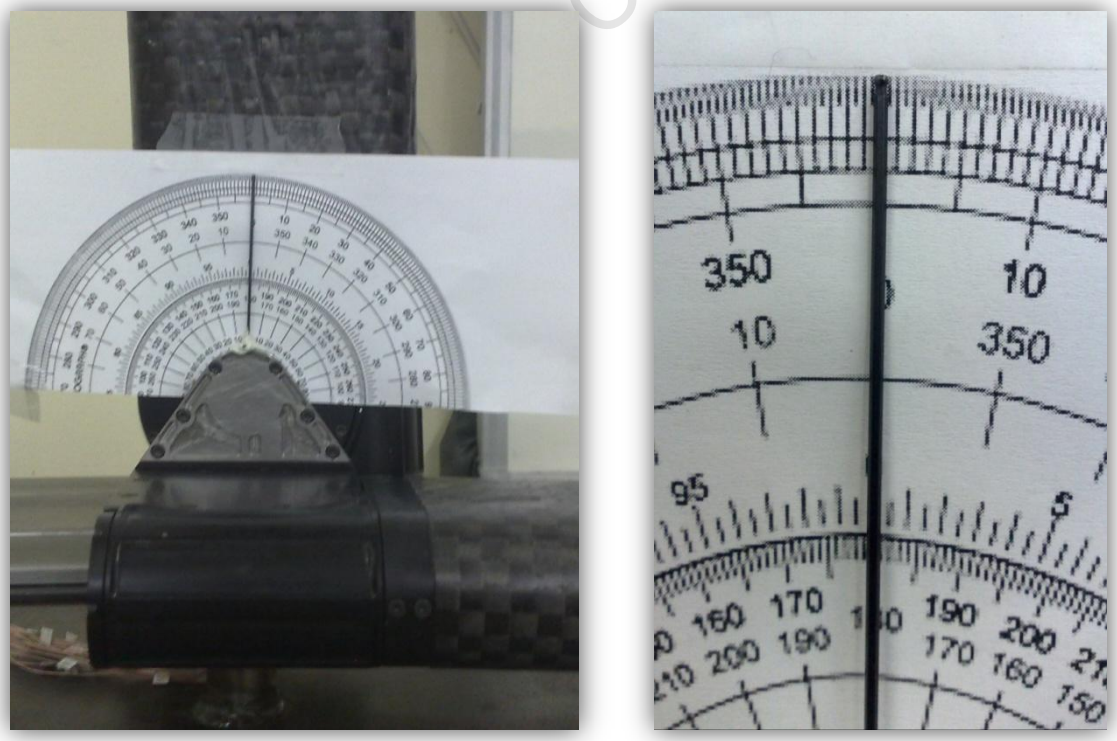

Figure 6-2: Pictures showing Backlash Test on Shoulder Joint

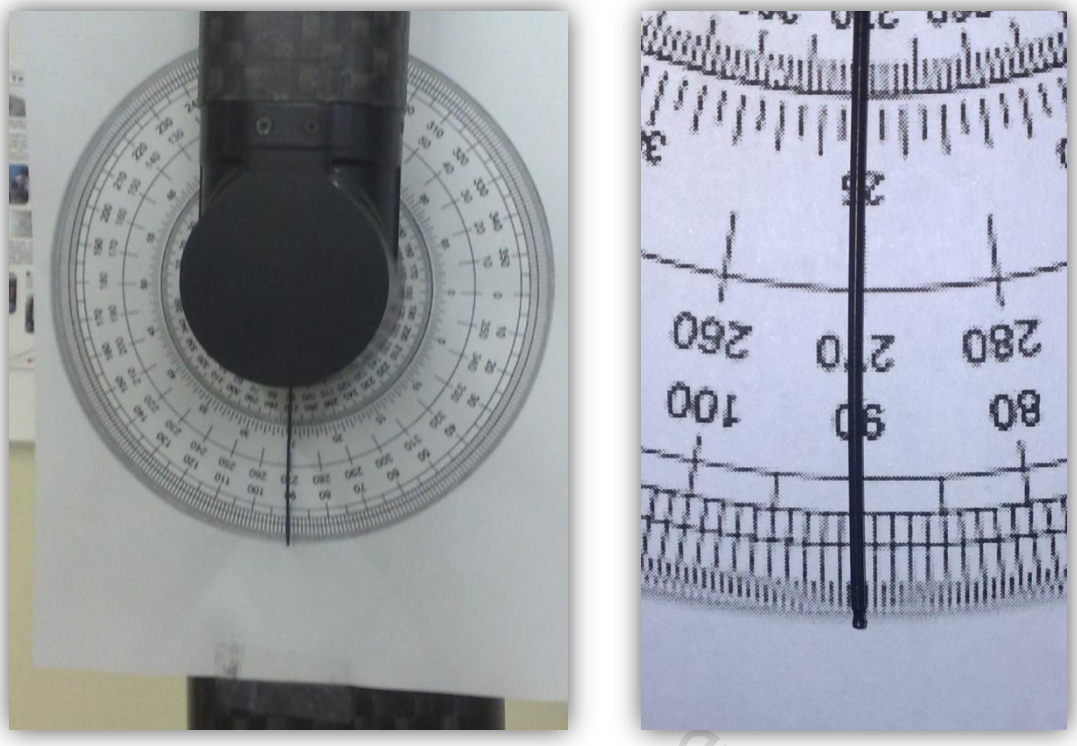

Figure 6-3: Pictures showing Backlash Test on Elbow 1 Joint

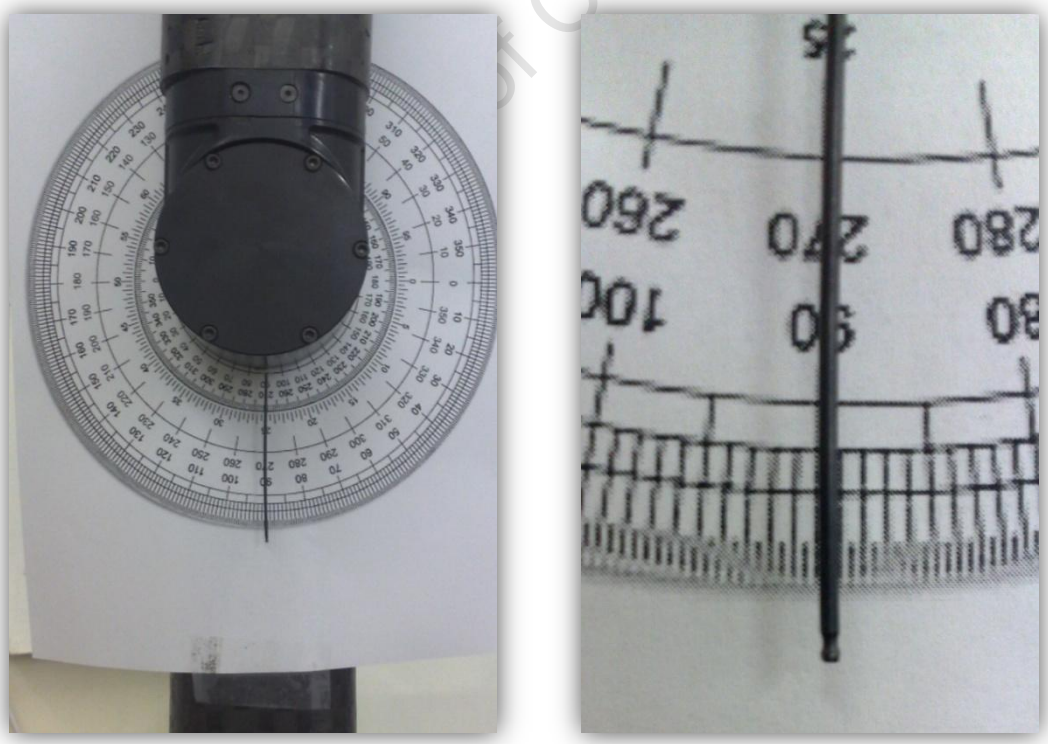

Figure 6-4: Pictures showing Backlash Test on Elbow 2 Joint

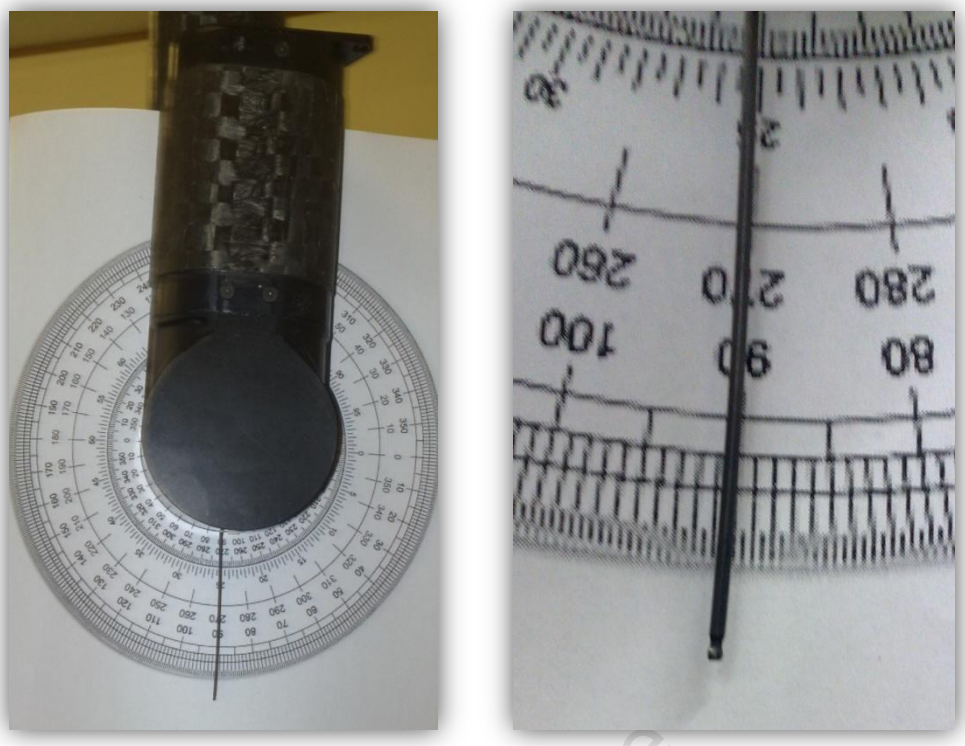

Figure 6-5: Pictures showing Backlash Test on Tilt Joint

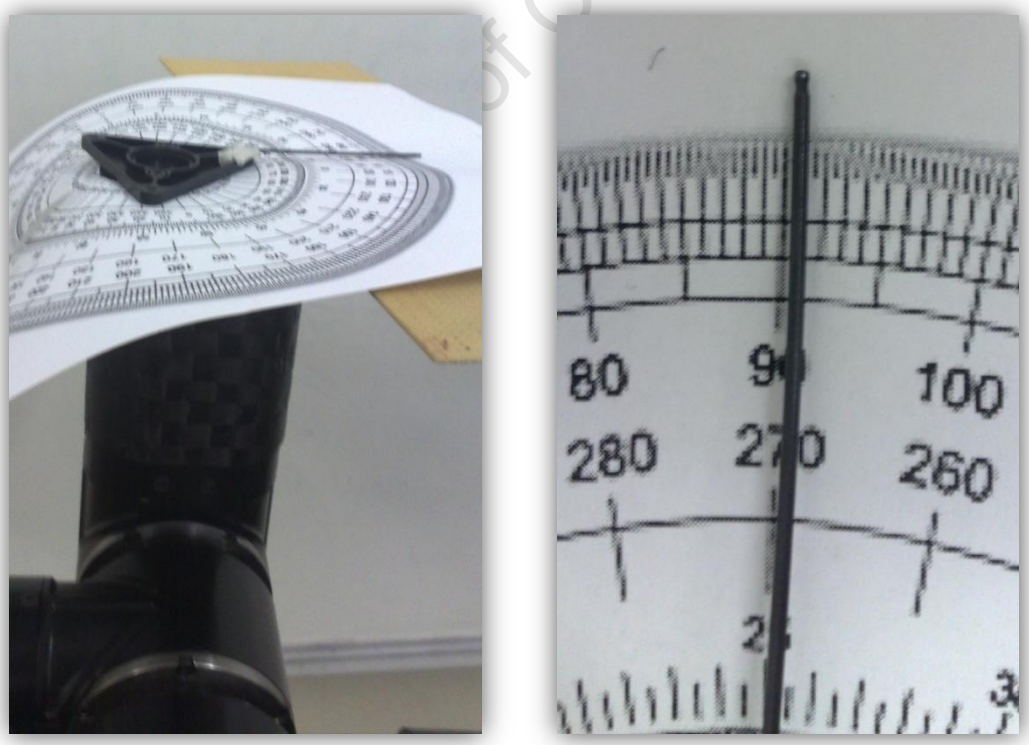

Figure 6-6: Pictures showing Backlash Test on Pan Joint

D7. Test 6: PackBot Comparison Test

Procedure:

a) Load arm with a payload of greater than 4.54kg. Extend arm to a 1.54m reach. Raise and lower the payload.
b) Extend arm to close in position (i.e. simulating lifting something right next to the robot base). Load to more than 13.61kg. Raise and lower the payload.

Measure: Capability of lifting more than the PackBot Manipulator 1.0.

Table 7-1: Table of Results for Test 6

Test 6	Reach	Payload Mass (kg)	Video
a	1.54m	5.1	2117
b	Close-in Position	15.7	2120

Figure 7-1: Pictures showing Manipulator Arm lifting 5.1kg at 1.54m Reach

Figure 7-2: Pictures showing Manipulator Arm lifing 15.7kg at Close in Position

Appendix E

Drawings

List of Drawings

E1. Overall System

E2. Turntable Section Exploded

E3. Turntable Section Assembled

E4. Bottom Section Exploded

E5. Bottom Section Assembled

E6. Mid Section Exploded

E7. Mid Section Assembled

E8. Top Section Exploded

E9. Top Section Assembled

E10. Pan Section Exploded

E11. Pan Section Assembled